

Aus dem Bereich Med. Physiologie  
Theoretische Medizin und Biowissenschaften  
der Medizinischen Fakultät  
der Universität des Saarlandes, Homburg/Saar

**Functions of SNARE Regulators and v-SNARE  
Transmembrane Domain in  $\text{Ca}^{2+}$ -triggered Exocytosis**

*Dissertation zur Erlangung des Grades eines Doktors der Naturwissenschaften*

**der Medizinischen Fakultät**

der UNIVERSITÄT DES SAARLANDES

2016

vorgelegt von: Antonio Yarzagaray  
geb.am: 18.12.1980 in Cartagena, Colombia

Homburg (Saar)

2016

### **Erklärung gemäß § 7 Abs. 1 Nr. 4**

Ich erkläre hiermit an Eides statt, dass ich die vorliegende Arbeit ohne unzulässige Hilfe Dritter und ohne Benutzung anderer als der angegebenen Hilfsmittel angefertigt habe. Die aus anderen Quellen direkt oder indirekt übernommenen Daten und Konzepte sind unter Angabe der Quelle gekennzeichnet.

Bei der Auswahl und Auswertung folgenden Materials haben mir die nachstehend aufgeführten Personen in der jeweils beschriebenen Weise unentgeltlich/entgeltlich geholfen:

1. ....
2. .... usw.

Weitere Personen waren an der inhaltlich-materiellen Erstellung der vorliegenden Arbeit nicht beteiligt. Insbesondere habe ich nicht die entgeltliche Hilfe von Vermittlungs- bzw. Beratungsdiensten (Promotionsberater/innen oder anderer Personen) in Anspruch genommen. Außer den Angegebenen hat niemand von mir unmittelbar oder mittelbar geldwerte Leistungen für Arbeiten erhalten, die im Zusammenhang mit dem Inhalt der vorgelegten Dissertation stehen.

Die Arbeit wurde bisher weder im Inland noch im Ausland in gleicher oder ähnlicher Form in einem anderen Verfahren zur Erlangung des Doktorgrades einer anderen Prüfungsbehörde vorgelegt.

Ich versichere an Eides statt, dass ich nach bestem Wissen die Wahrheit gesagt und nichts verschwiegen habe.

Vor Aufnahme der vorstehenden Versicherung an Eides Statt wurde ich über die Bedeutung einer eidesstattlichen Versicherung und die strafrechtlichen Folgen einer unrichtigen oder unvollständigen eidesstattlichen Versicherung belehrt.

Ort, Datum

Unterschrift der/des Promovierenden

Unterschrift der die Versicherung an Eides statt aufnehmenden Beamtin bzw. Des aufnehmenden Beamten

Tag des Promotionskolloquiums:

---

Dekan:

---

Vorsitzender:

---

Berichterstatter:

---

---

---

*To my grandmother*  
*Matilde Gómez Díaz*

## Summary

Calcium-dependent exocytosis mediates the release of neurotransmitters, hormones, neuropeptides, small proteins and digestive enzymes. During the past three decades, the key proteins that participate in this process have been well characterized. Several proteins work together to allow the membrane-bound secretory vesicles to fuse with the plasma membrane in order to release the aqueous content. SNARE proteins (soluble *N*-ethylmaleimide sensitive factor attachment protein receptor) have been identified as the core of the fusion machinery that requires auxiliary proteins to couple the triggering  $\text{Ca}^{2+}$ -stimulus to the fusion event.

The first part of this thesis work studied the functional role of two auxiliary proteins, ComplexinII (CpxII) and SynaptotagminI (SytI). These proteins have been implicated in regulating the function of SNARE proteins, but the precise mode of action and potential interaction have remained elusive. The present work shows that CpxII increases  $\text{Ca}^{2+}$ -triggered exocytosis and speeds up its secretory rates, contributing to two independent but synergistic functions, to increase synchronous release. In the framework of a structure-function analysis, it became clear that the C terminus enhances the pool of primed vesicles by impeding premature secretion at submicromolar  $\text{Ca}^{2+}$  concentrations, whereas the N terminus shortens the secretory delay and accelerates the stimulus-secretion coupling by increasing the  $\text{Ca}^{2+}$  affinity of secretion. The comparative analysis of single null mutants for CpxII and SytI, as well as their compound deficiency (double knock-out CpxII/SytI), shows that SytI and CpxII control the extent of evoked-release by different mechanisms. Overall, these results clarify how CpxII and SytI transform the constitutively active SNARE-mediated fusion mechanism into a highly synchronized,  $\text{Ca}^{2+}$ -triggered release apparatus.

Regulated exocytosis is expected not only to rely on protein-protein interactions but also protein-lipid interactions. Yet, the functional role of SNARE-lipid interactions has remained largely unclear. In particular, it is unknown whether transmembrane domains (TMDs) of SNARE proteins have functions that go beyond passive anchoring of the force-generating SNARE-apparatus. The present work shows that conformational

flexibility of the TMD of vesicular SynaptobrevinII is crucial for efficient  $\text{Ca}^{2+}$ -triggered exocytosis and dynamically supports membrane fusion. Specifically, the present work shows that a rigid  $\alpha$ -helical structure of the TMD (induced by helix-promoting leucine residues) spanning the outer leaflet of vesicular membrane strongly reduces secretion. Oppositely, increasing the number of helix-destabilizing,  $\beta$ -branched valine residues within the TMD rescues secretion to the wild-type level. These findings support a new model for membrane fusion, wherein SNARE force (generated by zipping SNAREs) together with membrane perturbation induced by structural flexibility of the v-SNARE TMD facilitates membrane merger.

## **Zusammenfassung**

Die Kalzium-abhängige Exocytose vermittelt die Freisetzung von Neurotransmittern, Hormonen, Neuropeptiden, kleinen Proteinen und Verdauungsenzymen. In den vergangenen drei Jahrzehnten wurden die wichtigsten Proteine, die an diesem Prozess beteiligt sind, identifiziert und charakterisiert. SNARE-Proteine („soluble *N*-ethylmaleimide sensitive factor attachment protein receptor“) wurden als Kern der Fusionsmaschinerie identifiziert, die akzessorische Proteine benötigt, um den auslösenden  $\text{Ca}^{2+}$ -Stimulus an das Fusionsereignis zu koppeln.

Der erste Teil dieser Arbeit untersucht die funktionelle Rolle von zwei akzessorischen Proteinen, dem ComplexinII (CpxII) und dem SynaptotagminI (SytI). Beide Proteine scheinen an der Regulation der SNARE-Proteine beteiligt zu sein, ihre eigentliche Wirkungsweise sowie potentielle Wechselwirkungen sind jedoch weitgehend unverstanden. Die vorliegende Arbeit zeigt, dass CpxII sowohl das Ausmaß der  $\text{Ca}^{2+}$ -gesteuerten Exozytose erhöht als auch die Stimulus-Sekretions-Kopplung beschleunigt. Somit vermittelt CpxII zwei unabhängige, aber synergistisch wirkende Funktionen, um die synchrone Transmitterfreisetzung zu steigern. Im Rahmen einer umfassenden Struktur-Funktions-Analyse wurde klar, dass einerseits der C-terminus von CpxII durch Inhibition vorzeitiger Sekretion bei submikromolaren  $\text{Ca}^{2+}$ -Konzentrationen die Akkumulation von Vesikeln im Exozytose-kompetenten Zustand erleichtert und der N-terminus andererseits die Sekretionsrate dieser Vesikel erhöht. Die vergleichende Analyse einzelner Nullmutanten für CpxII und SytI sowie der entsprechenden Doppel-Nullmutante (double knock-out CpxII/SytI) zeigt, dass SytI und CpxII in der Kontrolle der evozierten Transmitterfreisetzung kooperieren, jedoch ihre Wirkung durch unterschiedliche molekulare Mechanismen vermitteln. Insgesamt erlauben die erarbeiteten Befunde einen neuen Einblick in Mechanismen, mit denen CpxII und SytI die konstitutiv-agierende SNARE-Maschinerie in einen hoch-synchronisierten,  $\text{Ca}^{2+}$ -getriggerten Fusionapparat umwandeln.

Die  $\text{Ca}^{2+}$ -regulierte Exocytose beruht aller Voraussicht nach nicht nur auf Protein-Protein-, sondern auch auf Protein-Lipid-Wechselwirkungen. Im Gegensatz zu Protein-

Protein-Interaktion ist die funktionelle Rolle der SNARE-Lipid-Wechselwirkungen noch weitgehend unverstanden. So ist z.B. unklar, ob die Transmembrandomänen (TMDs) von SNARE-Proteinen neben ihrer Rolle als Membrananker noch zusätzliche, aktive Funktionen im Fusionsvorgang übernehmen. In der Tat legen die experimentellen Befunde nahe, dass konformationelle Flexibilität der TMD des vesikulären SynaptobrevinII die  $\text{Ca}^{2+}$ -getriggerte Exozytose entscheidend unterstützt. Es wird vermutet, dass die Fluktuationen in der Helixstruktur der TMD zu lokalen Membrandefekten führen und somit den Vorgang der Membranverschmelzung einleiten. So zeigen die Resultate, dass eine starre  $\alpha$ -helikale Struktur der TMD (induziert durch Helix-fördernde Leucinreste) im Bereich der äußeren Lipidschicht („outer leaflet“) der Vesikelmembran die Sekretionsantwort stark behindert. Im Gegensatz dazu erhöht die Anzahl Helix-destabilisierender,  $\beta$ -verzweigter Valinreste innerhalb der TMD die Sekretionsantwort auf das Niveau von Wildtypzellen.

Zusammengefasst unterstützen die Ergebnisse ein Modell, in dem nicht nur membranverbindende, Kraft-vermittelnde Interaktionen der SNARE Proteine (Protein-Protein-Wechselwirkung) sondern auch die Erzeugung lokaler Membrandefekte durch strukturelle Flexibilität der Membrananker von v-SNARE Proteinen (Protein-Lipid-Wechselwirkung) die Membranfusion erleichtert.



## **Acknowledgements**

I would like to appreciatively acknowledge my supervisor Prof. Dr. Dieter Bruns. I am highly indebted to him for providing me the lab space, constant help to successfully do the experiments, the consequent analyses of the results and scientific discussion.

I am also very grateful to Jun.-Prof. Dr. Ralf Mohrmann, Dr. Chad Grabner and Dr. Yvonne Schwarz for helping me throughout the projects, not only for being friendly open to discuss new ideas but also supporting me with experiments and analyses of data.

I also thank to Prof. Dr. Jens Rettig and all members of his lab, especially Dr. David Stevens and Dr. Claudia Schirra for not only discussing my results but also helping me with many aspects of flash photolysis experiments.

I want to express my thankfulness to Marina Wirth and all technical staff as well, Patrick Schmitt, Vanessa Schmitt, Katja Kingler, Anika Simon, Walentina Frisch, Birgit Bimperling and Martina Didion. Their effort to provide animals, reagents, keeping the lab with all necessary supplies was extremely important to perform the experiments. Also, I would like to thank Judith Arend for her administrative assistance.

And finally, my sincere thanks to all my colleagues for being more than just friends and supporting me at all facets of my work in the lab, Raúl Guzmán, Gustavo Guzmán, Madhurima Dhara, Soumyajit Dutta, Surya Gaya, Barbara Schindeldecker, Evgenii Bogatikov, Ahmed Shaaban, Ali Harb and Mazen Makke.

## Abbreviations

aa: amino acid  
ATP: Adenosine triphosphate  
BAPTA: 1,2-bis(o-aminophenoxy)ethane- N,N,N',N'-tetraacetic acid  
°C: Celsius  
Ca<sup>2+</sup>: Calcium  
CaCl<sub>2</sub>: Calcium chloride  
[Ca<sup>2+</sup>]<sub>i</sub>: Intracellular free calcium ion concentration  
cDNA: circular DNA  
cm: Centimeter  
Ceb: Cellubrevin  
C<sub>M</sub>: Membrane capacitance  
CO<sub>2</sub>: Carbon dioxide  
Cpx: Complexin  
CpxII ko: Complexin II ko  
CpxII/sytI Dko: Complexin II/synaptotagmin I double ko  
Cs: Cesium  
CsOH: Cesium hydroxide  
ΔC<sub>M</sub>: Delta (change) in membrane capacitance  
DDW: Double distilled water  
Dko: Double knockout  
DMEM: Dulbecco's Modified Eagle's Medium  
DMSO: Dimethylsulfoxide  
DNA: Deoxyribonucleic acid  
dNTP: Deoxyribonucleotide  
DOKO: Double knockout for Syb II/Ceb  
DPTA: 1,3-diaminopropane-N,N,N',N'-tetraacetic acid  
EB: Exocytotic burst  
EDTA: Ethylenediaminetetraacetic acid  
EGFP: Enhanced Green Fluorescent Protein  
EGTA: Ethyleneglycol tetraacetic acid

fF: Femtofarad  
 fF/s: Femtofarad per second  
 Fig: Figure  
 Fw-Primer: Forward Primer  
 g: gram  
 Gm: Membrane conductance  
 Gs: Series conductance  
 GTP: Guanosine triphosphate  
 h: Hour  
 H<sub>2</sub>O: Water  
 HEPES: 2-[4-(2-hydroxyethyl)piperazin-1-yl]ethanesulfonic acid  
 HCl: Hydrochloric acid  
 Hz: Hertz  
 kb: Kilobase pair  
 KCl: Potassium chloride  
 kDa: Kilodalton  
 kg: Kilogram  
 KHz: Kilohertz  
 ko: Knockout  
 LDCV: Large dense-core vesicles  
 μF: Microfarad  
 μg: Microgram  
 μL: Microliter  
 mg: Milligram  
 Mg<sup>2+</sup>: Magnesium  
 MgATP: Magnesium ATP  
 MgCl<sub>2</sub>: Magnesium chloride  
 min: Minutes  
 mL: Milliliter  
 mm: Millimeter  
 mM: Millimolar  
 mOsm: Milliosmol

ms: Milliseconds  
Munc-18: Mammalian uncoordinated-18  
mV: Millivolt  
MΩ: Megaohm  
n: Number of the elements (e.g., cells)  
Na<sub>2</sub>EDTA: Sodium EDTA  
Na<sub>2</sub>GTP: Sodium GTP  
NaHCO<sub>3</sub>: Sodium bicarbonate  
NaCl: Sodium chloride  
(NH<sub>4</sub>)<sub>2</sub>SO<sub>4</sub>: Ammonium sulfate  
nm: Nanometer  
nM: Nanomolar  
NMJ: Neuromuscular junction  
NP-EGTA: Nitrophenyl-EGTA  
nS: Nanosiemens  
NSF: N-ethylmaleimide sensitive factor  
p: Or p-value, probability value  
PCR: Polymerase chain reaction  
pF: Picofarad  
pM: Picomolar  
pS: Picosiemens  
R: Ratio  
Rev-Primer: Reverse Primer  
RNA: Ribonucleic acid  
rpm: Revolutions per minute  
RRP: Readily releasable pool  
s: Seconds  
SB-buffer: Soriano buffer  
SDS: Sodium dodecyl sulfate (detergent)  
SFV: Semiliki Forest Virus  
SNAP: Soluble NSF attachment protein  
SNAP-25: Synaptosomal-associated protein of 25 kDa

SNARE: The SNAP receptor  
 SR: Sustained rate  
 SRP: Slowly releasable pool  
 Syb: Synaptobrevin  
 SybII/ceb DOKO: Synaptobrevin II/cellubrevin double ko  
 Syt: Synaptotagmin  
 SytI ko: Synaptotagmin I ko  
 Syx: Syntaxin  
 t: Time  
 Tab: Table  
 TAE: Tris-acetate-EDTA  
 temp: Temperature  
 TMD: Transmembrane domain  
 TMR : Transmembrane region  
 TRIS: Tris(hydroxymethyl)aminomethane  
 t-SNARE: Target SNARE  
 UV: Ultraviolet  
 V: Volt  
 VAMP: Vesicle-associated membrane protein  
 v-SNARE: Vesicular SNARE  
 wt: Wildtype

## List of Figures and Tables

### Figures

- Figure 1. Representation of a vesicle motion and ultimate fusion
- Figure 2. SNARE complex formation
- Figure 3. SNARE regulators Complexin and Synaptotagmin
- Figure 4. Calcium indicators (Fura-2 and mag-Fura-2) and the calcium chelator NP-EGTA
- Figure 5. Flash photolysis technique on a chromaffin cell and the kinetic model of vesicle maturation
- Figure 6. Generation of the novel CpxII/SytI Dko
- Figure 7. Preparation and culturing of embryonic mouse chromaffin cells
- Figure 8. “Whole-cell” patch clamp configuration
- Figure 9. Excitation spectra of Fura-2
- Figure 10. Calibration curve
- Figure 11. CpxII determines magnitude and kinetics of  $\text{Ca}^{2+}$ -triggered exocytosis
- Figure 12. Typical recording of electrical properties in a chromaffin cell
- Figure 13. CpxII controls tonic secretion of chromaffin granules
- Figure 14. Loss of SytI in the absence of CpxII does not further aggravate the CpxII ko phenotype in chromaffin cells
- Figure 15. Absence of CpxII and not SytI determines the extent of tonic exocytosis
- Figure 16. Expression of CpxII full-length protein enhances the exocytotic burst and restores the kinetics in CpxII ko cells, but fails to do so in SytI ko
- Figure 17. Tonic exocytosis clamping accomplished by CpxII does not depend on SytI in chromaffin cells
- Figure 18. C- and N-terminal domains of CpxII control the magnitude and time course of synchronous exocytosis respectively
- Figure 19. Tonic secretion clamping done by CpxII depends on its C-terminal domain
- Figure 20. Expression in wt cells of either  $\Delta\text{C}$ - or  $\Delta\text{N}$ -mutant outcompete the endogenous CpxII altering the magnitude and kinetics of secretion

- Figure 21. The  $\Delta C$ - and  $\Delta N$ -mutant change the tonic secretion beyond levels recorded in wt cells, rising it and lowering it respectively
- Figure 22. N-terminal domain modifies the  $Ca^{2+}$  affinity of secretion
- Figure 23. The v-SNARE Transmembrane Domain (TMD)
- Figure 24. A rigid  $\alpha$ -helical structure of v-SNARE TMD reduces synchronous secretion
- Figure 25. Saturation of a  $\beta$ -branch amino acid in v-SNARE TMD is able to restore the exocytotic response
- Figure 26. Specific mutations on the two Valine residues do not affect the properties of the v-SNARE TMD
- Figure 27. Proline mutation in the v-SNARE TMD decreases regulated exocytosis
- Figure 28. The v-SNARE TMD spans both leaflets of the vesicle lipid bilayer
- Figure 29. The N-terminal half of the v-SNARE TMD provides its flexibility
- Figure 30. Alternating  $\beta$ -branch and non- $\beta$ -branch amino acids in v-SNARE TMD also rebuild synchronous secretion

**Tables**

- Table 1. PCR for CpxII and SytI
- Table 2. PCR for SybII
- Table 3. PCR for Ceb
- Table 4. PCR-programs
- Table 5. Proteins and their mutants expressed by SFV
- Table 6. Ratio 340/380 and Inverted Ratio for solutions containing BAPTA and DPTA
- Table 7. Scheme for preparation of solutions containing BAPTA
- Table 8. Scheme for preparation of solutions containing DPTA
- Table 9. CpxII domains and its truncated mutants

---

## List of Contents

Summary	I
Zusammenfassung	III
Acknowledgments	V
Abbreviations	VI
List of Figures and Tables	X
List of Contents	XII
 <b>1. Introduction</b>	 - 1 -
1.1 Regulated exocytosis	- 2 -
1.2 SNARE complex	- 4 -
1.3 SNARE regulators	- 7 -
1.3.1. Complexin	- 8 -
1.3.2. Synaptotagmin	- 9 -
1.4 Adrenal chromaffin cells as a model system for neuronal exocytosis	- 11 -
1.5 Kinetic model of vesicle maturation	- 14 -
1.6 Aim of the study	- 16 -
<b>2. Materials and methods</b>	- 17 -
2.1 Materials	- 17 -
2.2 Transgenic mice	- 17 -
2.3 Genotyping	- 18 -
2.4 Mouse chromaffin cell preparation	- 22 -
2.5 Virus production and infection	- 23 -
2.6 Electrophysiology	- 25 -
2.6.1 Capacitance recordings	- 25 -
2.6.2 Flash photolysis of caged $\text{Ca}^{2+}$ and calibration curve	- 28 -
2.6.3 Data acquirement and analysis	- 34 -
<b>3. Results</b>	- 36 -
3.1 CpxII function in $\text{Ca}^{2+}$ -triggered exocytosis	- 36 -
3.1.1 CpxII delimits the extent and kinetics of $\text{Ca}^{2+}$ -triggered exocytosis	- 37 -
3.1.2 CpxII regulates tonic release of chromaffin granules	- 39 -



---

3.1.3 CpxII and SytI have different mechanisms on regulated exocytosis	- 41 -
3.1.4 Clamping of premature exocytosis by CpxII does not depend on SytI	- 45 -
3.1.5 Distinct domains of CpxII control timing and extent of secretion	- 48 -
3.1.6 CpxII mutant protein can outcompete the endogenous protein	- 51 -
3.1.7 N terminus of CpxII rises the $\text{Ca}^{2+}$ affinity of secretion	- 53 -
3.2 Role of the v-SNARE TMD in $\text{Ca}^{2+}$ -triggered exocytosis	- 55 -
3.2.1 A rigid $\alpha$ -helical structure of the TMD reduces synchronous exocytosis	- 56 -
3.2.2 Flexibility of the TMD determines synchronous exocytosis	- 58 -
3.2.3 Single Valine mutations do not affect synchronous secretion	- 60 -
3.2.4 Proline mutation probably affects conformational changes in the TMD	- 61 -
3.2.5 The N-terminal half of the TMD determines fusogenicity	- 63 -
3.2.6 A TMD with alternating L and V residues support exocytosis like wt protein	- 65 -
<b>4. Discussion</b>	- 67 -
4.1 CpxII increases synchronous exocytosis by blocking premature secretion	- 68 -
4.2 CpxII regulates secretion by influencing SytI in $\text{Ca}^{2+}$ -triggered exocytosis	- 69 -
4.3 CpxII has different domains that synergize to elevate synchronous secretion	- 72 -
4.4 CpxII N-terminal domain changes the $\text{Ca}^{2+}$ -dependency of primed vesicle fusion	- 73 -
4.5 v-SNARE TMD provides conformational flexibility that facilitates secretion	- 74 -
4.6 Competing concepts on fusion pores: lipidic vs proteinaceous fusion pores	- 76 -
4.7 TMD flexibility within the outer vesicular membrane leaflet is crucial for membrane fusion	- 77 -
4.8 Concluding remarks	- 78 -
<b>5. Literature</b>	- 79 -
<b>6. Publications</b>	- 90 -

## 1. Introduction

Cellular activities are governed by different interconnected processes in order to provide to the living being the capability of irritability, development, reproduction and homeostasis. Many of these processes require a precise communication between cells, where molecules move constantly from the intra- to extracellular space. This form of active transport in which a cell carries molecules out of its compartment is called exocytosis (from Greek “exo” meaning out and English “cyto” cell, Figure 1). Exocytosis can be divided into five consecutive steps. The first, named “vesicle trafficking” implies that a newly formed vesicle, containing the substances to be released, move over a significant distance in the cytosol towards the plasma membrane. The next, “vesicle tethering”, which consists in a loose connection between the vesicle and the target membrane with a distance of more than about half the diameter of a vesicle. Later, the vesicular membrane and the plasma membrane are attached and held together in the “vesicle docking” stage. The fourth step is the “vesicle priming”, which comprises molecular organization and proteins-lipids adaptation that happen after initial docking. The final step, “vesicle fusion” reflects the merge between the two separate lipid bilayers, in response to an increase in intracellular calcium (for more details see review, Jahn, 2004). Exocytosis can be either constitutive or regulated. Constitutive exocytosis exists in all cells and its purpose is the discharge of components of the extracellular matrix, or the supply of integral membrane proteins. Regulated exocytosis is triggered when the cell receives an external signal in a tightly controlled reaction that is normally triggered by calcium ( $\text{Ca}^{2+}$ ). Several cellular processes use exocytosis, for example, the release of neurotransmitters from presynaptic neurons, the antigen presentation during the immune response, the acrosome reaction during fertilization and the secretion of proteins (like enzymes), peptide hormones and antibodies from the cell.

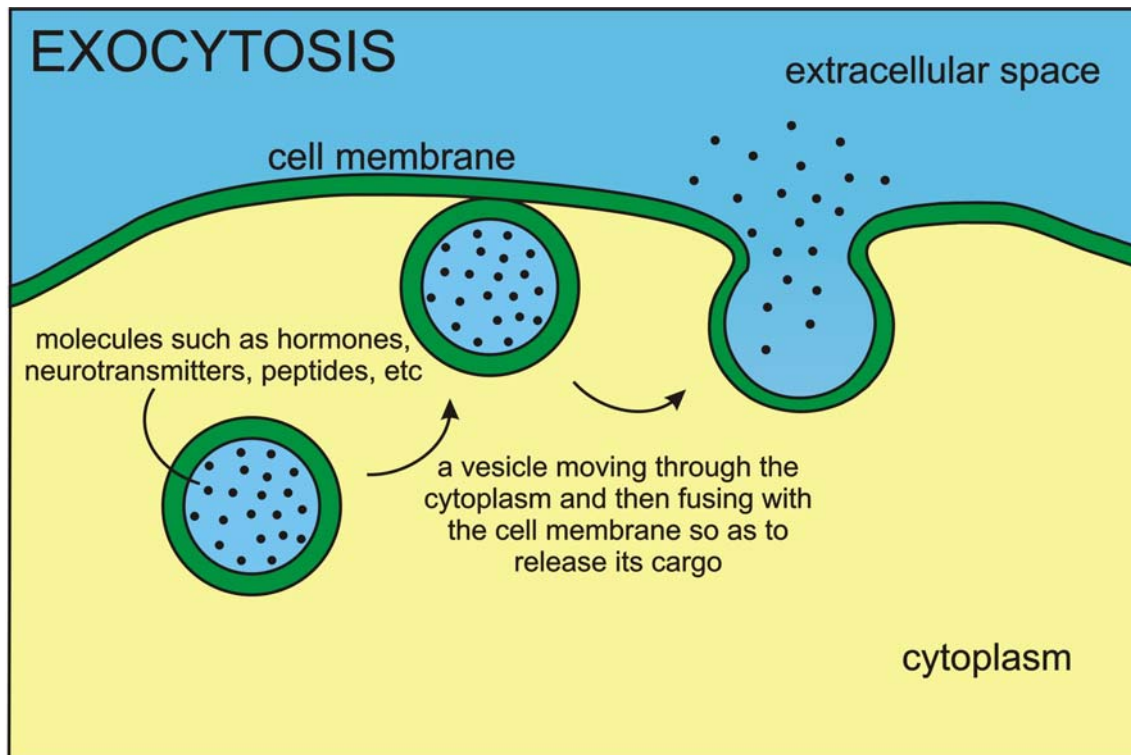


**Fig. 1. Representation of a vesicle motion and ultimate fusion.** A vesicle loaded (black dots) is moving inside the cell until fused with the plasma membrane releasing the cargo.

### 1.1 Regulated exocytosis

Regulated exocytosis is one of the fastest processes in eukaryotic cells. This complex consuming-energy, rapid and precise process requires a machinery made out of highly specialized proteins. Understanding the complexity of this process needs the characterization of the mechanism of membrane fusion and also how fusion is well-organized to happen at the correct time and with a defined probability. Intensive research on the underlying molecular mechanism started out more than 30 years ago and has led to the identification of numerous proteins involved in neurotransmitter release. Amongst the constituents of this machinery are proteins that have homologs in most kinds of intracellular membrane fusion events and comprise the Sec1/Munc18-1 (SM) protein Munc18-1 (an acronym for mammalian uncoordinated-18); *N*-ethylmaleimide sensitive factor (NSF); soluble NSF attachment proteins (SNAPs); the SNAP receptors (SNAREs) synaptobrevin (Syb, or VAMP, vesicle-associated membrane protein), syntaxin-1 (Syx) and SNAP-25 (not confused to SNAPs, it is an acronym for

synaptosomal-associated protein 25), also small GTPases from the Rab3 family (Rizo and Rosenmund, 2008). Discharge of neurotransmitters is strongly controlled by  $\text{Ca}^{2+}$ , and ensues within milliseconds after an increase in the intracellular  $\text{Ca}^{2+}$  ( $[\text{Ca}^{2+}]_i$ ) (Bollmann et al., 2000; Schneggenburger and Neher, 2000). The optimization of vesicle fusion for speed is a critical and crucial characteristic of neurosecretion with vital physiological effects (Sørensen, 2004).

Before final fusion with the plasma membrane, vesicles have to go through some maturation steps, beginning with their biogenesis and followed by translocation and physical connection to the plasma membrane. Cells establish a pool of vesicles that have already overcome the slower maturation stages in order to respond quickly to stimulation. The presence of vesicles in distinct maturation phases becomes clear upon persistent stimulation, where diverse kinetics of the secretory response varying in their release readiness: an early, very fast “exocytotic burst”, that occurs on a milliseconds scale, is followed by a slower sustained phase of secretion (Sørensen, 2004).

Defining releasable pools and their properties depends on the experimental design i.e. on the ability to synchronize secretion and simultaneously to make a proper measurement of the release response. At a small number of synapses, voltage-clamp of the presynaptic terminal has been accomplished in order to define presynaptic calcium currents (Forsythe, 1994). Yet, it was quickly noted that although calcium currents were even, the calcium signal in the terminal was not, because of high gradients close to channels and not-homogeneous scattering of calcium channels, therefore creating calcium microdomains nearby channels (Simon and Llinas, 1985). By using photo-labile calcium chelators (e.g. ethylene glycol tetraacetic acid, EGTA, and related products), problems with the calcium signal being not homogeneous have been surpassed. Using these techniques, different systems have shown outstanding results where different release-ready pools could be distinguished, like in rat pituitary cells (Thomas et al., 1993), goldfish retinal bipolar neurons (Heidelberger et al., 1994), calyx of held (Bollmann et al., 2000; Schneggenburger and Neher, 2000; Felmy et al., 2003), and chromaffin cells (Heinemann et al., 1994).

Synthesis of a highly specific calcium chelator nitrophenyl-EGTA (NP-EGTA) along with capacitance recordings and depolarizing protocols have contributed to the present understanding of vesicle pools in neuroendocrine cells (Voets et al., 1999; Ashery et al., 2000; Voets, 2000). Vesicles that initially merge with a time constant of roughly 20 - 40 ms (at 20  $\mu\text{M}$   $[\text{Ca}^{2+}]_i$ ) fit in to the readily releasable pool (RRP) and contain the fast burst component (for more details see section 1.5 kinetic model of priming and fusion in chromaffin cells). Vesicles that merge with a time constant of roughly 200 ms (at 20  $\mu\text{M}$   $[\text{Ca}^{2+}]_i$ ) derive from the slowly releasable pool (SRP) and form the slow burst component. Nevertheless, even if vesicles from both pools (RRP and SRP) can be released upon prolonged  $[\text{Ca}^{2+}]_i$ , a physiological stimulus like an action potential, preferentially causes the release of vesicles from the RRP (Becherer and Rettig, 2006).

## 1.2 SNARE complex

More than 35 years ago, Schekman and colleagues discovered genes that are crucial for the steps in the secretory pathway in *S. cerevisiae* (Novick et al., 1980). A decade later, Rothman and colleagues identified mammalian homologues of Sec18 and Sec17, named NSF (*N*-ethylmaleimide sensitive factor) and SNAP (soluble NSF attachment protein), as soluble factors that are essential for intracellular membrane-fusion reactions (Wilson et al., 1989; Clary et al., 1990). Proteins identified as receptors for SNAP were isolated from bovine brain, thus introducing for the first time the term SNARE (SNAP receptors, Söllner et al., 1993). Those proteins formed a complex (only SNARE complexes serve as SNAP receptors and not individual SNAREs) containing a vesicular protein named VAMP (vesicle-associated membrane protein, or synaptobrevin, Syb) and proteins from the plasma membrane, syntaxin (Syx) and SNAP-25. This led to a functional classification as v-SNAREs, for vesicle-membrane SNAREs, and t-SNAREs, for target-membrane SNAREs (Söllner et al., 1993).

The crucial roles of the SNAREs were verified by the finding that they are the targets of clostridial neurotoxins (Blasi et al., 1993). Instead, NSF seemed to be a priming factor and not needed for fusion by studying the *in vitro* fusion of vacuoles (Mayer et al., 1996). Besides, it has also been shown that neuronal SNARE proteins are aligned in

parallel in the SNARE complex, which led to the “zipper” model of SNARE function (Hanson et al., 1997; Lin et al., 1997). SNAREs were also shown to be sufficient to fuse membranes of liposomes without the need for other factors (Weber et al., 1998). In summary, stable “SNARE complex” is formed to induce membrane fusion and is taken apart upon binding to SNAPs and NSF through the ATPase action of NSF.

The structure of the SNARE complex (2.4 Å resolution of a complex containing Syb-II, Syx-1A and SNAP-25B) was resolved by X-ray crystallography, which consists in a highly twisted and parallel four-helix bundle (Sutton et al., 1998; Figure 2). Conserved leucine-zipper-like layers (16 hydrophobic stacked layers) were found in the complex. Within these layers, an ionic layer comprising of an arginine (R) and three glutamine (Q) residues was shown. Henceforward, SNAREs were reclassified as Q- and R-SNAREs, holding glutamine and arginine residues respectively (Fasshauer et al., 1998).

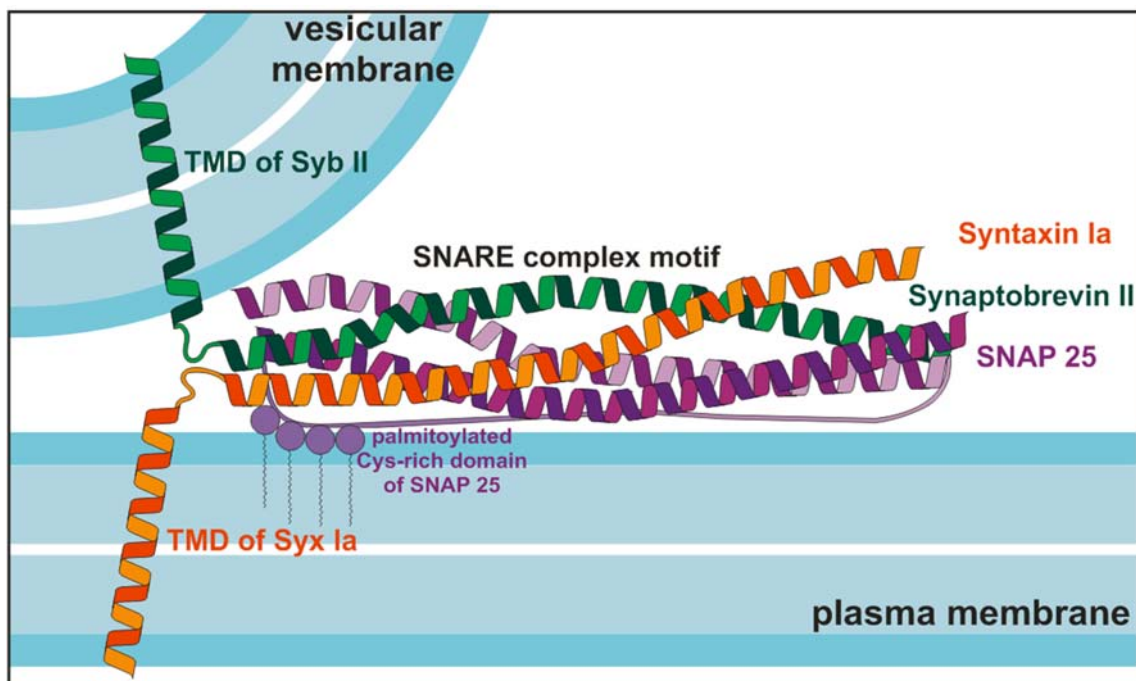


**Fig. 2. SNARE complex formation.** A four helical bundle is formed by the three proteins (Syntaxin, Synaptobrevin and SNAP 25) in order to bring vesicle membrane to a close approximation to the plasma membrane. Syb II and Syx Ia are anchored through carboxy-terminal transmembrane domains (TMD) to the vesicle and plasma membrane respectively, while SNAP 25 is attached by palmitoyl modifications to the plasma membrane. The complex conformation starts from the N terminus towards C terminus of the SNARE proteins. The SNARE motifs (heptad-regions involving coiled-coil interactions) confer stability. Drawing of the complex is taken and modified from Sutton et al., 1998.

SNAREs proteins Syx and Syb are anchored to the membrane by C-terminal transmembrane domains (TMD), while SNAP-25 is anchored to the membrane by palmitoyl groups. Short linkers connect the TMDs to the SNARE motifs that form the core complex. Monomeric SNARE motifs are unstructured, but when correct arrays of SNAREs are combined, they form helical core complexes of great stability. In addition to SNARE motifs and TMDs, many SNAREs possess autonomously folding N-terminal domains, which can control SNARE assembly. For instance, Syx1 is folded into a self-restricted closed conformation binding Munc18-1. Munc13s open Syx1 coordinating SNARE complex association in an NSF-SNAP-resistant fashion along with Munc18-1 (see reviews Bruns and Jahn, 2002; Jahn and Scheller, 2006, Rizo and Xu, 2015). Using mouse chromaffin cells, it has been shown that v-SNAREs control exocytosis of vesicles from priming to fusion (Borisovska et al., 2005). Furthermore, a tight molecular coupling between the complex forming SNARE domain and TMD of SybII is decisive for priming of chromaffin granules, their exocytosis initiation and fusion pore expansion (Kesavan et al., 2007). During fast fusion, regulatory proteins like Complexin (Cpx), which prevents full zippering of SNARE (Giraudo et al., 2006) and Synaptotagmin (Syt), which act as  $\text{Ca}^{2+}$  sensor for secretion (Chapman, 2008), are required to provide speed and precision. Yet, the precise function and fundamental mechanisms of these two proteins remain controversial as will be discussed below (section 1.3).

Although SNARE motifs have been intensively studied, as well as SNAREs N-terminal domains, other structures, like TMDs, have unclear function. TMDs could function as anchors to hold the SNAREs proteins to the membrane or, alternatively promoting membrane merger. SNARE TMDs have the particular feature of overrepresentation of  $\beta$ -branched amino acids.  $\beta$ -branched residues (valine, isoleucine and threonine) have a non-hydrogen substituent attached to their beta-carbon, thus generating steric hindrance for a strict  $\alpha$ -helix arrangement. Valine and isoleucine are present in approximately 40% of all residues in SNARE TMDs (Langosch et al., 2001). An *in vitro* approach based on lipid mixing has shown that the fusogenicity of “peptides mimics of SNAREs TMD segments” decreased with increasing stability of the  $\alpha$ -helical structure within TMD. This suggests that structural flexibility of TMD is important for SNARE function at a late step in membrane fusion (Langosch et al., 2001). Moreover,

simulation studies have shown a tendency of the SNARE TMDs as well as the viral hemagglutinin fusion peptide to disrupt lipid packing, enabling lipid splay (first encounter of the acyl chains of lipid moieties between contacting membranes) and generation of an initial lipid bridge between membranes (Kasson et al., 2010; Markvoort and Marrink, 2011; Risselada et al., 2011).

### 1.3 SNARE regulators

Since the SNARE complex suffices for membrane fusion *per se*, it is necessary to be regulated in order to avoid uncontrolled complex formation and premature exocytosis. Also, regulated exocytosis is characterized to be precise and fast, which is a demanding task that requires proteins functioning as regulators. Quite a few molecules have been recognized that are necessary for  $\text{Ca}^{2+}$ -dependent exocytosis, the most outstanding of which are Complexin (Cpx) or Synaptotagmin (Syt) (Figure 3).

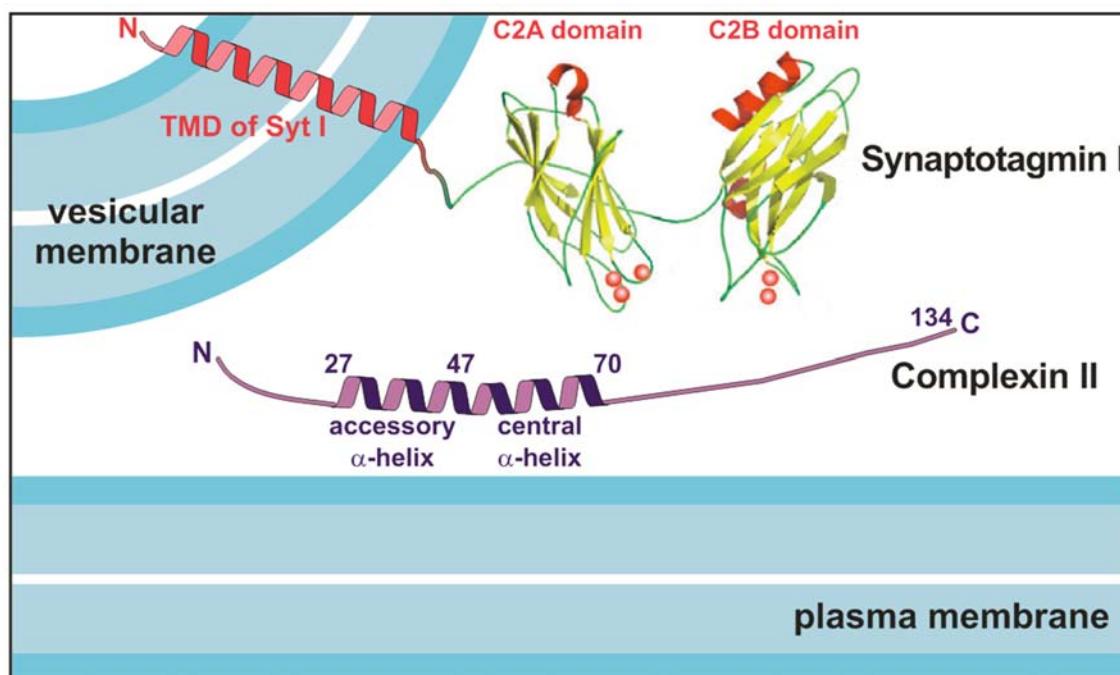


**Fig. 3. SNARE regulators Complexin and Synaptotagmin.** Synaptotagmin is a vesicular protein with a helical Transmembrane Region (TMR) attached to two cytosolic C2 domains. These two domains react to  $\text{Ca}^{2+}$  (showed as red spheres), which is crucial in regulated exocytosis. Complexin is a short cytosolic protein with four domains, i.e., N-terminal, accessory  $\alpha$ -helix, central  $\alpha$ -helix and C-terminal domains. Drawing of Synaptotagmin molecule is taken and modified from Chapman, 2008.



### 1.3.1 Complexin

Since SNARE proteins assemble spontaneously, fast  $\text{Ca}^{2+}$ -triggered fusion necessitates regulatory proteins. Cpxs are among the best characterized SNARE regulators known nowadays. In mammals, Cpx constitutes a family of four proteins, that are small (134 - 160 residues, 15 – 20 kDa), polar (charged) and present in the cytosol (Brose, 2008). Whereas CpxI and CpxII are present in neurons, CpxII has been observed in non-neuronal tissues like chromaffin cells (McMahon et al., 1995; Archer et al., 2002). CpxIII and CpxIV are principally expressed in the retina where they are clearly restricted to ribbon synapses of photoreceptors and bipolar neurons. CpxIII and CpxIV have at the very C terminus a CAAX box (C as cysteine, A as any aliphatic residue and X any residue), which operates as a farnesylation consensus motif (Reim et al., 2005).

Cpx shows weak interaction with Syx and not with Syb and SNAP-25, but tight interaction with the SNARE complex (McMahon et al., 1995). A combined X-ray and NMR study showed the crystal structure of Cpx/SNARE complex. Cpx has a central short  $\alpha$ -helix (23 aa) that binds to the groove between Syb and Syx in the SNARE complex (Chen et al., 2002). The Cpx helix binds in an antiparallel manner in relation to the four helical bundle of SNARE, the N terminus of Cpx faces the C terminus of the SNARE complex (Chen et al., 2002). Mutations of any amino acid in the central  $\alpha$ -helix of Cpx, which interacts with the SNARE complex, prevents Cpx from binding, while the rest of the mutations outside of the SNARE interface do not (Xue et al., 2007). Experiments using deuterium exchange with Cpx and SNARE complex showed that Cpx binding stabilizes the Syb/Syx interface, indicating a critical stage to guarantee efficient and fast neurotransmitter release upon  $\text{Ca}^{2+}$  influx (Chen et al., 2002). These experiments also suggest a model where Cpx binding indeed stabilizes SNARE complex and thus keeping them in a highly fusogenic state (Marz and Hanson, 2002).

The function of Cpx in vesicle fusion has been investigated *in vitro* (liposomes) and in cells of primary cultures and cell lines (e.g., neurons, neuroendocrine cells, PC12 cells,  $\beta$ -pancreatic cells, sperm cells, mast cells). Many experimental approaches have been performed, e.g., overexpression of Cpx, RNAi-knockdown of Cpx expression and

genetic deletion of Cpx. However, the real function of Cpx in the vesicle fusion process has remained unclear, because depending on the cell type, organism or experimental method, Cpx seems to have either facilitatory or inhibitory effect on regulated exocytosis, or both (Brose, 2008).

In particular, knockout studies and investigations on specific mutations have caused conflicting interpretations about the functional role of Cpx. Disturbing Cpx function produces an increase in spontaneous release, which led to the proposal that Cpx acts as fusion clamp that prevents premature exocytosis. Nevertheless, clamping release cannot be the only action of Cpx because several studies reported for a positive role of Cpx in  $\text{Ca}^{2+}$ -triggered exocytosis. In the same line, hippocampal neurons lacking all Cpx isoforms showed reduced spontaneous and triggered release (Brose, 2008). Structure-function analyses emphasized the two-faced effects of Cpx by showing that the very N terminus of murine Cpx is essential for its facilitatory role, whereas the adjacent accessory helix has a mild inhibitory effect (Xue et al., 2007). The N terminus of Cpx is believed to position close to the C-terminus end of the SNARE complex (i.e., the TMD of Syb and Syx) as judged from NMR analysis (Chen et al., 2002). This observation led to the assumption that the N terminus of Cpx interacts with the C terminus of the SNARE complex supporting fusogenicity (Xue et al., 2007; Xue et al. 2010). It has been also shown that after Cpx binds to SNARE complex, its N terminus activates and clamps the force created by SNARE complex assembly (Maximov et al., 2009).

Despite many studies, the role of Cpx is matter of discussion and requires more experiments so as to clarify the real function of this SNARE regulator in vesicle fusion.

### **1.3.2 Synaptotagmin**

Synaptotagmin comprises a family (16 isoforms in mammals, Craxton, 2004) of membrane-trafficking proteins that have an N-terminal transmembrane region (TMR), two C-terminal C2-domains, the C2A and the C2B domain, and a short cytosolic domain that links the TMR to the C2 domains (Südhof and Rizo, 1996). Other proteins, like rabphilin and Doc2s, also have C2A- and C2B-domains. However, they are not

classified in the Syt family, because they lack TMR (Südhof and Rizo, 1996). Syt was discovered in a screen for synaptic proteins and its capability of binding  $\text{Ca}^{2+}$  suggested a role as a  $\text{Ca}^{2+}$  sensor in regulated exocytosis (Brose et al., 1992). However, not all Syts bind  $\text{Ca}^{2+}$ , eight of them have shown  $\text{Ca}^{2+}$ -dependent phospholipid binding, Syt-1, -2, -3, -5, -6, -7, -9, and -10; Syt-1, -2, and -9 (with a role as  $\text{Ca}^{2+}$  sensors for fast release; Xu et al., 2007) and Syt-12 (which does not bind  $\text{Ca}^{2+}$ , but controls release) are localized on synaptic vesicles (Maximov et al., 2006). The other Syts are perhaps sorted to different types of vesicles or to the cell membrane. In Syt-1, the C2A and C2B domains bind two and three  $\text{Ca}^{2+}$  ions, respectively, via similar  $\text{Ca}^{2+}$ -binding sites (Shao et al., 1996; Ubach et al., 1998; Fernandez et al., 2001).

There are conflicting views on the function of Syt in regulated exocytosis. Pioneering electrophysiological observations on Syt-1, studying synaptic responses from isolated pairs of pyramidal neurons (primary culture of mice hippocampus) in whole-cell patch clamp configuration, have shown that the deletion of Syt-1 leads to a loss of synchronous secretion (with low  $\text{Ca}^{2+}$  affinity that facilitates more than 90% of the release), whereas the slow asynchronous component is unchanged (Geppert et al., 1994). At the neuromuscular junction (NMJ) of *Drosophila larvae* lacking Syt, electrophysiological experiments also showed that significant levels of evoked secretion are maintained, but this release was not anymore strongly coupled to the depolarizing stimulus (Yoshihara and Littleton, 2002). These discoveries suggested that Syt is necessary to transform the asynchronous release events into rapidly triggered synchronous secretion. These conclusions are compatible with the idea that another function for Syt could rely on the formation, or stabilization, of a vesicles pool with the capability of being quickly released (Voets et al., 2001). Nonetheless, these results raised numerous questions, including which  $\text{Ca}^{2+}$  sensor mediates efficient, though slow, exocytosis in the absence of SytI (Chapman, 2008).

Various types of exocytosis are driven by  $\text{Ca}^{2+}$ , comprising neuropeptide secretion in neurons, catecholamine-secreting process like in chromaffin cells, mast cell degranulation, and acrosomal exocytosis in sperm. The same Syt variants mediating synaptic vesicle fusion (SytI, SytII, SytIX) seem to be also involved in these types of

exocytosis. Furthermore, SytVII has been reported to serve as a  $\text{Ca}^{2+}$  sensor in neurons and neuroendocrine cells (Südhof, 2011; Schonh et al., 2008). Specially, for chromaffin granule exocytosis,  $\text{Ca}^{2+}$  triggering process appear to be equally regulated by both SytI and SytVII. Only in the absence of both proteins (SytI/VII double ko), the secretion is entirely abolished (Schonh et al., 2008). Indeed, in pancreatic cells (either alfa- or beta cells, releasing glucagon and insulin, respectively) SytVII has emerged as the principal  $\text{Ca}^{2+}$  sensor (Gustavsson et al., 2008, 2009), while SytII is the main variant for mast cell degranulation (Melicoff et al., 2009). In chromaffin cells, Cpx proteins are required cofactors for exocytosis mediated by Syt (Cai et al., 2008). Cpx may bind to the SNARE complex for the following Syt action and this preserved task of both drives, mostly, if not all,  $\text{Ca}^{2+}$ -regulated forms of secretion (Südhof, 2011).

Furthermore, it has been proposed that Syt may well have two different roles in the control of release. An initial model hypothesized that Syt functions as a clamp that hinders SNARE-catalyzed fusion awaiting the  $\text{Ca}^{2+}$  influx (Söllner et al., 1993; Popov and Poo, 1993). If this notion is right, it is predictable that knock-out (ko) of Syt would increase spontaneous synaptic vesicle exocytosis or in general regulated exocytosis. A clamping role was supported by initial investigation of Syt ko in *Drosophila larvae*, where spontaneous SV fusion in NMJ was increased. This finding was independently confirmed by various research groups (Littleton, 1994; DiAntonio and Schwarz, 1994; Mackler, 2002). However, no change was reported from Syt ko mice in frequency of mEPSC in primary hippocampal cells culture (Geppert et al., 1994). Conversely, mouse cortical neurons lacking Syt showed higher mini frequencies (Pang et al., 2006). Hence, it is unclear whether Syt clamps fusion before the  $\text{Ca}^{2+}$  signal.

#### **1.4 Adrenal chromaffin cells as a model system for neuronal exocytosis**

Since the 1960s, it is clear that  $\text{Ca}^{2+}$  is the fundamental trigger for regulated exocytosis (Douglas and Rubin, 1963). However, debates continue due to the limitations to measure local  $\text{Ca}^{2+}$  signals in confined domains that govern exocytosis and the strategies used to measure secretion. Many methods have been developed to study the different pathways involved exocytosis with the  $\text{Ca}^{2+}$  signaling. Several methods

provide benefits and downsides. While various neuronal preparations have been shown to be suitable for studying synaptic vesicle fusion, the small size of the presynaptic release compartment made it inherently difficult to measure the relevant  $\text{Ca}^{2+}$  signal. In contrast, chromaffin cells have been demonstrated as an appropriate model system that permits researchers to study exocytosis with high time resolution to determine a wide range  $[\text{Ca}^{2+}]_i$  with high accuracy. Chromaffin cells are neuroendocrine cells of the adrenal glands, which are placed at the rostral side of the kidneys in mammals. Indeed, chromaffin cells are the endocrine matching part of postganglionic sympathetic neurons and are frequently designated as adrenal paraneurons. Physiologically, upon sympathetic stimulation, chromaffin cells release their substances into the bloodstream in a  $\text{Ca}^{2+}$ -dependent fashion (Stevens et al., 2011). The main molecules are the catecholamines, adrenaline and noradrenaline, which regulates tasks of the autonomous nervous system, like heart rate, blood pressure and the control of glucose levels. The large dense-core vesicles (LDCVs) are the compartments where catecholamines are located (along with other substances like chromogranin or neuropeptide Y, also known as NPY), with spherical shape and size in diameter of  $\sim 150\text{-}200\text{ nm}$  (Borisovska et al., 2005; Stevens et al., 2011). The adrenal chromaffin cell is the preferred model system to closely observe and investigate molecular mechanisms of regulated exocytosis.

The adrenal chromaffin cell has various benefits for assessing vesicle pools. Chromaffin cells, when put in dissociated cultures, are circle-shape cells with a diameter of about  $10\text{ }\mu\text{m}$ , allowing the measurement of LDCVs as a rise in membrane capacitance following stimulation. Therefore, measurements in whole cell patch-clamp configuration and the subsequent exchange of intracellular solution (with NP-EGTA in order to photo-liberate  $\text{Ca}^{2+}$ ) containing in a glass pipette, are relatively easy to achieve. Voltage-clamp permits recordings of capacitance increase reflecting the merge of vesicular membrane to the plasma membrane and can also be simultaneously combined with amperometric measurements representing direct evidence for catecholamines release (Bruns, 2004). Catecholamines are oxidizable molecules, and by the means of amperometry technique is possible to precisely assess the distinct fusion kinetic events with high time resolution (Bruns, 2004). Flash photolysis of caged- $\text{Ca}^{2+}$  in chromaffin cells, that causes synchronized secretion, allows to differentiate vesicle pools that are produced and

modulated by defined proteins over a diverse maturation stages (Sørensen, 2003). With the help of the  $\text{Ca}^{2+}$  chelator NP-EGTA and dyes with high- and low-affinity of  $\text{Ca}^{2+}$  (Figure 4), simultaneous measurements of the capacitance membrane and intracellular calcium concentrations ( $[\text{Ca}^{2+}]_i$ ) can be done in order to study regulated exocytosis in a wide range of  $\text{Ca}^{2+}$  concentrations. Moreover, total internal fluorescence microscopy can also be used to observe and quantify maturation stages such as docking and priming (Becherer et al., 2012). Considering all these advantages, chromaffin cells are an appropriate and suitable system to study  $\text{Ca}^{2+}$ -triggered exocytosis.

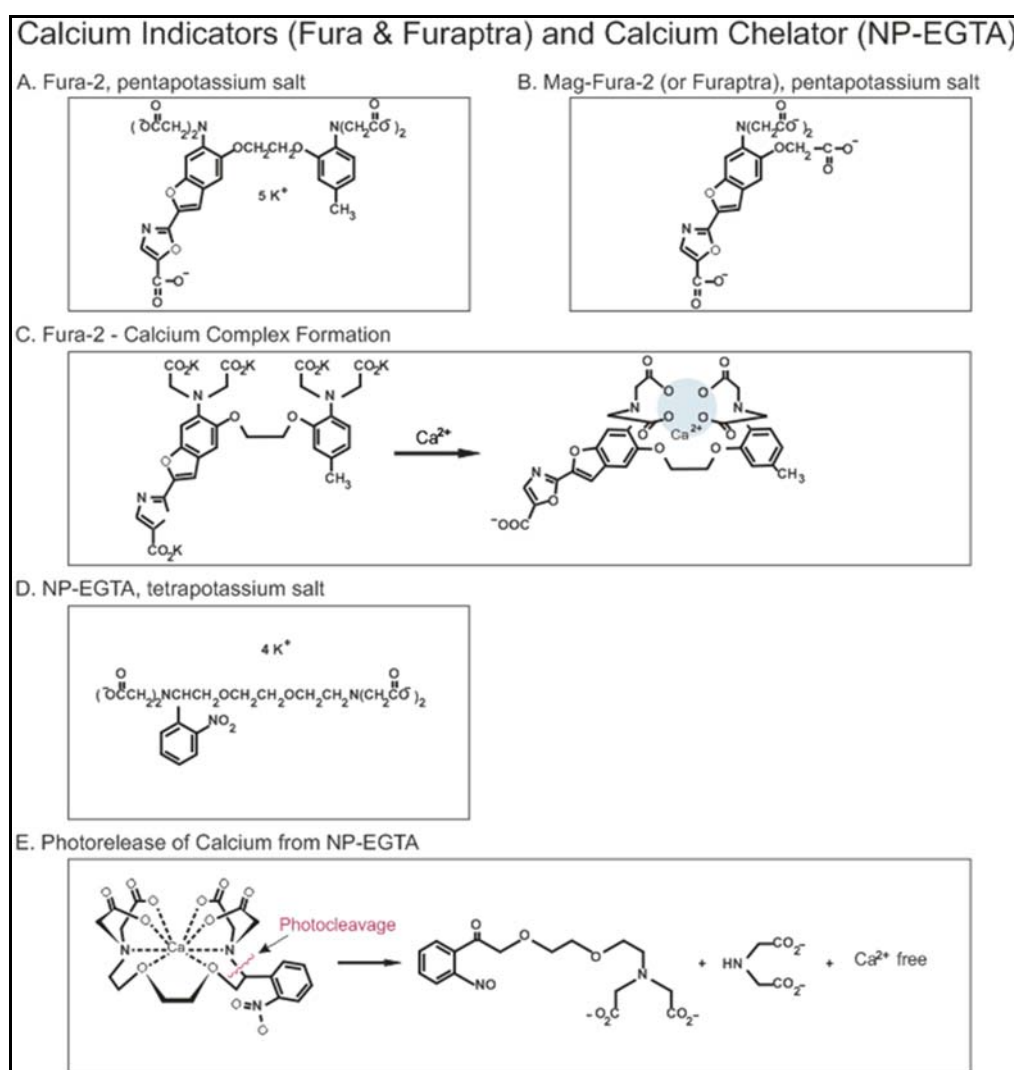


**Fig. 4. Calcium indicators (Fura-2 and mag-Fura-2) and the calcium chelator NP-EGTA.** (A) Structure of the high-affinity  $\text{Ca}^{2+}$  probe Fura-2. (B) Structure of the low-affinity  $\text{Ca}^{2+}$  dye Mag-Fura-2. (C) Formation of the Fura-2- $\text{Ca}^{2+}$  complex. (D) Structure of the  $\text{Ca}^{2+}$  chelator NP-EGTA. (E) Photochemical reaction of the NP-EGTA- $\text{Ca}^{2+}$  complex (Modified from Ellis-Davis and Kaplan, 1994).

### 1.5 Kinetic model of vesicle maturation

Spatial arrangements between  $\text{Ca}^{2+}$  channels and release sites are highly variable in chromaffin cells and stimulation by trains of depolarizations (high  $\text{Ca}^{2+}$  influx through the  $\text{Ca}^{2+}$ -channels) produces secretion, but the release of primed vesicles is not synchronized (Klingauf and Neher, 1997). Alternatively, chromaffin cells can be stimulated by  $[\text{Ca}^{2+}]_i$  that is increased rapidly upon flash photolysis of NP-EGTA, an UV-sensitive  $\text{Ca}^{2+}$ -chelator (Ellis-Davis and Kaplan, 1994), so as to synchronize primed vesicles release. Uncaging of  $\text{Ca}^{2+}$  is accomplished by a brief and strong UV light flash leading to a photolysis of NP-EGTA (Figure 4, E). The cleaved products exhibit a reduced affinity and consequently  $[\text{Ca}^{2+}]_i$  increases rapidly by nearly hundreds of nanomolar to tens of micromolar in a step-like fashion. Using this approach, it has been possible a description of distinct vesicle pools in chromaffin cells (Figure 5), which is possible by simultaneous whole-cell capacitance recordings and flash photolysis of caged  $\text{Ca}^{2+}$  (for review see Rettig and Neher, 2002; Sørensen, 2003).

Two kinetically distinct phases can be seen from a typical wild type chromaffin cell capacitance (Heinemann et al., 1994; Voets et al., 1999). A very rapid phase (known as exocytotic burst) that appears roughly 1 s following flash, exhibiting the LDCVs secretion from the release-ready stage and the later sustained component (generally believed to denote the recruitment of new vesicles to secretion competence or “priming”). Keeping the  $[\text{Ca}^{2+}]_i$  sufficiently high, primed vesicles that undergo fusion give rise to the sustained growth in membrane capacitance. The response ( $C_M$ ) can be fitted by using a double exponential function and a linear component (sustained phase):

$$C_M(t) = A_0 + A_{RRP}(1 - e^{-t/\tau_{RRP}}) + A_{SRP}(1 - e^{-t/\tau_{SRP}}) + kt$$

It has been suggested that fusion reaction of vesicles from the RRP and the SRP relies on cooperative binding of at least three  $\text{Ca}^{2+}$  ions (Heinemann et al., 1994; Voets et al., 2000). This dependence indicates that the fusion rate constant of primed vesicles is low at basal  $[\text{Ca}^{2+}]_i$ , but abruptly rises by augmenting  $[\text{Ca}^{2+}]_i$ , thus enabling the synchronization of secretion.

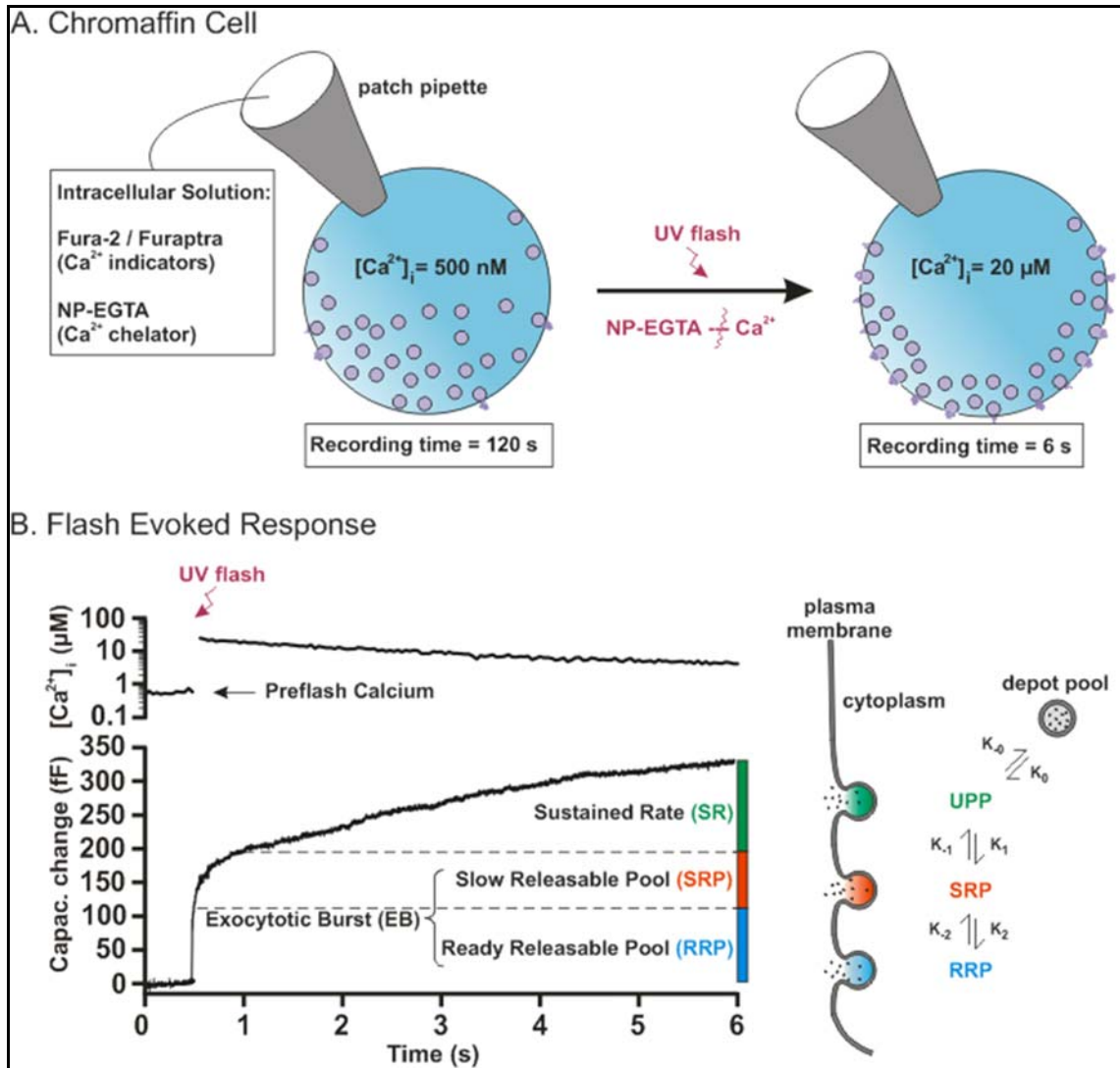


**Fig. 5. Flash photolysis technique on a chromaffin cell and the kinetic model of vesicle maturation.**

(A) Representation of a chromaffin cell (blue sphere) after being loaded (solution containing  $\text{Ca}^{2+}$  chelator and dyes) and the subsequent application of a brief UV flash in order to quickly elevate  $[\text{Ca}^{2+}]_i$ , resulting in synchronous release. (B) A typical trace of a simultaneous measurement of capacitance and  $[\text{Ca}^{2+}]_i$ . Note the rapid increase in the capacitance after the application of the UV flash causing the so-called flash evoked response. It can be fitted by two exponentials and a straight line. Initial burst is fast (blue) with a time constant  $\tau \sim 10\text{-}20 \text{ ms}$  (RRP) followed by slower phase (red) with  $\tau \sim 100\text{-}300 \text{ ms}$  (SRP). Sustained phase (SR, green) is measured as femtoFarad per second (ranges from 5-50 fF/s). Beside the graph, a drawing of the vesicle pools. Vesicles from the depot pool reversibly dock to the plasma membrane establishing a pool of docked, but unprimed vesicles (UPP, green). Docked vesicles reversibly prime in a  $[\text{Ca}^{2+}]_i$ -dependent manner, forming the SRP (red). From the SRP, vesicles either undergo fusion or transit into the RRP (blue). Sequential binding of three  $\text{Ca}^{2+}$  ions triggers fusion of vesicles from the RRP and the SRP. Model modified from Rettig and Neher, 2002.



## 1.6 Aim of the study

$\text{Ca}^{2+}$ -triggered exocytosis of synaptic vesicles at the presynaptic active zone is vital to release neurotransmitters that allow intercellular communication between neurons. Similarly, neuroendocrine cells secrete hormones into the bloodstream in order to produce a response in a specific target organ or group of cells.  $\text{Ca}^{2+}$ -triggered exocytosis depends on an organized chain of events, where some proteins support docking, priming and/or fusion of vesicles with the plasma membrane. SNARE complex and its role in exocytosis have been intensively investigated over the last three decades. However, the functions of regulatory proteins that govern SNARE action to fulfill the speed requirements of  $\text{Ca}^{2+}$ -triggered exocytosis, have remained controversial. The aim of this work is to determine the precise mode of action and potential interplay of SNARE regulator proteins Complexin II (CpxII) and Synaptotagmin I (Sytl) in  $\text{Ca}^{2+}$ -triggered exocytosis. By using single null mutants for CpxII and Sytl, as well as their combined deficiency (double knock-out CpxII/Sytl), this work intends to define the actions of these two proteins on the vesicle release process and clarify to what extent they regulate the  $\text{Ca}^{2+}$ -triggered apparatus. Moreover, by using virus expressing either CpxII protein or its truncated mutants, this work additionally intends to assign specific functions, if so, to particular regions within CpxII protein. Furthermore,  $\text{Ca}^{2+}$ -triggered exocytosis relies not only on protein-protein interactions but also on protein-lipid interactions. Nevertheless, the functional role of SNARE-lipid interactions has remained uncertain. Particularly, it is unknown whether transmembrane domains (TMDs) of SNARE proteins have functions that go beyond passive anchoring of the SNARE-apparatus. This work also aims to delineate the functional role of the SynaptobrevinII (SybII) TMD in  $\text{Ca}^{2+}$ -triggered exocytosis by systematically mutating its core residues (amino acid positions 97-112). This structure-function analysis allows to better understand how crucial properties of the amino acids within SybII-TMD would affect the surrounding lipids of the vesicular membrane. Overall, this work aims to offer new insight into the functions of SNARE regulators and v-SNARE TMD in  $\text{Ca}^{2+}$ -triggered exocytosis.

## 2. Materials and Methods

### 2.1 Materials

All reagents and chemicals were obtained from Sigma-Aldrich (St. Louis, MO, U.S.A.) unless otherwise noted. And all related products (falcon tubes, Petri dishes, six-well plates, etc) were from Life Technologies (Carlsbad, California, U.S.A.).

### 2.2 Transgenic mice

All experiments were performed on mouse chromaffin cells derived from wild-type (wt), ComplexinII ko (CpxII ko), SynaptotagminI ko (SytI ko), ComplexinII/SynaptotagminI double ko (CpxII/SytI dko) and SynaptobrevinII/Cellubrevin (SybII/ceb) double ko of either sex at E17.5–E18.5. Animals were kept according to German Animal Health Care Regulations.

Animals that are genetically deficient for CpxII ko and SytI ko were kindly provided by Drs N. Brose (MPI Göttingen, Germany) and T. Sudhof (Stanford, USA) respectively. From the offspring of heterozygous CpxII or SytI animals, null mutants were obtained at the expected Mendelian ratio. When observed instantly after birth, homozygous, heterozygous, and wt mice are phenotypically impossible to differentiate. However, homozygous mutant SytI mice become gradually weaker and eventually die within few hours (Geppert et al., 1994). Since CpxII ko mice are viable and fertile, it was possible to breed heterozygous SytI mice with CpxII ko in order to get a mouse strain that is heterozygous for both. Then, this mouse strain was bred with homozygous CpxII ko, so that a mouse strain that is heterozygous for SytI and homozygous-ko for CpxII could be generated. This latter was used in order to obtain a novel CpxII/SytI Dko with a normal number of offspring compatible with a Mendelian distribution (Figure 6). Animals that are genetically deficient for both SybII and ceb (from now on named DOKO) were generated as it has previously described Borisovska et al., 2005.

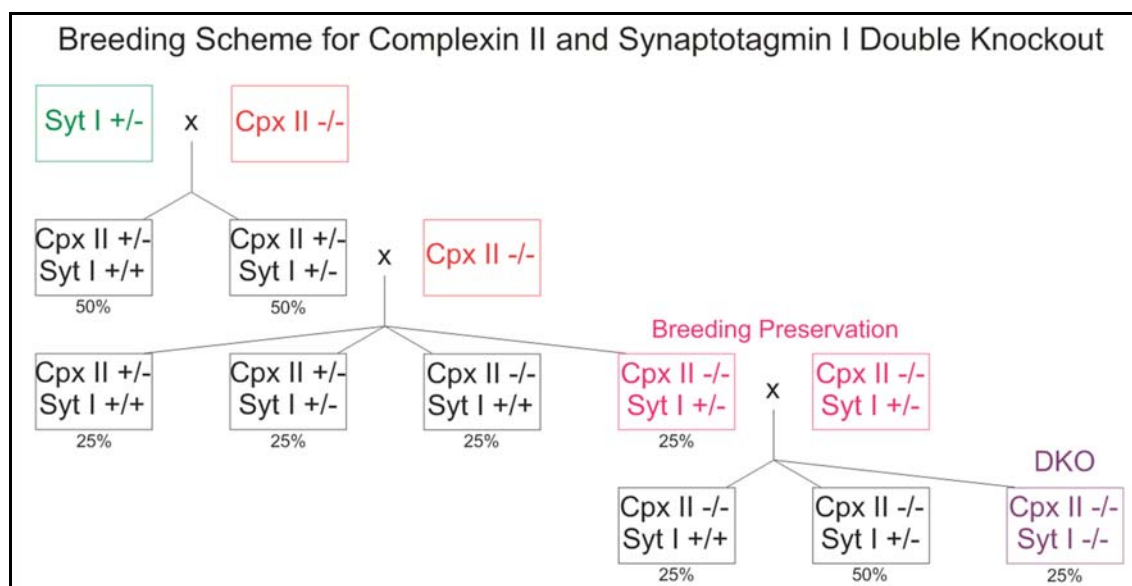


**Fig. 6. Generation of the novel CpxII/SytI Dko.** Breeding scheme depicting how the double ko mouse strain for CpxII and SytI was generated. Because CpxII ko is viable and fertile, it was used to breed with heterozygous SytI to get heterozygous for both CpxII and SytI. Then, this was bred with CpxII ko and heterozygous SytI and homozygous ko CpxII was generated, which was used for breeding preservation to produce continuously CpxII/SytI dko. Mendelian distribution is represented as percentages.

## 2.3 Genotyping

Genotyping was done by PCR in order to determine the genotype of the newborn mice, a rapid method for amplification of a specific DNA fragment using single stranded oligonucleotide primers flanking the regions to be amplified. The procedure as follows:

First, DNA was extracted from the embryonic mouse tails. For CpxII ko, SytI ko and CpxII/SytI Dko (and their respective controls), 1 – 3 mm of the embryonic tails were digested by incubation at 75°C in a solution containing 88 µL DDW (double-distilled water), 10 µL Fast Extract Buffer (KAPPA Mouse Genotyping - Peqlab) and 2 µL Fast Extract Enzyme Buffer (KAPPA Mouse Genotyping - Peqlab). After 15 min digestion, the tails were kept another 15 minutes for inactivation at 95°C. Tubes were then centrifuged on a table top centrifuge at 13000 rpm for 2 min and 1 µL supernatant of each tube containing the DNA was used for PCR reaction. For DOKO, the DNA extraction was different, since it is needed a higher and cleaner amount of DNA in order to amplify and detect better SybII gene. Embryonic tails with length of ~1 cm were

placed in 200  $\mu$ L Eppendorf tubes and put under incubation at 56°C in the shaker for at least 4 hours in 400  $\mu$ L SNET buffer (in mM: 20 Tris-HCl, 5 EDTA, 100 NaCl, 1% SDS) supplemented with 8  $\mu$ L Proteinase K (Quiagen). Tubes were then centrifuged at 13000 rpm for 5 min and 350  $\mu$ L supernatant transferred into a fresh one. Precipitation of DNA was accomplished by adding 350  $\mu$ L isopropanol (100% Merck), and white pellet was visible after 10 min centrifugation at 13000 rpm. Then, supernatant was removed and 400  $\mu$ L ethanol (100% Merck) added in order to wash the DNA. Ethanol was removed and the tubes were kept at 30°C so as to dry the precipitate, and later 100 – 200  $\mu$ L of water (Sigma quality) was added. DNA was dissolved at 30°C for ~1 h on the shaker. Then, tubes were centrifuged on a table top centrifuge at 13000 rpm for 2 min and 1  $\mu$ L supernatant of each tube containing the DNA was used for PCR reaction.

For the PCR reaction, primers were purchased from Eurofins MWG Operon (Ebersberg, Germany) and used at a final concentration 25 pM/ $\mu$ L. Two distinct PCR reactions, one for wt and the other one for the mutant allele, were designed to verify the genotype.

**Tab. 1. PCR for CpxII and SytI.** Ingredients for 1X PCR CpxII and SytI reactions with their respective primer sequences. C: cytosine, G: guanidine, A: adenine, T: Thymidine.

DDW	7.25 $\mu$ L
Green KAPPA Mix	12.5 $\mu$ L
DMSO	12.5 $\mu$ L
MgCl <sub>2</sub>	0.5 $\mu$ L
Fw-Primer (wt and CpxII or SytI mutants)	1.25 $\mu$ L
Rev-Primer (wt and CpxII or SytI mutants)	1.25 $\mu$ L
Fw-Primer CpxII-wt: 5'-CGG CAG CAG ATC CGA GAC AAG-3'	
Rev-Primer CpxII-wt: 5'-GAG AGG GGC ATG AAG TCA AGT CAG-3'	
Fw-Primer CpxII-ko: 5'-CGC GGC GGA GTT GTT GAC CTC G-3'	
Rev-Primer CpxII-ko: 5'-CAG GCA CAC TAC ATC CCA CAA ACA-3'	
Fw-Primer SytI-wt: 5'-GTA TTC AGT GCG TCT CAG AGA C-3'	
Rev-Primer SytI-wt/ko: 5'-AAC TAT AAT TTG TCA CAG GCA TTG CCT TTC A-3'	
Fw-Primer SytI-ko: 5'-GAG CGC GCG CGG CGG AGT TGT TGA C-3'	

**Tab. 2. PCR for SybII.** Ingredients for 1X PCR SybII reactions with its respective primer sequences. SB-buffer (Soriano buffer, in mM: 83 (NH<sub>4</sub>)<sub>2</sub>SO<sub>4</sub>, 335 Tris-HCl, 33.5 MgCl<sub>2</sub>, 25 β-mercaptoethanol), 10XPCR-buffer (in mM: 100 Tris-HCl, pH 8.3 at 25°C; 500 KCl; 15 MgCl<sub>2</sub>; 0.01% gelatin).

SybII wt		SybII mutant	
DDW	18.0 µL	DDW	24.0 µL
SB-buffer	5.0 µL	10XPCR-buffer	3.0 µL
DMSO	2.0 µL	MgCl <sub>2</sub>	0.5 µL
dNTP's	0.5 µL	dNTP's	0.5 µL
Fw-Primer	0.5 µL	Fw-Primer	0.5 µL
Rev-Primer	0.5 µL	Rev-Primer	0.5 µL
Amersham Polymerase	1.0 µL	RedTag Polymerase	1.0 µL
Fw-Primer SybII-wt: 5'-GCC CAC GCC GCA GTA CCC GGA TG-3'			
Rev-Primer SybII-wt: 5'-GCG AGA AGG CCA CCC GAT GGG AG-3'			
Fw-Primer SybII-ko: 5'-CAC CCT CAT GAT GTC CAC CAC-3'			
Rev-Primer SybII-ko: 5'-CAG CAG ACC CAG GCC CAG CG-3'			

**Tab. 3. PCR for Ceb.** Ingredients for 1X PCR ceb reactions with its respective primer sequences.

DDW	20.0 µL
10XPCR-buffer	3.0 µL
MgCl <sub>2</sub>	0.5 µL
dNTP's	0.5 µL
Fw-Primer (wt and ceb mutant)	0.5 µL
Rev-Primer (wt and ceb mutant)	0.5 µL
RedTag Polymerase	1.0 µL
Fw-Primer ceb-wt: 5'-CAG ACT CAC TGA ACC TAT GAG AG-3'	
Rev-Primer ceb-wt/ko: 5'-CTC ACC TGA TAC ATG CAG CAC-3'	
Fw-Primer ceb-ko: 5'-CAG CGC ATC GCC TTC TAT CGC-3'	

For every genotyping, the ingredients depicted in Tables 1, 2 and 3 were carefully mixed on ice and DNA template was added (1.0 µL for CpxII and SytI reactions; 4.0 µL for SybII and Ceb reactions). To amplify the genomic DNA, PCR-programs were performed in a Thermocycler as shown in Table 4.

**Tab. 4. PCR-programs.** Programs for all genotypes, temp.: temperature.

CpxII-wt reaction			CpxII-ko reaction			SytI-wt/ko reaction		
temp.	time	cycles	temp.	time	cycles	temp.	time	cycles
94°C	05:00	41X	94°C	05:00	41X	94°C	05:00	35X
94°C	00:30		94°C	00:45		94°C	00:30	
64°C	00:45		59°C	00:30		60°C	00:45	
72°C	01:00		72°C	01:00		72°C	01:30	
72°C	07:00		72°C	07:00		72°C	10:00	
SybII-wt reaction			SybII -ko reaction			ceb-wt/ko reaction		
temp.	time	cycles	temp.	time	cycles	temp.	time	cycles
95°C	05:00	35X	95°C	04:00	40X	95°C	04:00	40X
95°C	00:50		95°C	00:30		95°C	00:30	
55°C	00:45		60°C	00:30		60°C	00:30	
65°C	01:30		72°C	02:00		72°C	02:00	
65°C	10:00		72°C	10:00		72°C	10:00	

Agarose gel electrophoresis was used to separate DNA fragments from the PCR products of different lengths. The gel was made by using 1.8 g of agarose powder mixed with 100 mL of 1X TAE (Tris-acetate-EDTA) buffer (40 mM TRIS, 20 mM acetic acid and 1 mM EDTA) and then heated in a microwave oven until completely dissolved. Ethidium bromide (final concentration 0.5 µg/mL) was added to the agarose solution to enable visualization of DNA fragments after electrophoresis. After cooling the agarose solution to around 60°C, it was transferred to a casting tray containing sample comb and permitted to become solid at room temperature. Once the gel was solidified, the comb was removed and the gel along with the tray was introduced into the electrophoresis chamber (Bio-Rad) and covered with 1X TAE buffer. DNA samples were then pipetted into the sample wells. The first well was always occupied with 5 µL of 1 kb DNA ladder as standard. The lid and power leads were positioned on the machine and a current was applied. The electrophoresis was done at a voltage of 5 V/cm. The distance DNA has traveled in the gel was adjudicated by observing the migration of dyes in the loading buffer and when adequate migration had followed, the gel was put on an ultraviolet illuminator and photographed (Bio-Rad).

## 2.4 Mouse chromaffin cell preparation

All experiments were executed on chromaffin cells prepared from embryos at developmental stage E-18. Embryos from wt, CpxII ko, SytI ko and CpxII/SytI dko were not phenotypically different, but DOKO animals exhibited an unusual body shape, with a curved look and a shoulder hump (Borisovska et al., 2005), that it is similar with the SybII ko phenotype (Schoch et al., 2001). Despite the gene deficient, embryos showed no developmental changes and the adrenal glands were physically normal. Adrenal glands were quickly prepared under a dissecting microscope and placed in a petri dish containing a drop of Locke's solution (in mM: 154 NaCl, 5.6 KCl, 3.6 NaHCO<sub>3</sub>, 5.6 glucose and 5.0 HEPES, pH 7.3 and osmolality 320 mOsm/kg). The connective tissues adjoining the glands were detached by using fine forceps under a dissecting microscope. Then, the clean glands were treated with Papain (15 units/mL, Worthington, Lakewood, NJ) in a sterile 15 mL-Falcon tube containing 200 µL enzyme solution (50 mg L-Cysteine, 2.5 mL CaCl<sub>2</sub>·2H<sub>2</sub>O of 100 mM and 2.5 mL Na<sub>2</sub>EDTA of 50 mM in 250 mL DMEM-Fisher 1074-8424, pH 7.3 and osmolality 340 mOsm/kg). Falcon tubes were placed in a water bath with gentle shaking for 20 min. incubation at 37°C. Afterwards, solution from every Falcon tube was removed off and 1 mL DMEM was added in order to rinse out the glands. This solution was immediately removed and the enzyme Papain activity was stopped by adding 200 µL of inactivating solution (25 mL fetal calf serum-Fisher, 1066-4083, 625 mg trypsin inhibitor-Fisher, 1077-9414 and 625 mg albumin in 225 mL DMEM, pH 7.3 and osmolality 340 mOsm/kg) and incubating for another 3 min. in the water bath. After inactivation process, solution from every Falcon tube was replaced by 1 mL DMEM without harming the glands in order to rinse them out. 200 µL culture medium (DMEM with penicillin-streptomycin-Fisher VX15140122 and Insulin-Transferrin-SeleniumX-Fisher, 1052-4233, 0.4 mL and 1 mL respectively for 100 mL DMEM) was added and the glands were softly triturated by pipetting up and down until complete dissociation. Then, 1 mL of culture medium was additionally added. 100 µL of the cell suspension was plated on coverslips (diameter 25 mm) and allowed to settle for 30 minutes. 3 mL per well of culture medium was added and the 6-well plates were incubated at 37°C and 9% CO<sub>2</sub>. Cells were used for patch clamp experiments on days 1 – 2 of culture (Figure 7).

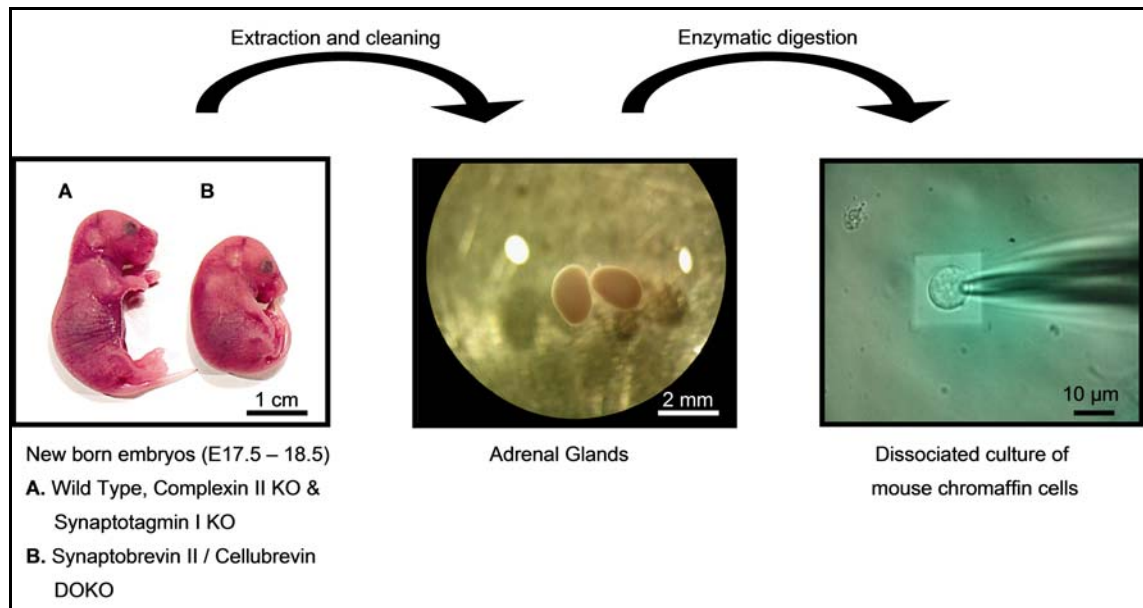


**Fig. 7. Preparation and culturing of embryonic mouse chromaffin cells.** New born embryos were taken and their adrenal glands removed, so as to make a dissociated culture. Embryos were alive, but DOKO died after few minutes and unlike the others (wt, CpxII ko, SytI ko and CpxII/SytI dko), exhibit a tucked posture with hardly movements. Under a dissecting microscope, glands were cleaned of connective tissue, then dissociated, kept at 37°C/9% CO<sub>2</sub> and after two days used for recordings.

## 2.5 Virus production and infection

For expression of the proteins and their mutants (Tab. 5) in chromaffin cells, cDNAs were subcloned into the viral plasmid pSFV1 (Invitrogen, Sand Diego, CA) upstream of an independent open reading frame that encodes for enhanced green fluorescent protein (EGFP). Infected cells were identified by EGFP labeling. Mutant constructs having either amino acids removal or substitutions were generated using the overlapping primer method. DNA sequence analysis (Eurofins MWG Operon, Germany) confirmed all mutations. Semliki Forest Virus (SFV) particles were produced as described previously (Ashery et al., 1999). Concisely, virus cDNA was transcribed in vitro by using SP6 RNA polymerase (Ambion, USA) after linearization with SpeI. Then, BHK21 cells were transfected by electroporation (400 V, 975  $\mu$ F) with a combination of the protein of interest (10  $\mu$ g) and pSFV-helper2 RNA. 15 h incubation (31°C, 5% CO<sub>2</sub>) and virions released into the supernatant were gathered by low speed centrifugation (200 g, 5 min), snap-frozen and stored at -80°C. Infection of cells with virus particles (for ~5.5 h) was done at room temperature on day 2 culture and used for patch clamp recordings.



**Tab. 5. Proteins and their mutants expressed by SFV.** Proteins and mutants (either deletions or replacements) were expressed in chromaffin cells by using SFV gene expression system.  $\Delta C$  and  $\Delta N$  indicate truncated versions of the protein without C-terminal and N-terminal domains respectively. Numbers indicate the position of the amino acids (aa) in the protein. Transmembrane domain (TMD) of SybII (aa 95-112), was either unchanged or some aa substituted. M, L, G, V, C, A indicate methionine, leucine, glycine, valine, cysteine and alanine respectively.

Name		Description
CpxII and their mutants	CpxII	Full length of CpxII protein amino acids 1-134
	CpxII- $\Delta C$	Truncated CpxII amino acids 1-72 (without C-terminus)
	CpxII- $\Delta N$	Truncated CpxII amino acids 28-134 (without N-terminus)
SybII and their mutants	SybII	Full length of SybII protein, amino acids 1-116 TMD unchanged, aa 95-112: MMILGVICAILIIIV
	poly-L	SybII with substitution of 16 amino acids in the TMD MMLLLLLLLLLLLLLLLL
	poly-V	SybII with substitution of 16 amino acids in the TMD MMVVVVVVVVVVVVVVVV
	poly-LV	SybII with substitution of 16 amino acids in the TMD MMLVVLVVLVVLVVLV
	V112A	SybII with substitution of 1 amino acid in the TMD MMILGVICAILIIIA
	V101A	SybII with substitution of 1 amino acid in the TMD MMILGAICAILIIIV
	V101P	SybII with substitution of 1 amino acid in the TMD MMILGPICAILIIIV
	poly-LN	SybII with substitution of 8 amino acids in the TMD MMLLLLLLIIILIIIV
	poly-LC	SybII with substitution of 8 amino acids in the TMD MMILGVICALLLLLLL

## 2.6 Electrophysiology

### 2.6.1 Capacitance recordings

The patch-clamp technique allows to investigate electrical properties of small excitable cells. It was first used to study single ion channel, and later modified for numerous different applications in the cell physiology (Neher and Sakmann, 1976; Hamill et al., 1981), like high time resolution membrane capacitance determination (Neher and Marty, 1982). The generation of a constricted electrical seal (Giga-Ohm range) between the glass pipette tip and the plasma membrane considerably decreases the noise of the recording and allows to investigate a single ion channel action in the electrically secluded membrane patch. This is known as the “cell-attached” configuration. Breaking the membrane patch, underneath the pipette, creates an electrical access inside the cell, a recording mode also referred to as the “whole-cell” configuration. The low access resistance (range to 1 – 10 M $\Omega$ ) provides an excellent control of the cell’s membrane voltage. Additionally, this technique enables a fast exchange of the cytosol with the pipette solution (for instance ions or molecules), which facilitates defined membrane conductances (for details see “Single Channel Recording”, edited by Sakmann and Neher, 1995).

The electrical features of a round-shape cell resemble a plate capacitor ( $C_M$ ) coupled in parallel to a resistor ( $R_m$ , Figure 4). The cell membrane acts electrically as a capacitor with a specific membrane capacitance ( $C_M$ ) of  $\sim 1\mu\text{F}/\text{cm}^2$  (Cole, 1968). Hence, measurements of membrane capacitance faithfully represent changes in the surface cell area due to exo- and endocytosis (Rabl et al., 2005; Yamashita et al., 2005). The experiments performed for this thesis work made use of whole-cell capacitance recordings in order to report chromaffin granule exocytosis.

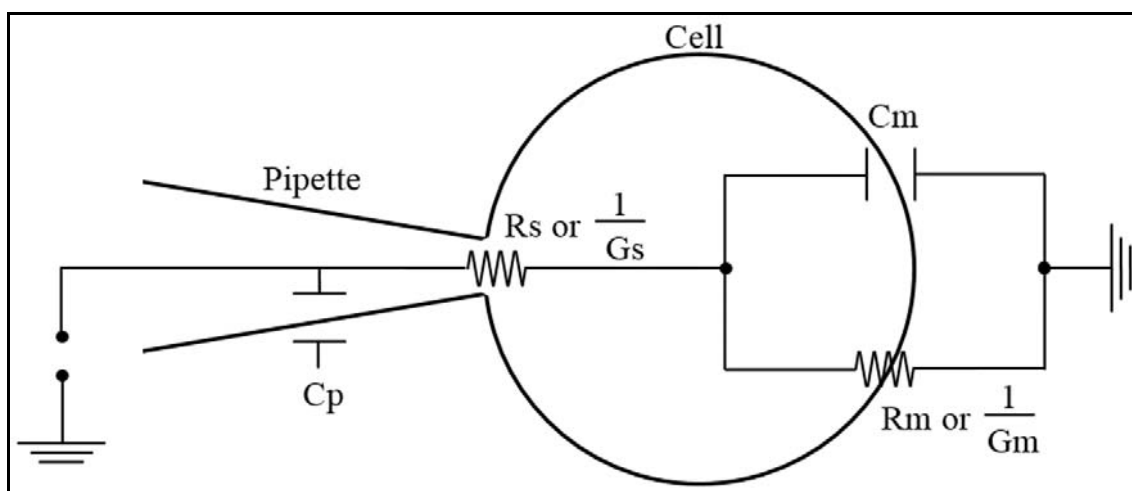


**Fig. 8. “Whole-cell” patch clamp configuration.** A glass patch-pipette is hermetically attached to the plasma membrane, the link between patch-pipette and the cytosol is roughly by access resistance ( $R_s$ )  $\sim 10$  MOhm. The bilayer membrane is identical to a resistor ( $R_m \sim 1$  MOhm) and capacitor ( $C_m$ ) coupled in parallel (known as RC circuit).  $R_m$  is delimited by ion channels and pores in the plasma membrane. Voltage is typically clamped to  $-70$  mV. The drawing exemplifies the minimal corresponding circuit of the cell, patched in the “whole-cell” configuration. Measurements of capacitance cell membrane are feasible with a high-time resolution (Modified from Gillis, 1995).

An alteration in stimulus voltage causes charging of the membrane capacitance. Hence, the current that goes on the cell membrane (capacitor) can be quantified and is proportional to the membrane capacitance. This is the principle in which membrane capacitance recordings are based. A stepwise alteration of the voltage ( $\Delta V$ ) arises in two-component current signal, a first transient current ( $I_c$ ) that decreases exponentially and a constant current ( $I_r$ ). The time course is well defined by the equation:

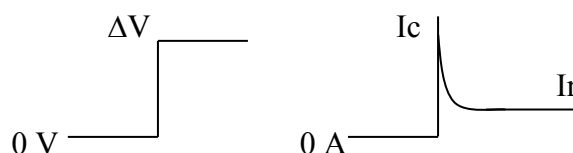
$$i(t) = (I_c - I_r)e^{(-t/\tau)} + I_r,$$

where  $\tau$  refers to the time constant of the decay of  $I_o$  and  $t$  is the time after the voltage application. This equation can be fitted to the current response to get approximations on the circuit parameters showed in Fig. 8 ( $R_s$ ,  $R_m$ ,  $C_m$ ):

$$R_s = \Delta V / I_c$$

$$R_m = (\Delta V - R_s I_r) / I_r$$

$$C_m = \Delta (1/R_s + 1/R_m)$$



This method, even though is simple and relatively easy to understand, has some drawbacks restricting its utility. A precise calculation of  $I_c$  is always difficult to get, due to the filtering of the current and voltage signals. Also, the current peak amplitude estimation is not entirely reliable because of the poorly compensation of pipette capacitance (Fig. 8,  $C_p$ ). Furthermore, the temporal resolution of the capacitance measurement is limited by the time interval between voltage steps being enough to permit the recharging of  $C_M$ . Sinusoidal excitation is the most common stimulation protocol (Gillis, 1995), favored and convenient for high-time resolution capacitance recordings. Upon sinusoidal excitation, the linear circuit (consisting of resistors, capacitors and inductors) outputs a sinusoidal carried signal with altered amplitude and phase.

If a sinusoidal voltage waveform is employed to an RC circuit (in the bilayer cell membrane), the current will be sinusoidal as well, but displaced relative to the voltage input and the subsequent phase alteration is correlated to the capacitance. In other words, a sinusoidal voltage ( $v(t)=V_o\cos\omega t$ , where  $\omega$  is a frequency) is put on an resistor ( $R$ ), thus resulting in a current given by Ohm's law:  $I_R(t) = v(t)/R = (V_o/R)\cos\omega t$ . Consequently, sine wave amplitude of the output current is inversely proportional to the resistance. Once a sine wave is applied across an ideal capacitor, it brings out a  $90^\circ$  phase shift between the applied voltage and the subsequent current:  $I_C(t) = Cdv(t)/dt = -\omega CV_o\sin\omega t$ .

Accordingly, the divergence between input voltage and output current signals, regarding the amplitude and phase, convey the information of the circuit and its electrical properties. Nevertheless, a sine wave gives only two exclusive values (magnitude and phase), that can be used to define the three cell's parameters  $R_s$ ,  $R_m$  and  $C_M$ . On one hand, the "piecewise linear" technique considers that slight changes in  $R_s$  and  $R_m$  have little influence on the estimation of  $C_M$  changes (Neher and Marty, 1982). On the other hand, the "sine wave + DC" technique (extensively performed) employs a DC current along with the stimulus sine wave, thereby rendering a third independent value ( $R_s+R_m$ ; Lindau and Neher, 1988). Evidently, both methods are only suitable for cells that are round and have compact shape, which can be depicted by the simple three-

component electric circuit shown on Fig. 8. In the present thesis work, the “sine wave + DC” method was used to study chromaffin cells secretion.  $R_s$ ,  $R_m$  and  $C_m$  calculation is based on the complex notation (imaginary part of the equations). It requires the phase-sensitive detector lock-in amplifier enabling the calculation of the variables  $R_s$ ,  $R_m$  and  $C_m$  from real and imaginary components of a complex admittance signal (Gillis, 2000). The phase shift (angle) and amplitude (size) of a sine wave are determined from one sine wave period. Value of membrane capacitance is acquired every millisecond when used a 1 kHz stimulation. As a result, the frequency of the used sine wave defines the time resolution of capacitance recordings. The accuracy (signal to noise ratio) of these measurements are influenced by the amplitude of the sine wave, even though it should not be increased significantly in order to avoid activation of voltage-gated channels. Movement of charges throughout gating of voltage-dependent channels causes a variation in specific conductance, which goes along with differences between the measured capacitance and the membrane area (Fernández et al., 1982).

In the present thesis work, DC-holding potential was set to -70 mV, sine-wave stimulus to 1000 Hz and peak-to-peak amplitude to 35 mV. Patch pipettes (borosilicate glass, GC150F10, Harvard Apparatus LTD, Edenbridge, UK) and an EPC-9 patch-clamp amplifier (HEKA, Lambrecht, Germany) were used to perform the whole-cell recordings. Current signals were digitized at 20 kHz and  $R_s$ ,  $R_m$  and  $C_m$  were computed with the use of implemented lock-in unit in the Pulse software.

### **2.6.2 Flash photolysis of caged $\text{Ca}^{2+}$ and calibration curve**

UV-light flash-photolysis of caged  $\text{Ca}^{2+}$  was used to synchronize exocytosis of large dense-core vesicles from isolated mouse chromaffin cells, hence enabling the study of the physiological process of excitation-release coupling. A  $\text{Ca}^{2+}$  cage compound (NP-EGTA, supplied by Dr. Ellis-Davis, MCP Hahnemann University, Philadelphia, PA) was placed into the cell by using patch-pipettes in combination with  $\text{Ca}^{2+}$  indicators (FURA-2 and FuraFura, supplied from Molecular Probes, Eugene, OR), thus continuously observing changes in the intracellular calcium concentration ( $[\text{Ca}^{2+}]_i$ ).

FURA-2 and Fura-2 have different  $\text{Ca}^{2+}$  affinities, which help to supervise the  $[\text{Ca}^{2+}]_i$  changes through an extensive range of concentrations. FURA-2 with the  $K_d$  of 224 nM offers a good resolution in detecting  $[\text{Ca}^{2+}]_i$  lower than 1  $\mu\text{M}$ , while Fura-2 with  $K_d$  of 25  $\mu\text{M}$  allows  $[\text{Ca}^{2+}]_i$  estimations in the micromolar range (subsequent flash application). After binding to  $\text{Ca}^{2+}$ , FURA-2 and Fura-2 display an absorption shift that can be perceived by scanning the excitation spectrum between 300 nm and 400 nm, whereas monitoring the emission at  $\sim 510$  nm (Fig. 9, Grynkiewicz et al., 1985; Konishi et al., 1991).

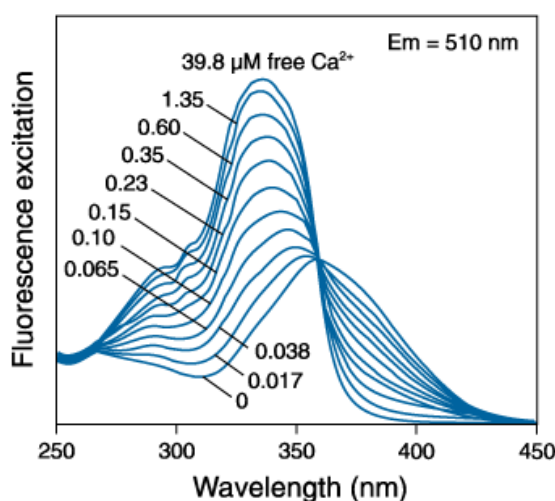


**Fig. 9. Excitation spectra of Fura-2.** Fura-2 in solutions with the specified free  $\text{Ca}^{2+}$  concentrations (0 – 39.8  $\mu\text{M}$ ) determined at emission wavelength 510 nm. Intensity of emission is rising with increasing free  $\text{Ca}^{2+}$  concentrations as excited by wavelength in the range 279–360 nm, but then diminishing in the excitation range of 360–440 nm. Downloaded from Molecular Probes homepage.

In the present thesis work, ratiometric recordings were done by interchanging FURA-2 and Fura-2 fluorescence by fluctuating their excitation at 340/380 nm by means of a quickly switching monochromator (Polychrome IV, TILL Photonics, Planegg, Germany) and emission measured at  $\sim 510$  nm. Calibration of  $[\text{Ca}^{2+}]_i$  were done in vivo employing whole-cell recordings with known calcium concentrations solutions (Fig. 10). Considering that Fura-2 (also known as mag-FURA-2) was initially intended to measure  $\text{Mg}^{2+}$  concentration ( $K_d = \sim 1.9$  mM), calibration solutions were set to have similar free  $[\text{Mg}^{2+}]_i$  of  $\sim 370$   $\mu\text{M}$ . The  $\text{Ca}^{2+}$  chelators, 1,2-bis(2-aminophenoxy) ethane- $\text{N,N,N',N'}$ -tetra acetate (BAPTA) and 1,3-diaminopropane-2-ol- $\text{N,N'}$ -tetra acetate (DPTA), were used in order to buffer the free  $[\text{Ca}^{2+}]_i$  (Table 6, 7, 8).

**Table 6. Ratio 340/380 and Inverted Ratio for solutions containing BAPTA and DPTA.** Solutions containing known  $[Ca^{2+}]_i$  and the ratio R 340/380 experimentally done.

Solutions with:	Free $[Ca^{2+}]_i$ ( $\mu M$ )	Ratio 340/380	1/R
BAPTA	0	0.1170	8.5470
	0.1539	0.2016	4.9603
	0.3016	0.2441	4.0967
	0.4981	0.2818	3.5486
DPTA	4.90	0.3362	2.9744
	19.48	0.4154	2.4073
	61.24	0.6177	1.6189
	104.6	0.7003	1.4280
	353.7	1.2500	0.8000

**Table 7. Scheme for preparation of solutions containing BAPTA.** Solutions containing BAPTA.

Stock solutions (final volume each = 1000 $\mu L$ )							
Sln N°	$Ca^{2+}$ mM	$CaCl_2$ , $\mu L$ 100 mM	BAPTA, $\mu L$ 100 mM	Cs-Glu 4X, $\mu L$	$H_2O$ ddW, $\mu L$	Osmolality	pH
1	0	0	328	267	405	337	7.37
2	13.7	137	328	252	283	334	7.32
3	19.2	192	328	231	249	351	7.33
4	23.0	230	328	224	218	355	7.36

**Table 8. Scheme for preparation of solutions containing DPTA.** Solutions containing DPTA.

Stock solutions (final volume each = 1000 $\mu L$ )									
#	$Ca^{2+}$ mM	$Mg^{2+}$ mM	$CaCl_2$ , $\mu L$ 100 mM	$MgCl_2$ , $\mu L$ 100 mM	DPTA, $\mu L$ 100 mM	Cs-Glu 4X, $\mu L$	$H_2O$ ddW, $\mu L$	Osmolality	pH
1	2.8	6.5	28	35	400	205	302	358	7.36
2	9.0	5.5	90	55	400	195	260	338	7.31
3	20	3.5	200	35	400	182	183	357	7.34
4	25	2.5	250	25	400	175	150	362	7.32
5	35	0.5	350	5	400	163	82	376	7.30

Small fraction (64  $\mu\text{L}$ ) of every stock solution (either containing BAPTA or DPTA) was taken and mixed with both 10X MgATP/Na<sub>2</sub>GTP solution (8  $\mu\text{L}$ ) and 10X Fura-2/Furaptra solution (8  $\mu\text{L}$ ). Osmolality (280 – 320 mOsm/Kg) and pH (7.2 – 7.3) of these solutions were checked out again.

Note: DPTA is a pH sensitive chelator and changes the pH upon binding to Ca<sup>2+</sup>, therefore for all solutions containing DPTA the pH was additionally adjusted with CsOH. Moreover, Furaptra also binds Mg<sup>2+</sup> and for that reason the solutions were adjusted according to the free Mg<sup>2+</sup> concentration by adding MgCl<sub>2</sub>.

As it is shown in the Table 6, the calibration curve was made covering a wide range of [Ca<sup>2+</sup>]<sub>i</sub> by using indicators with different K<sub>d</sub> values.

The ratiometric measurements (380/340) obtained from several experiments for each [Ca<sup>2+</sup>]<sub>i</sub> were plotted in a logarithmic scale and fitted using the following equation:

$$R = R_{\min} - R_1([Ca^{2+}]_i / ([Ca^{2+}]_i + K_{\text{fura}})) - R_2([Ca^{2+}]_i / ([Ca^{2+}]_i + K_{\text{furaptra}}))$$

where, R<sub>min</sub> represents R at [Ca<sup>2+</sup>]<sub>i</sub> = 0 M (30 mM BAPTA, no CaCl<sub>2</sub>), (R<sub>min</sub> - R<sub>1</sub> - R<sub>2</sub>) represents the ratio measured when cells were perfused with the solution containing 10 mM CaCl<sub>2</sub> and no chelator. The parameters estimated after fitting (R<sub>min</sub>=8.6; R<sub>1</sub>=5.7; R<sub>2</sub>=2.5; K<sub>fura</sub>=80.3 nM; K<sub>furaptra</sub>=64.8  $\mu\text{M}$ ) were further used to convert ratiometric signal into [Ca<sup>2+</sup>]<sub>i</sub>.



The  $[Ca^{2+}]_i$  was calculated as follows:

if  $[Ca^{2+}]_i = x$ , then,

$$R = R_{min} - R_1 \cdot x / (x + K_{fura}) - R_2 \cdot x / (x + K_{furaptra})$$

$$R - R_{min} = - R_1 \cdot x / (x + K_{fura}) - R_2 \cdot x / (x + K_{furaptra})$$

$$R - R_{min} = - [(R_1 \cdot x) \cdot (x + K_{furaptra}) + (R_2 \cdot x) \cdot (x + K_{fura})] / [(x + K_{fura}) \cdot (x + K_{furaptra})]$$

$$(R - R_{min}) \cdot (x + K_{fura}) \cdot (x + K_{furaptra}) = - [(R_1 \cdot x) \cdot (x + K_{furaptra}) + (R_2 \cdot x) \cdot (x + K_{fura})]$$

$$(R - R_{min}) \cdot (x + K_{fura}) \cdot (x + K_{furaptra}) + (R_1 \cdot x) \cdot (x + K_{furaptra}) + (R_2 \cdot x) \cdot (x + K_{fura}) = 0$$

$$(R - R_{min}) \cdot [x^2 + x \cdot (K_{fura} + K_{furaptra}) + K_{fura} \cdot K_{furaptra}] + x^2 \cdot R_1 + x \cdot R_1 \cdot K_{furaptra} + x^2 \cdot R_2 + x \cdot R_2 \cdot K_{fura} = 0$$

$$x^2 \cdot (R - R_{min}) + x \cdot (K_{fura} + K_{furaptra}) \cdot (R - R_{min}) + K_{fura} \cdot K_{furaptra} \cdot (R - R_{min}) + x^2 \cdot R_1 + x \cdot R_1 \cdot K_{furaptra} + x^2 \cdot R_2 + x \cdot R_2 \cdot K_{fura} = 0$$

$$x^2 \cdot (R - R_{min} + K_{fura} + K_{furaptra}) + x \cdot [(K_{fura} + K_{furaptra}) \cdot (R - R_{min}) + R_1 \cdot K_{furaptra} + R_2 \cdot K_{fura}] + K_{fura} \cdot K_{furaptra} \cdot (R - R_{min}) = 0$$

and this is a quadratic equation of the form  $ax^2 + bx + c = 0$ , where

$$a = (R - R_{min} + K_{fura} + K_{furaptra}),$$

$$b = [(K_{fura} + K_{furaptra}) \cdot (R - R_{min}) + R_1 \cdot K_{furaptra} + R_2 \cdot K_{fura}] \text{ and}$$

$$c = K_{fura} \cdot K_{furaptra} \cdot (R - R_{min}),$$

which is solved as:  $x = [-b \pm (b^2 + 4ac)^{1/2}] / 2a$

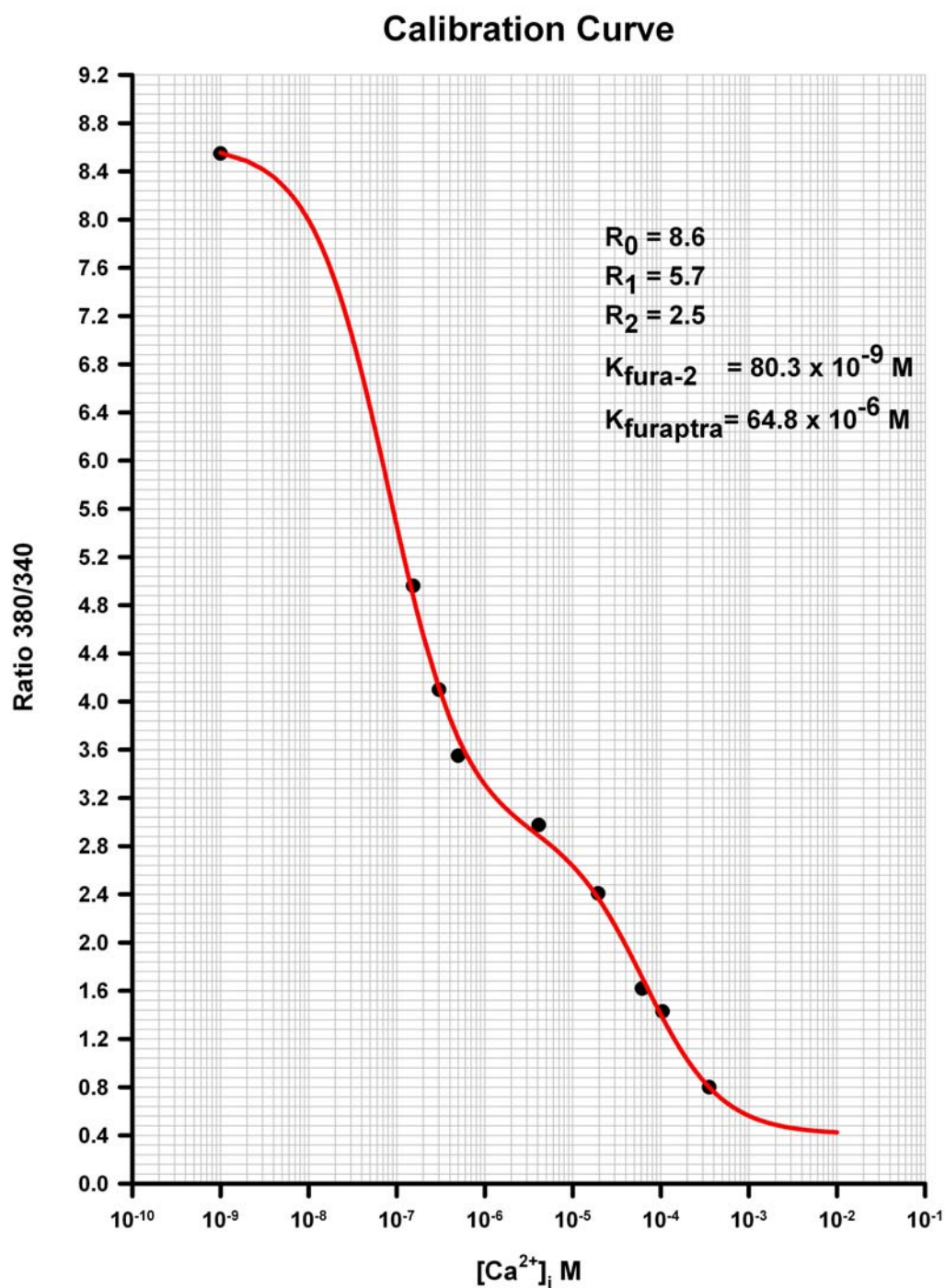


**Fig. 10. Calibration curve.** In Vivo Calibration Curve for a Fura-2-Fura-2 mix. In vivo ratios of the fluorescent signal during illumination at 340 and 380 nm were measured using pipette solutions with  $[Ca^{2+}]_i$  buffered to the indicated concentrations. Inset, the calculated parameters of the fitted curve.

Using this equation, it is possible to successfully determine the  $[Ca^{2+}]_i$  in a wide range and with simultaneously measurements of the capacitance membrane to carefully study stimulus-release coupling in chromaffin cells.

### 2.6.3 Data acquirement and analysis

After days 1 – 2 of culture, coverslips were transferred under laminar flow cabinet into bath solution (extracellular solution, pH 7.3 adjusted with NaOH, osmolality 320 mOsm/kg) containing:

NaCl	140 mM
KCl	4 mM
CaCl <sub>2</sub>	2 mM
MgCl <sub>2</sub>	1 mM
Glucose	30 mM
HEPES	10 mM

Experiments were performed with patch pipettes and an EPC-9 amplifier (HEKA, Lambrecht, Germany). Patch pipettes (GC150F10, Harvard Apparatus, USA) were pulled with a programmable puller (P-87, Sutter Instruments, CA, USA) and heat polished. Tip sizes were 1 – 2  $\mu\text{m}$  and pipette resistances 4 – 6 M $\Omega$ .

Whole-cell membrane capacitance recordings simultaneously with ratiometric measurements  $[\text{Ca}^{2+}]_i$  were done by combining the indicator dyes Fura-2 and Fura-2/AM (Molecular Probes, Eugene, OR), excited at 340/380nm with a monochromator (Polychrome IV, TILL Photonics, Planegg, Germany). Photolysis of NP-EGTA was executed by using a quick discharge of the high-pressure Xenon lamp (Rapp OptoElectronics, Hamburg - Germany). UV-light flash was filtered (UV-3, FT 400, AHF Analysentechnik AG, Tübingen - Germany) and focused into a Zeiss objective (40x, Fluar, 1.3) of an inverted microscope (Axiovert 200, Zeiss - Germany). The epifluorescence lighting structure and UV-light flash were attached via a dual port enclosing a quartz cover slip as a beam splitter. This port permits the passage of approximately 15% of light origin at the side port (for epifluorescence illumination) and ~85% of the light source at the back port (for UV light) regardless of wavelength.

The pipette solution (intracellular solution, pH 7.3, osmolality 310 mOsm/kg) for flash experiments, used for intracellular perfusion of chromaffin cells (approximately for 2 min) before the UV flash, contained:

Cs-glutamate	110 mM
NaCl	8 mM
HEPES-CsOH	20 mM
CaCl <sub>2</sub>	3.5 mM
NP-EGTA	5 mM
Fura-2	0.2 mM
Furaptra	0.3 mM
MgATP	2 mM
Na <sub>2</sub> GTP	0.3 mM

Data were collected by using high time resolution PULSE software (HEKA, Lambrecht, Germany) and lower time resolution X-Chart plug-in module of the Pulse software so as to observe capacitance alterations before and after stimulus (high Ca<sup>2+</sup>) with low time resolution and with high time resolution respectively. Capacitance measurements were completed in accordance with the Lindau–Neher technique (sine wave stimulus: 1000 Hz, 35mV peak-to-peak amplitude, DC-holding potential -70 mV). Current signals were digitized at 20 kHz and membrane capacitance was evaluated with customized IgorPro routines (Wavemetrics, Lake Oswego, OR) Recordings were implemented at room temperature.

The flash-induced capacitance response was approximated with the following function:

$$f(t) = A_0 + A_1(1 - e^{-t/\tau_1}) + A_2(1 - e^{-t/\tau_2}) + kt$$

where  $A_0$  denotes the cell capacitance prior to flash. The parameters  $A_1$ ,  $\tau_1$ , and  $A_2$ ,  $\tau_2$  render the amplitudes and time constants of RRP and SRP, respectively.

### 3. Results

Granule exocytosis in cultured chromaffin cells was synchronized using flash photolysis of caged  $\text{Ca}^{2+}$  (NP-EGTA), and changes in  $[\text{Ca}^{2+}]_i$  were measured with a combination of calcium indicators (Fura-2 and Fura-2/AM). Photolytic “uncaging” of  $[\text{Ca}^{2+}]_i$  leads to a step-like increase in  $[\text{Ca}^{2+}]_i$  that stimulates granule exocytosis in wt cells, which is detected by measuring the membrane capacitance at high time resolution. The secretory response of a wt chromaffin cell to such a stimulus can be roughly divided into two kinetically distinct phases (Heinemann et al, 1994; Voets et al, 1999): an initial phase (also referred to as EB), reflecting the exocytosis of granules from a release-ready state and a subsequent sustained phase that is thought to represent refilling of the just emptied pool by recruitment of new vesicles into the exocytosis-competent state (priming). At high  $[\text{Ca}^{2+}]_i$ , priming is instantly followed by fusion producing a sustained increase in membrane capacitance. At resting levels of  $[\text{Ca}^{2+}]_i$ , the balance between “forward-directed” priming and “backward-directed” depriming reactions should determine the pool size of release-ready vesicles (Voets, 2000; Rettig and Neher, 2002).

#### 3.1 CpxII function in $\text{Ca}^{2+}$ -triggered exocytosis

*In vitro* experiments have shown that SNARE proteins alone are able to cause fusion, although slowly (Weber et al, 1998). Regulatory proteins are needed, like Cpx and Syt, for contribution of the speed and precision of fusion (Carr and Munson, 2007). The high speed of stimulus–secretion coupling in  $\text{Ca}^{2+}$ -triggered exocytosis emerges because synaptic vesicles get accumulated at active zones in a release ready or primed state. At this “priming” stage, the SNARE complexes are partially assembled, but clamped, thus preventing from achieving the vesicle fusion (Wojcik and Brose, 2007). It has been proposed that Cpxs act at a post-priming step, either by keeping a fusogenic state of stable SNARE complexes (Reim et al., 2001; Xue et al., 2007), or by clamping SNARE complexes to hinder fusion. The clamp is released when Syt is activated by  $\text{Ca}^{2+}$  and subsequently binding to the SNARE complex (Schaub et al., 2006; Giraudo et al., 2006; Huntwork et al., 2007).

The function of complexins has been difficult to clarify because of apparently incompatible data. Cpxs have been shown to play a positive and/or negative role in exocytosis. Neurons lacking both CpxI and CpxII exhibited a reduction in synchronous neurotransmitter release (Reim et al., 2001). In contrast, injection of recombinant Cpx into *Aplysia* nerve terminals caused inhibition of evoked neurotransmitter secretion (Ono et al., 1998); additionally, when Cpx peptides binding Syx were microinjected into the presynaptic terminals of giant squid, a clear reduction of evoked neurotransmitter release was observed (Tokumaru et al., 2001). Furthermore, Cpxs possess four domains with different disputed functions (Brose, 2008). In murine neurons, Cpx N-terminal domain is essential for activating fast fusion (Xue et al., 2007; Maximov et al., 2009), however, at NMJ of *C. elegans* has no influence (Hobson et al., 2011; Martin et al., 2011). The accessory  $\alpha$ -helix plays a negative role in *in vivo* studies (Xue et al., 2007; Maximov et al., 2009; Yang et al., 2010), probably by preventing the “zipper” of partially assembled SNARE complexes before the  $\text{Ca}^{2+}$  signal (Giraudo et al., 2009; Krishnakumar et al., 2011; Kummel et al., 2011). The central  $\alpha$ -helix binds to the groove between SyxI and SybII inside the SNARE complex (Bracher et al., 2002; Chen et al., 2002) and is necessary for all Cpx functions (Brose, 2008). The C-terminus binds either to Syt (Tokumaru et al., 2008) or to phospholipids (Malsam et al., 2009; Seiler et al., 2009) and has been proposed either to be inactive (Xue et al., 2007) or to clamp spontaneous fusion (Cho et al., 2010; Martin et al., 2011; Kaeser-Woo et al., 2012). Given these controversies, the present thesis work tries to explain the precise Cpx action in  $\text{Ca}^{2+}$ -triggered exocytosis, clarify to what extent Cpx role is controlled by SytI and fundamental features of Cpx and Syt to fulfill the speed requirements of  $\text{Ca}^{2+}$ -triggered exocytosis.

### 3.1.1 CpxII delimits the extent and kinetics of $\text{Ca}^{2+}$ -triggered exocytosis

Studying the secretion response of CpxII null mutants shows that loss of CpxII strongly reduces the exocytotic burst (EB) component that is commonly detected in response to a step-like increase in  $[\text{Ca}^{2+}]_i$  (Figure 11A). Both components of the EB, the rapid and the slow phases (RRP and SRP, respectively), are equally decreased, but the following sustained rate (SR) remains unaffected (Figure 11C). Fitting of the capacitance response

displays slowdown of the RRP and SRP kinetics (Figure 11D). Normalization of the signals corroborates the changed kinetic properties of the EB (Figure 11B). Additionally, absence of CpxII results in a longer delay between the stimulus and the onset of the secretory response (Figure 11B inset, 11E). Moreover, wt cells expressing CpxII (wt + CpxII) show a larger EB size in comparison with controls expressing GFP (wt + GFP; Figure 11A). Both the RRP and the SRP are considerably augmented, and the SR is diminished (Figure 11C), but no change was observed in the time constants of the EB components (Figure 11D). Accordingly, CpxII is a rate limiting factor for the extent of regulated exocytosis in chromaffin cells. Furthermore, the speed of stimulus–release coupling is severely affected in its absence.

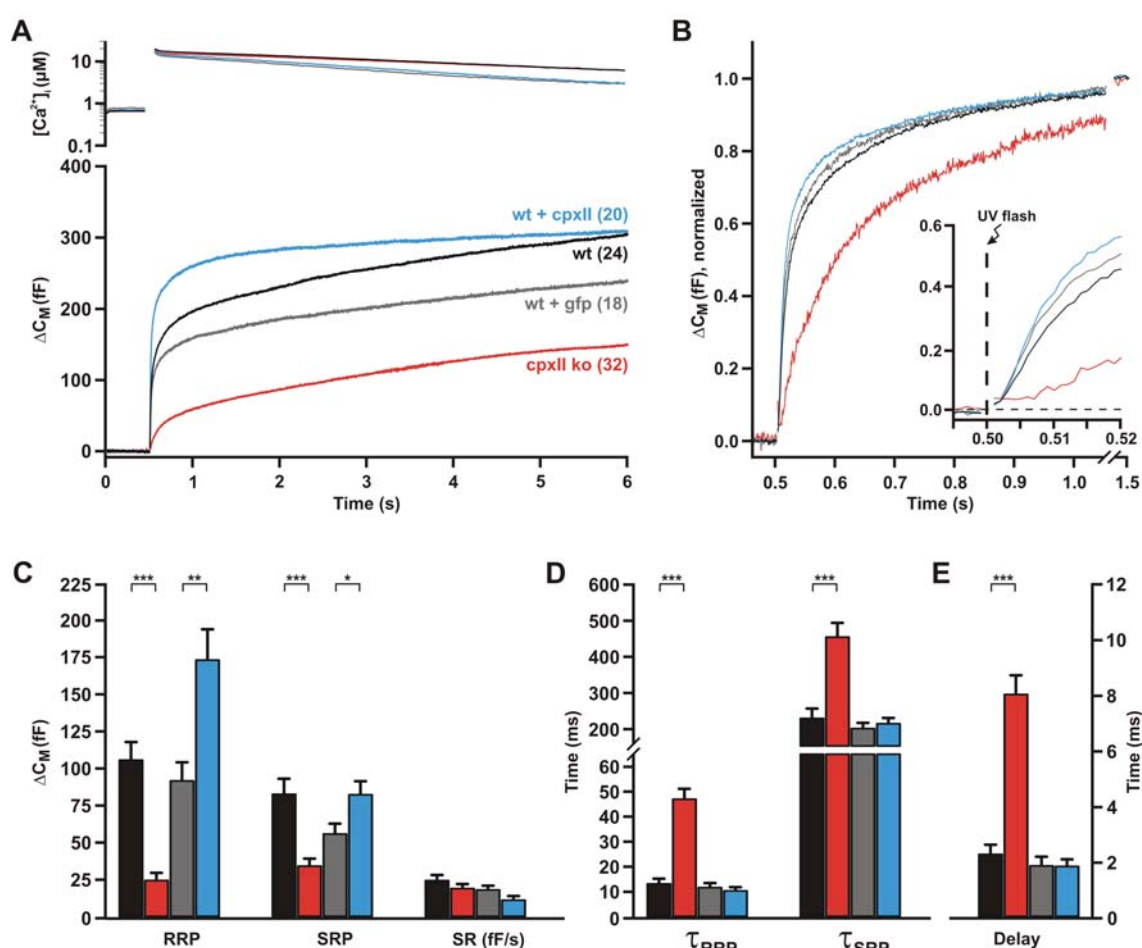


**Fig. 11. CpxII determines magnitude and kinetics of  $Ca^{2+}$ -triggered exocytosis.** (A) Averaged flash-induced  $[Ca^{2+}]_i$  levels (top panel) and corresponding capacitance responses (bottom panel) of wt cells (black; n=24), CpxII ko (red; n=32), and wt cells expressing either GFP (gray, wt + gfp; n=18) or CpxII (blue, wt + CpxII; n=20). Flash is at t=0.5 s. (B) Normalized capacitance signals (as shown in A) of the

exocytotic burst size (0.5 s after the flash) after subtraction of the sustained component. Note the slower release for CpxII ko. The inset shows an extended scaling of the normalized capacitance signals during the first 20 ms after flash (arrow) illustrating the delayed onset of CpxII ko secretion. (C) Quantification of the capacitance in their different components RRP, SRP and SR determined from fitting individual cellular responses (bars with same color code as shown in A). RRP and SRP size are reduced in the absence and increased with overexpression of CpxII. (D) Detailed analysis of the time constants of RRP and SRP revealed that the time course of secretion is higher for CpxII ko. (E) The mean exocytotic delay is also higher for CpxII ko. Error bars represent SEM. \* $p < 0.05$ , \*\* $p < 0.01$ , \*\*\* $p < 0.001$ , Student's  $t$ -test. Figure is taken and modified from Dhara, Yarzagaray et al., 2014.

### 3.1.2 CpxII regulates tonic release of chromaffin granules

Chromaffin cells were perfused with the NP-EGTA (free  $[Ca^{2+}]_i = \sim 500$  nM), in order to facilitate  $Ca^{2+}$ -dependent priming of LDCVs, for 2 minutes prior flash-induced release. Simultaneously, CM, series and membrane conductance as well as  $[Ca^{2+}]_i$  were monitored (Figure 12). Analysis of the preflash recording reveals that during the 2 minutes of the intracellular solution perfusion,  $C_m$  is clearly increased ( $142 \pm 21$  fF,  $n = 32$ ). This increase of  $C_m$ , which has been shown to be associated with granule exocytosis (Borisovska et al, 2012), is considerably higher in the absence of CpxII ( $326 \pm 40$  fF,  $n = 26$ ) and strongly diminished upon expression of CpxII in wt cells ( $16 \pm 27$  fF,  $n = 23$ ; Figure 13A and B), despite similar  $[Ca^{2+}]_i$  (Figure 13D). These results shows that CpxII controls not only the extend of synchronous exocytosis but also governs the tonic release at submicromolar  $[Ca^{2+}]_i$ . When both types of secretion (tonic and synchronous) are analyzed in the very same cells, a correlation is obtained, where the size of the EB is inversely proportional to the foregoing tonic secretion ( $r^2 = 0.94$ ; Figure 13C). Thus, changes in the tonic release determine and directly affect the EB size. Taken together, these results provides strong evidence that CpxII is essential to restrict the vesicle release at submicromolar  $[Ca^{2+}]_i$ , thereby preserving the pool for synchronous secretion.



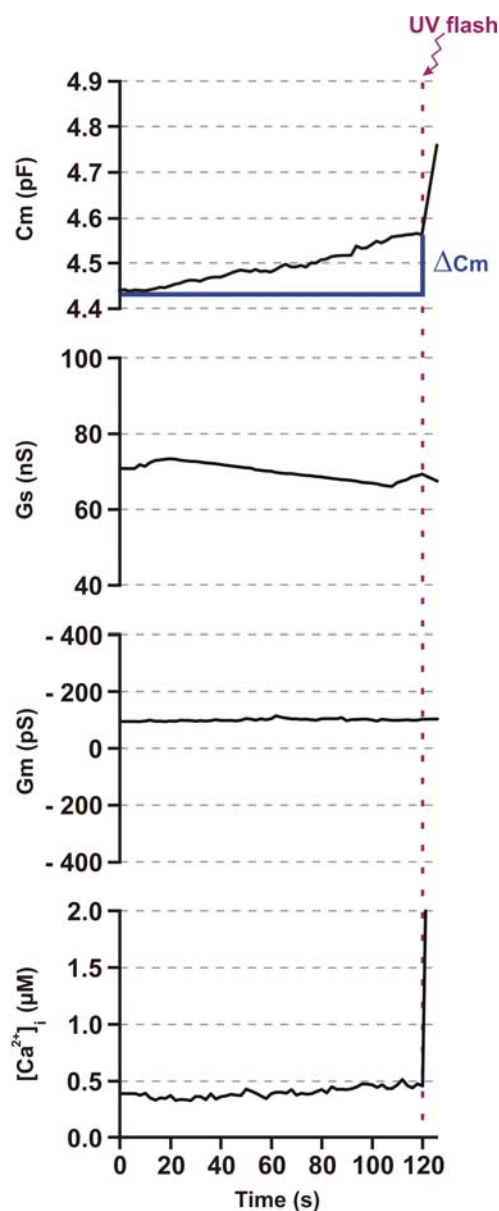


**Fig. 12. Typical recording of electrical properties in a chromaffin cell.** Measurement of cell membrane capacitance ( $C_m$ ), series conductance ( $G_s$ ), membrane conductance ( $G_m$ ), and  $[Ca^{2+}]_i$  during application of submicromolar  $Ca^{2+}$  in about 2 min. (120 s). Note the shallow but steady rise in membrane capacitance ( $\Delta C_m$ ) before the ultraviolet flash (UV, arrow), indicating the exocytosis of chromaffin granules. Figure is taken and modified from Dhara, Yarzagaray et al., 2014.

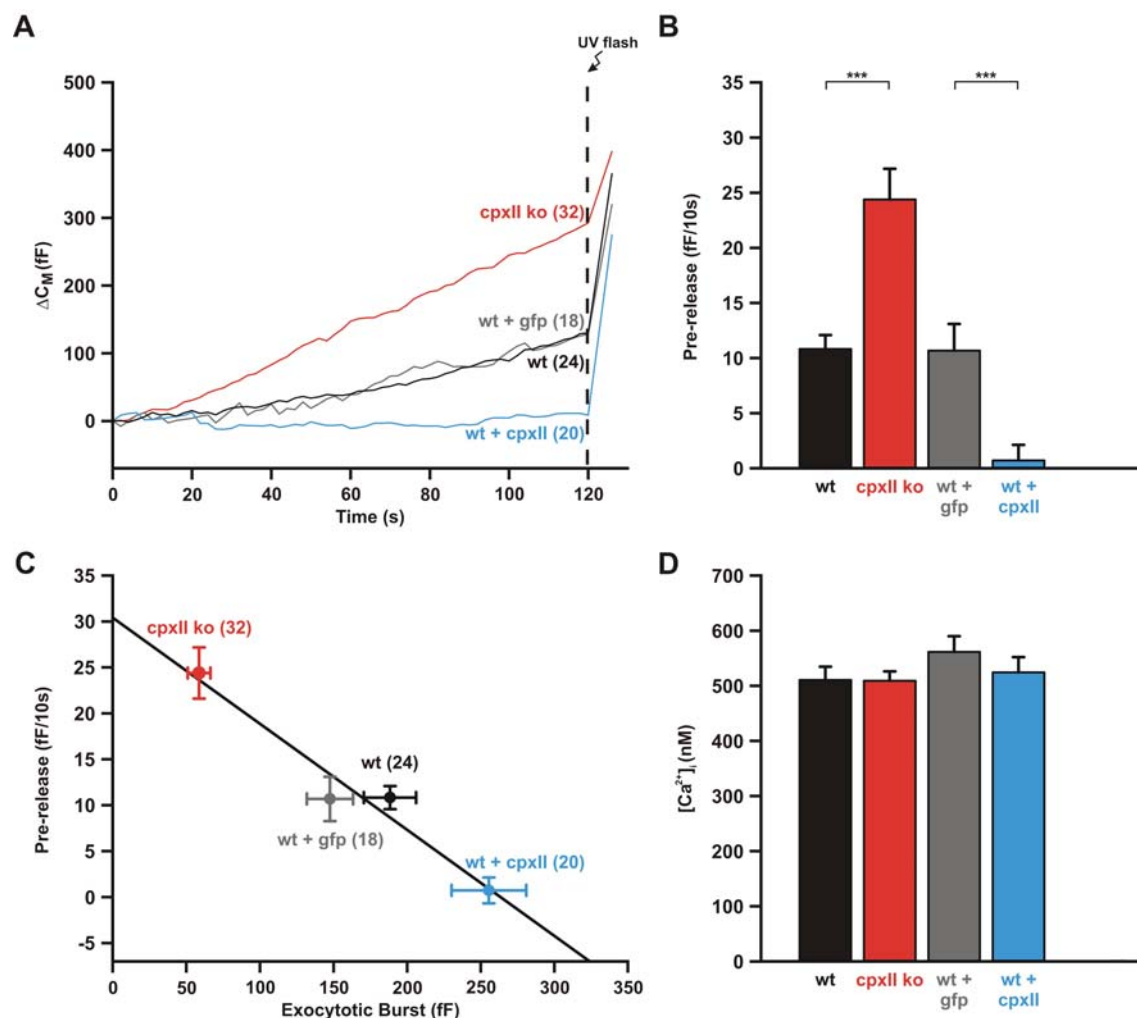


**Fig. 13. CpxII controls tonic secretion of chromaffin granules.** (A) Averaged capacitance responses before and after the  $Ca^{2+}$ -triggered stimulus by the UV-flash (dashed line) for the same group of cells as shown in Fig. 1, wt cells (black; n=24), CpxII ko (red; n=32), and wt cells expressing either GFP (gray, wt + gfp; n=18) or CpxII (blue, wt + CpxII; n=20). (B) Quantification of capacitance responses before flash. Compared with control, loss of CpxII causes a strong increase in capacitance before the flash-evoked response, while it is almost abolished with overexpression of CpxII. (C) Correlation between the release before flash-induced response (y-axis) and the exocytotic burst (x-axis) for the indicated groups. Note that both types of secretion are negatively correlated. (D) Similar submicromolar  $[Ca^{2+}]_i$  levels before flash for the designated groups. Error bars represent SEM. \*\*\* $p < 0.001$ , Student's  $t$ -test. Figure is taken and modified from Dhara, Yarzagaray et al., 2014.

### 3.1.3 CpxII and SytI have different mechanisms on regulated exocytosis

SytI has been described as a  $Ca^{2+}$  sensor for exocytosis (Brose et al., 1992). In its absence, the EB is reduced with an almost abolished RRP and unchanged SRP

component (Figure 14A, C). Furthermore, fusion kinetics were slow, which is consistent with its function as the main  $\text{Ca}^{2+}$  sensor in secretion from chromaffin cells (Voets et al., 2001; Nagy et al., 2006; Schonn et al., 2008; Figure 14B, D and E). The sustained rate (SR), determined as the slope of a line fitted to the  $C_m$  traces between 1.5 and 6 s after flash, was not affected in the null mutant, suggesting that the vesicle supply (forward-directed priming) does not depend on SytI. Additionally, analysis of the preflash  $C_m$  trace shows that SytI ko is similar compared to wt at similar submicromolar  $[\text{Ca}^{2+}]_i$  (Figure 15). Therefore, loss of SytI does not modify tonic secretion, indicating that clamping of premature release is characteristic for CpxII and not a universal attribute of SNARE regulators in chromaffin cells.

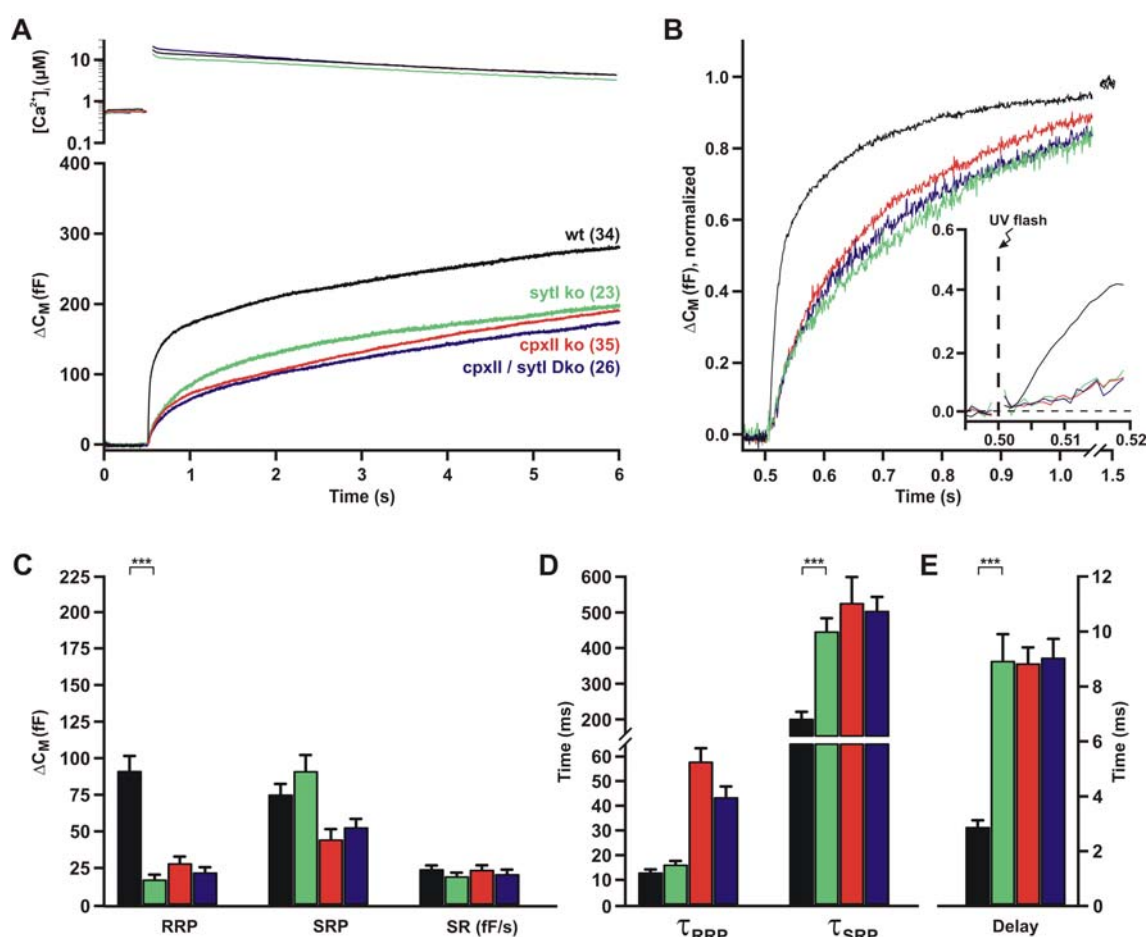


**Fig. 14. Loss of SytI in the absence of CpxII does not further aggravate the CpxII ko phenotype in chromaffin cells.** (A) Mean flash-induced  $[\text{Ca}^{2+}]_i$  levels (upper panel) and corresponding capacitance responses (lower panel) of wt cells (black; n=34), CpxII ko (red; n=35), SytI ko (green; n=23) and CpxII/SytI double ko (purple, n=26). Flash is at t=0.5 s. (B) Capacitance signals (as shown in A) are normalized to the exocytotic burst size (0.5 s after the flash) after subtraction of the sustained component. Note the slower release for all knock out phenotypes. Normalized capacitance signals (inset) during the

first 20 ms after flash (arrow) depicting the delayed onset of CpxII ko, SytI ko and CpxII/SytI double ko secretion. (C) Amplitudes of the two exocytotic burst components (RRP, SRP) and the rate of sustained release (fF/s) for the indicated groups (identical color code as shown in A). Compared with control, the averaged RRP of SytI ko is nearly abolished. CpxII ko and CpxII/SytI double ko appear with both exocytotic burst components reduced. (D) Mean RRP and SRP time constants. SytI ko exhibits a slower SRP. CpxII ko and CpxII/SytI double ko are equally slow. (E) The secretory delay is strongly increased for all knock out phenotypes. Error bars represent SEM. \*\*\* $p < 0.001$ , Student's  $t$ -test.

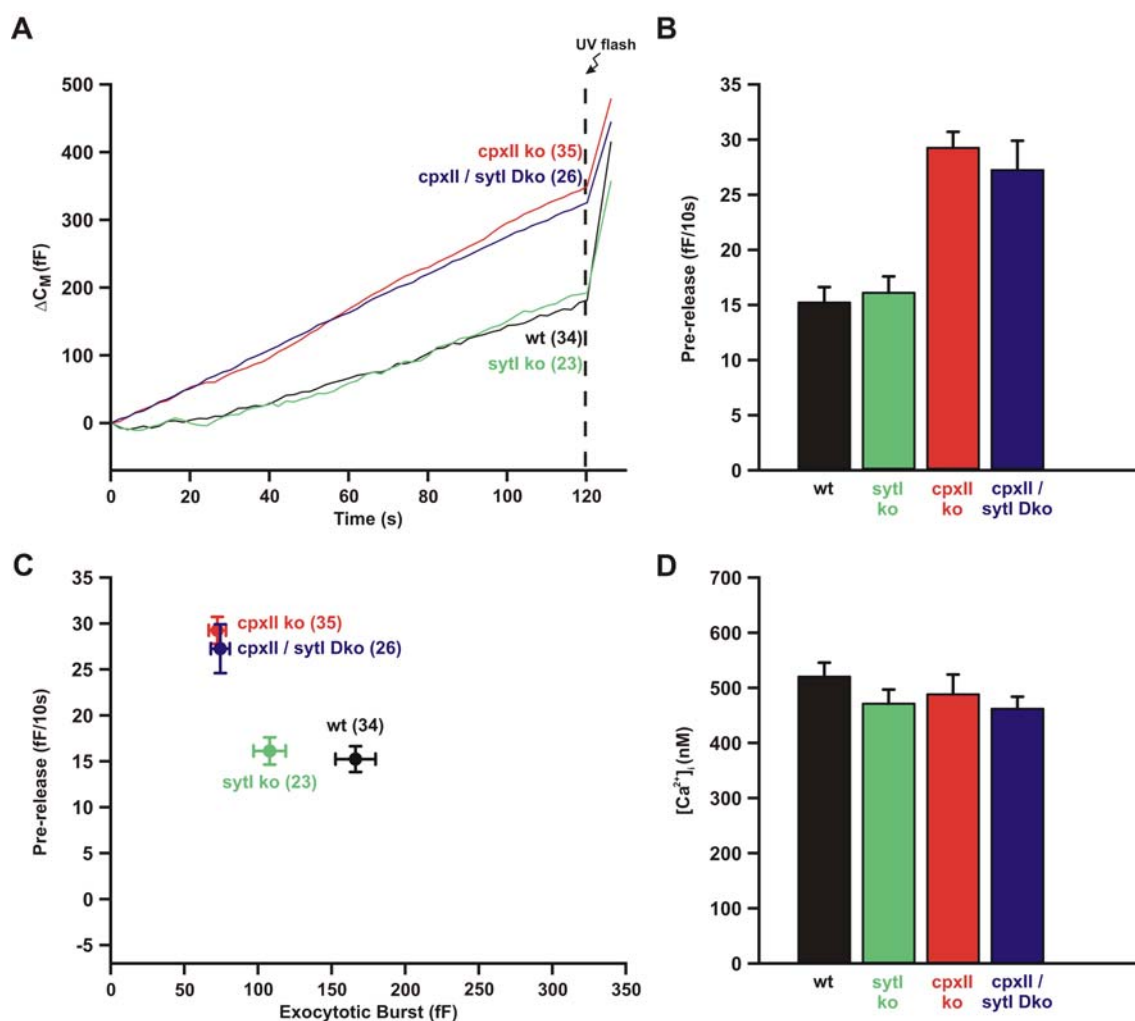


**Fig. 15. Absence of CpxII and not SytI determines the extent of tonic exocytosis.** (A) Mean tonic exocytosis (dashed line illustrates the flash) from the cells shown in Fig. 3, wt cells (black; n=34), CpxII ko (red; n=35), SytI ko (green; n=23) and CpxII/SytI Dko (purple, n=26). (B) Amplitudes of capacitance responses before the high-Ca<sup>2+</sup> stimulus. Loss of SytI exhibits similar response to that of wt cells. CpxII ko and CpxII/SytI dko show a similar high tonic exocytosis. (C) Correlation between the release before flash-induced response (y-axis) and the exocytotic burst (x-axis) for the indicated groups. Note that the additional absence of SytI in CpxII (Dko) does not further change the amplitude of both types of secretion. (D) Similar submicromolar [Ca<sup>2+</sup>]<sub>i</sub> before flash for the indicated groups. Error bars: SEM.

To better understand the functional interplay between CpxII and SytI and whether the remaining evoked secretion of CpxII null mutant could be further aggravated with additional loss of SytI, we took advantage of a novel double knockout mouse (CpxII/SytI dko) that was generated in our lab. Surprisingly, loss of SytI in the absence of CpxII does not additionally aggravate the CpxII ko secretion phenotype. CpxII ko and CpxII/SytI dko evoked-flash responses are nearly identical regarding their magnitudes of the EB components and their kinetic properties of release (Figure 14A, C). Similarly, tonic secretion at similar sub-micromolar  $[Ca^{2+}]_i$  of CpxII ko and CpxII/SytI dko are similar (Figure 15). Several remarks can be outlined from these results:

1. The slow kinetics of the EB components seen with the single null mutants are not additive, since CpxII/SytI dko kinetic properties are not slower than CpxII ko. This might happen because a further slow down of the EB cannot be distinguished from the sustained rate of release. Alternatively, CpxII/SytI dko may affect exocytosis timing by the same molecular mechanism.
2. As discussed before, CpxII ko leads to elevated premature exocytosis at submicromolar  $[Ca^{2+}]_i$ , thereby reducing both EB components (RRP and SRP). Instead, SytI selectively abolishes the RRP component without affecting premature release. Therefore, both SNARE regulators control the magnitude of synchronous secretion by different molecular mechanisms.
3. Unlike SytI ko, CpxII ko leads to loss of vesicles before  $Ca^{2+}$ -triggered exocytosis, therefore absence of CpxII results in the high tonic secretion seen in the CpxII/SytI dko.
4. SytI ko slows down the stimulus-secretion coupling, which can be explained since SytI protein contains  $Ca^{2+}$ -binding domains. However, absence of Cpx also affects exocytosis timing, therefore CpxII must interact (either directly or indirectly) with  $Ca^{2+}$  sensor proteins, since CpxII lacks any  $Ca^{2+}$ -binding domains.
5. Chromaffin cells express two syt isoforms, SytI and SytVII (Schonn et al., 2008). SytI is the major  $Ca^{2+}$  sensor for exocytosis at different  $[Ca^{2+}]_i$ , and can be functionally replaced by sytVII. Therefore, SytVII might support exocytosis at low  $[Ca^{2+}]_i$  in an unperturbed-fashion in SytI ko.

Collectively, these results suggest that both CpxII and SytI play an important role in the magnitude of synchronous secretion and exocytosis timing by different mechanisms, by interacting either with each other or with the SNARE complex. Although, a previous study suggested that these two proteins physically interact (Tokumaru et al., 2008), it is still unclear when and how those interactions occur. Further experiments considering molecular interactions between the proteins are needed to clarify this point.

### 3.1.4 Clamping of premature exocytosis by CpxII does not depend on SytI

Additional experiments were performed by expressing CpxII full-length protein on cells that were deficient either in CpxII or in SytI. These experiments verified the previous findings. Clamping of premature exocytosis depends solely on CpxII and not on SytI.

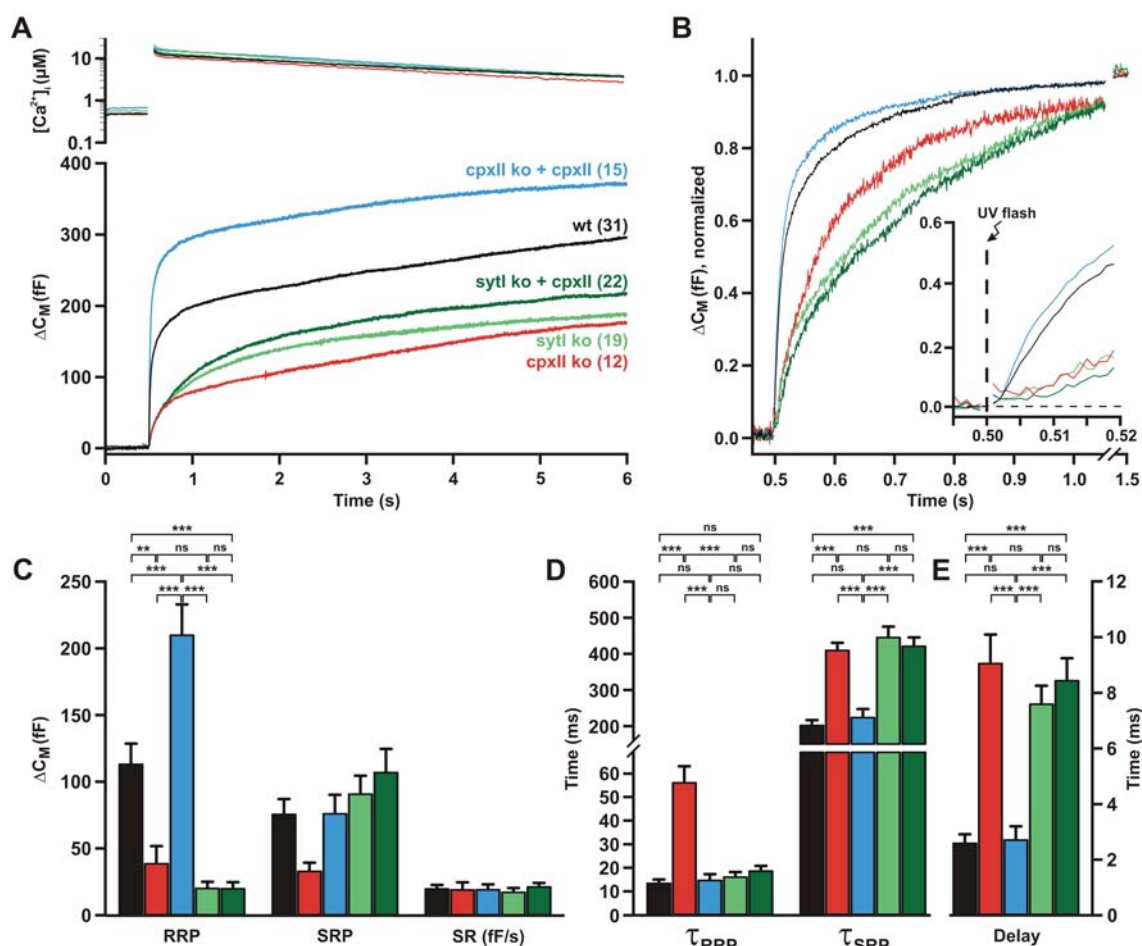


**Fig. 16. Expression of CpxII full-length protein enhances the exocytotic burst and restores the kinetics in CpxII ko cells, but fails to do so in SytI ko.** (A) Averaged flash-evoked  $[Ca^{2+}]_i$  increases (top) and parallel capacitance recordings (bottom) of wt cells (black; n=31), CpxII ko (red; n=12), SytI ko

(light green; n=19) and expression of CpxII full-length protein in either CpxII ko (blue, CpxII ko + CpxII; n=15) or SytI ko (dark green, SytI ko + CpxII; n=22). Flash is at t=0.5 s. (B) Capacitance traces (as shown in A) were scaled to the same amplitude of the exocytotic burst after subtraction of the sustained release, so that comparison of kinetic properties are possible. Note that CpxII ko, SytI ko and SytI ko expressing CpxII are slower. (Inset) Expanded view of the scaled capacitance signals during the first 20 ms after the uncaging flash (arrow). (C) Individual capacitance traces were fitted in order to get information on the pool amplitudes (color code as shown in A). RRP is enhanced and SRP is restored on CpxII ko cells as CpxII is expressed, while on SytI ko cells the expression of CpxII has no effect. (D, E) The fitted data also provides information about the time constants ( $\tau_{RRP}$ ,  $\tau_{SRP}$ ) and exocytotic delay. CpxII, when expressed on CpxII ko cells, “rescues” the kinetics to the wt level, but it is unable to do it as expressed on SytI ko. Error bars: SEM. ns: no significant, \*\* $p < 0.01$ , \*\*\* $p < 0.001$ , one way ANOVA test.

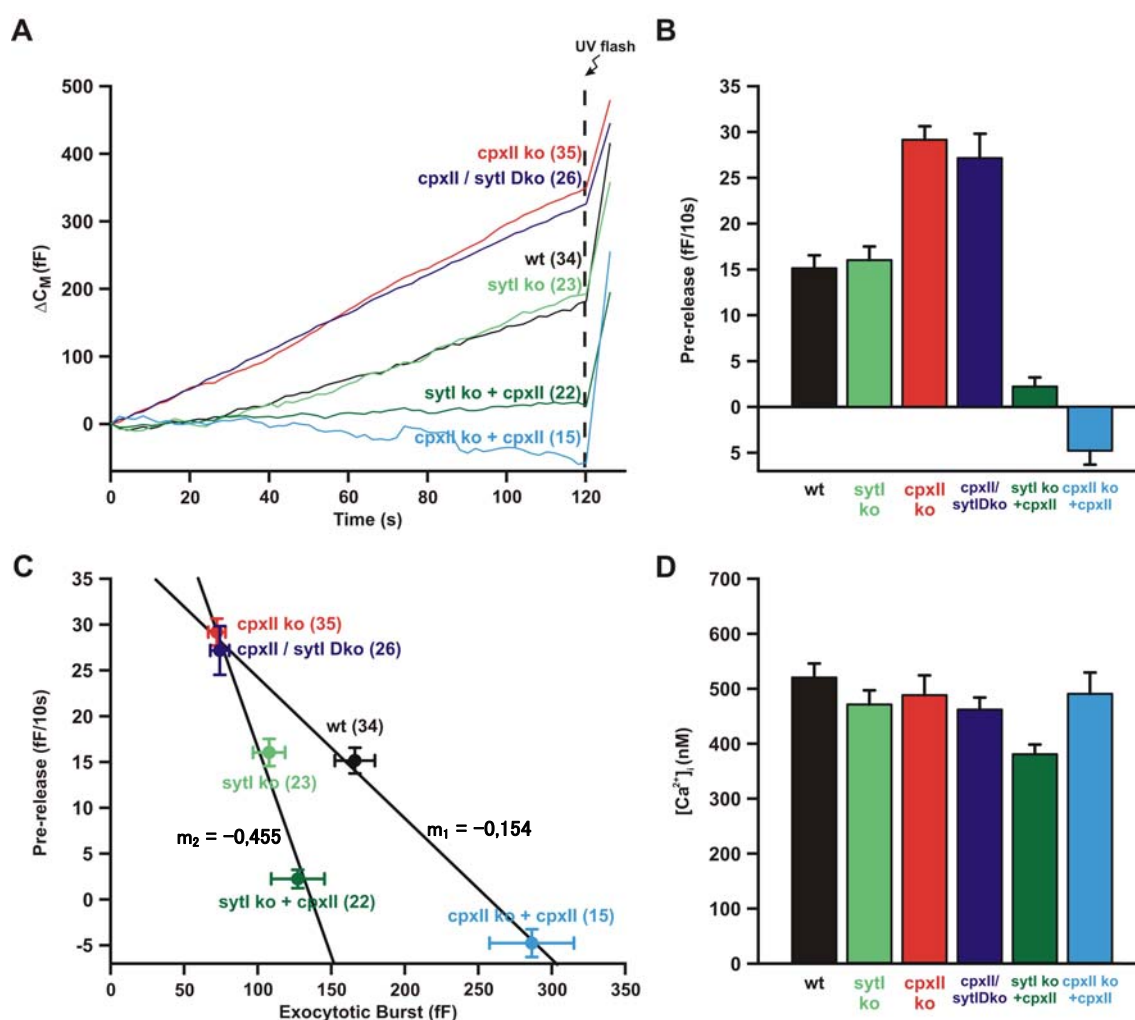


**Fig. 17. Tonic exocytosis clamping accomplished by CpxII does not depend on SytI in chromaffin cells.** (A) Mean capacitance traces before and after the step-like elevation of  $[Ca^{2+}]_i$  (flash at arrow and dashed line) for the same group of cells as shown in Fig. 5, wt cells (black; n=31), CpxII ko (red; n=12), SytI ko (light green; n=19), CpxII/SytI double ko (purple, n=26) and expression of CpxII full-length protein in either CpxII ko (blue, CpxII ko + CpxII; n=15) or SytI ko (dark green, SytI ko + CpxII; n=22).



(B) Size of capacitance responses prior to the flash stimulus. Expression of CpxII full-length protein in either CpxII ko or SytI cells is able to clamp tonic secretion. (C) Correlation between the tonic release (y-axis) and the exocytotic burst (x-axis) for the indicated groups. The two regression lines that correlate the tonic release and EB for CpxII and SytI have slopes of -0.154 and -0.455 respectively, indicating a stronger dependency tonic/EB for CpxII than SytI. Neither the absence of CpxII nor the absence of SytI avoids CpxII protein clamp tonic secretion, although the EB is not enhanced in Syt ko cells. (D) Similar submicromolar  $[Ca^{2+}]_i$  levels before flash for the designated groups. Error bars represent SEM. ns: no significant, \*\*\* $p < 0.001$ , one way ANOVA test.

The results show that the expression of CpxII on CpxII ko cells boosts EB beyond wt levels (Figure 16). Also, it strongly reduces the tonic secretion at similar submicromolar  $[Ca^{2+}]_i$  (Figure 17), showing an identical phenotype when expressed CpxII on wt cells. However, expression of CpxII on SytI ko does not enhance the exocytotic response (Figure 16), but do decrease its tonic secretion (Figure 17). These results confirm that the clamping of tonic secretion by CpxII does not depend on SytI in chromaffin cells.





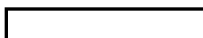
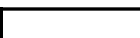
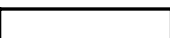
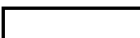
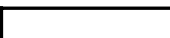
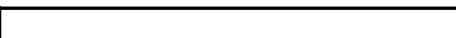
A correlation between premature exocytosis and exocytotic burst of six groups were studied (Figure 17C; wt, CpxII ko, SytI ko, CpxII/SytI dko, CpxII ko+CpxII and SytI ko+CpxII). Two regression lines were determined for CpxII ko, wt and CpxII ko+CpxII (slope -0.154) and for CpxII/SytI dko, SytI ko and SytI ko+CpxII (slope -0.455). The changes in tonic release (y-axes) account for alterations in the size of the EB (x-axes). A related reciprocal (negative slope) dependency was previously described for the first set of experiments with CpxII ko (Figure 13). The results show that CpxII ko supports high tonic secretion and consequently a fewer vesicles released after high- $Ca^{2+}$  stimulus. Wt cells show a balanced release via tonic and synchronous pathway of secretion. Furthermore, expression of CpxII strongly suppresses tonic release with a consequence increase in EB component of synchronous exocytosis. Similarly, presence of CpxII even in the absence of SytI determines the amount of tonic release as seen in CpxII/SytI dko, SytI ko and SytI ko+CpxII, albeit with a shallower slope of -0.455. Presence of CpxII protein in SytI ko hardly restores the EB of synchronous release, suggesting that SytI is the major determinant of  $Ca^{2+}$ -triggered exocytosis. Together, these results show that CpxII controls synchronous release by preventing premature exocytosis, whereas SytI supports synchronous secretion by functioning as the major  $Ca^{2+}$  sensor. Thus, these two SNARE regulators employ two distinct mechanism to govern regulated exocytosis.



### 3.1.5 Distinct domains of CpxII control timing and extent of secretion

NMR analysis has revealed that Cpxs do not show a tertiary structure, but show an  $\alpha$ -helix in the central region of its sequence (approximately 58 aa), while the very end of both N- and C terminus remain unstructured (Pabst et al., 2000). Moreover, a combined X-ray and NMR study has shown that the  $\alpha$ -helical region from amino acid number 48 to 70 binds tightly to the SNARE complex (stoichiometry 1:1) in an antiparallel manner (Chen et al., 2000). Different controversial functions have been assigned to the Cpx domains (see review, Brose, 2008). Motivated by the preceding discoveries, we next examined which CpxII domains control excitation–release coupling and clamp tonic secretion. By using SFV system, we expressed the protein Cpx and truncated mutants in cultured chromaffin cells. Table 9 shows the four domains present in CpxII and the investigated mutants.

**Tab. 9. CpxII domains and its truncated mutants.** Description of the four domains present in CpxII and illustration (boxed) of the expressed full-length protein and mutants.  $\Delta$ C and  $\Delta$ N indicate without C-terminal and N-terminal domains respectively. Numbers specify the place of the aa in the protein.

	N-Terminal Domain aa 1-27	accessory $\alpha$ -helix aa 28-47	Central $\alpha$ -helix aa 48-72	C-Terminal Domain aa 73-134
full length				
$\Delta$ C				
$\Delta$ N				

Remarkably, expression of an N-terminally truncated mutant ( $\Delta$ N mutant, CpxII aa 28–134) in chromaffin cells lacking CpxII greatly restores the EB as observed with CpxII full-length protein expression (Figure 18A). Oppositely, a C-terminally truncated mutant, which does not have the last 62 aa ( $\Delta$ C mutant, CpxII aa 1–72), practically fails to restore the EB. Furthermore, the  $\Delta$ N mutant is incapable to rescue the EB kinetic properties and the delayed onset of secretion, while the  $\Delta$ C mutant restore the kinetic properties in a similar way that CpxII protein does (Figure 18B, D and E). Changes in the protein's ability to clamp exocytosis were observed. The  $\Delta$ N mutant clamps tonic secretion like the wt, whereas the  $\Delta$ C mutant fails to do so (Figure 19).

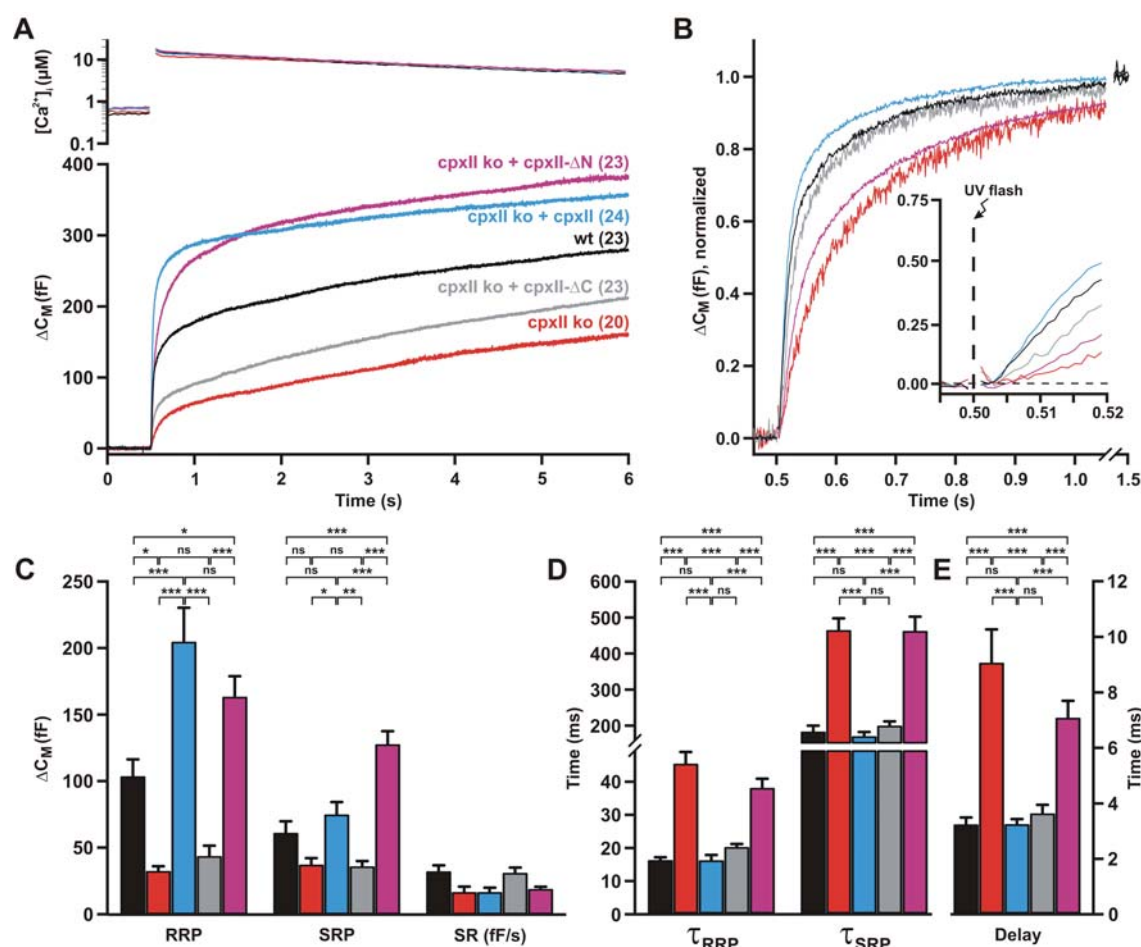


**Fig. 18. C- and N-terminal domains of CpxII control the magnitude and time course of synchronous exocytosis respectively.** (A) Mean flash-evoked  $[Ca^{2+}]_i$  increases (upper panel) and consequent capacitance traces (lower panel) of wt cells (black; n=23), CpxII ko (red; n=20), and CpxII ko expressing either CpxII full-length (blue, CpxII ko + CpxII; n=24), or its truncated mutants (gray, CpxII ko + CpxII- $\Delta C$ ; n=23; magenta, CpxII ko + CpxII- $\Delta N$ ; n=23). Flash is at t=0.5 s. (B) Normalized capacitance responses (as shown in A) of the exocytotic burst size (0.5 s after the flash) after subtraction of the sustained component. The inset displays an extended view of the normalized capacitance signals during the first 20 ms after flash (arrow) revealing the delayed onset of secretion for the indicated groups. (C) Analysis of the size of burst phases (RRP and SRP) and sustained rate of secretion (SR) by capacitance measurements (bars with same color code as shown in A). Exocytotic burst is highly increased when CpxII- $\Delta N$  is expressed as CpxII full-length, but it is not when CpxII- $\Delta C$  is expressed in the same CpxII ko cells. (D) Kinetic analysis of the individual traces revealed that the truncated mutant CpxII- $\Delta C$  is able to restore the kinetics of the CpxII ko to the wt level, while CpxII- $\Delta N$  is not. (E) Mean exocytotic delay for the indicated groups. Error bars represent SEM. \* $p$ <0.05, \*\* $p$ <0.01, \*\*\* $p$ <0.001, one way ANOVA test. Figure is taken and modified from Dhara, Yarzagaray et al., 2014.

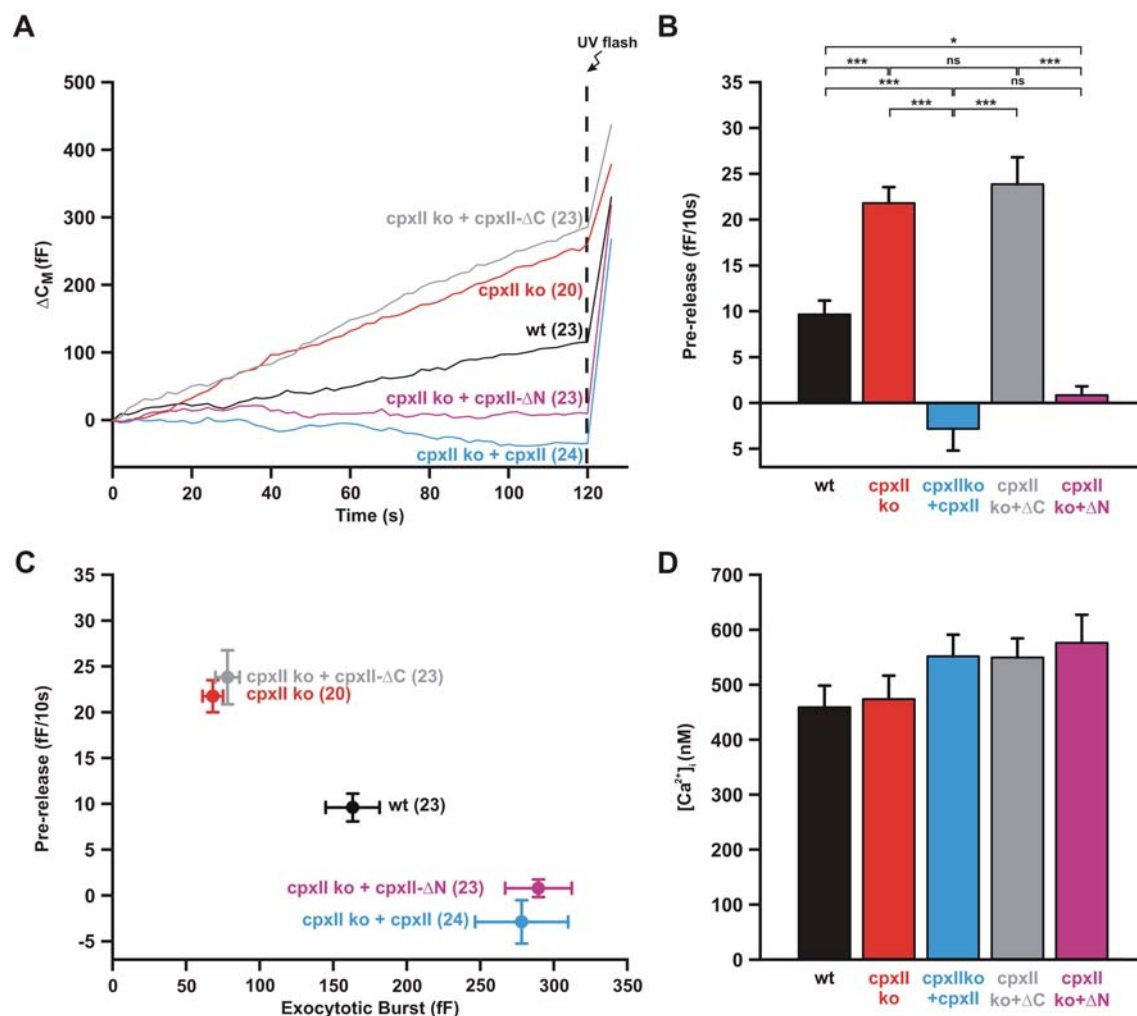


**Fig. 19. Tonic secretion clamping done by CpxII depends on its C-terminal domain.** (A) Averaged capacitance responses before and after the Ca<sup>2+</sup>-triggered stimulus by the UV-flash (dashed line) for the same group of cells as shown in Fig. 7, wt cells (black; n=23), CpxII ko (red; n=20), and CpxII ko expressing either CpxII full-length (blue, CpxII ko + CpxII; n=24), or its truncated mutants (gray, CpxII ko + CpxII-ΔC; n=23; magenta, CpxII ko + CpxII-ΔN; n=23). (B) Amplitudes of capacitance responses before the high-Ca<sup>2+</sup> stimulus. When CpxII-ΔN is expressed in CpxII ko cells, the tonic exocytosis is strongly reduced, but CpxII-ΔC is unable to clamp. (C) Correlation between the tonic release (y-axis) and the exocytotic burst (x-axis) for the indicated groups. Note the similarity between CpxII ko + CpxII-ΔC and CpxII ko, as well as the same pattern for CpxII ko+CpxII-ΔN and CpxII ko+CpxII. (D) [Ca<sup>2+</sup>]<sub>i</sub> levels before flash are not different for the indicated groups. Error bars denote SEM. ns: no significant, \**p*<0.05, \*\*\**p*<0.001, one way ANOVA test. Figure is taken and modified from Dhara, Yarzagaray et al., 2014.

Collectively, the ΔN and ΔC mutant allowed us to separate the two functional defects that were observed in the absence of CpxII. This suggests that different domains of this protein offer distinct and independent roles for Ca<sup>2+</sup>-triggered exocytosis.

### 3.1.6 CpxII mutant protein can outcompete the endogenous protein

To test whether CpxII mutant proteins can compete with the endogenous CpxII and bind to productive SNARE complexes, we repeated these experiments in wt cells. Indeed, comparable results were seen with wt cells expressing the truncated mutant variants.  $\Delta N$  mutant expressed in wt cells caused an enhanced pool of primed vesicles like wt cells expressing CpxII, albeit fusing with slower kinetics. Conversely, the  $\Delta C$  mutant reduced evoked release (with similar EB size that CpxII ko cells exhibit), clearly acting as a dominant negative mutant protein (Figure 20).

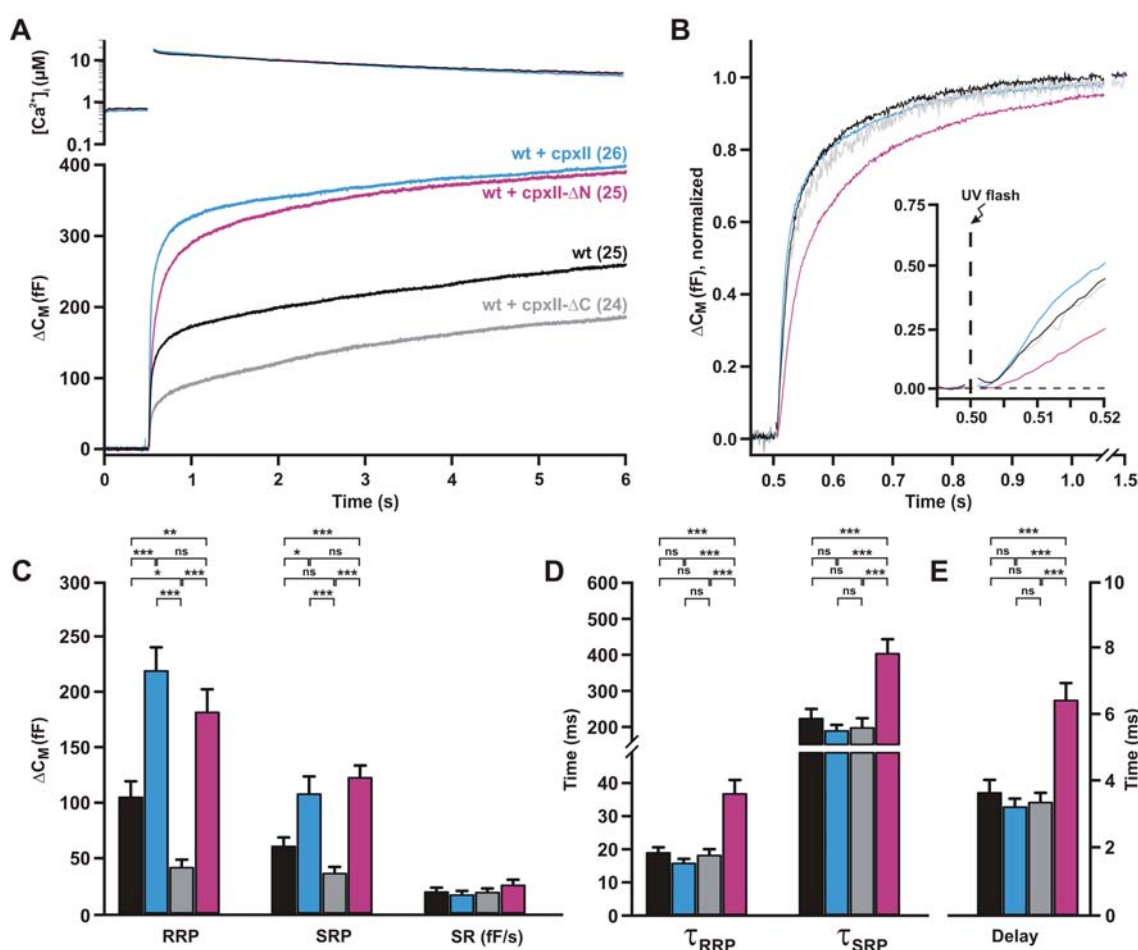


**Fig. 20. Expression in wt cells of either  $\Delta C$ - or  $\Delta N$ -mutant outcompete the endogenous CpxII altering the magnitude and kinetics of secretion.** (A) Averaged flash-induced  $[Ca^{2+}]_i$  levels (top panel) and corresponding capacitance responses (bottom panel) of wt cells (black; n=25), and wt cells expressing either CpxII full-length (blue, wt + CpxII; n=26), or its truncated mutants (gray, wt + CpxII- $\Delta C$ ; n=24; magenta, wt + CpxII- $\Delta N$ ; n=25). Flash is at t=0.5 s. (B) Normalized capacitance signals (as

shown in A) of the exocytotic burst size (0.5 s after the flash) after subtraction of the sustained component.  $\Delta N$ -mutant is able to slow down the response. The inset shows an extended scaling of the normalized capacitance signals during the first 20 ms after flash (arrow) showing the delayed onset of secretion for wt + CpxII- $\Delta N$ . (C) Amplitudes of the two exocytotic burst components (RRP, SRP) and the rate of sustained release (fF/s) for the indicated groups (identical color code as shown in A).  $\Delta N$ -mutant boosts the exocytotic burst as seen with CpxII full-length protein, whereas  $\Delta C$ -mutant strongly reduces it. (D) Detailed analysis of the time constants of RRP and SRP revealed that the time course of secretion is higher for wt + CpxII- $\Delta N$ . (E) Mean exocytotic delay for the indicated groups showing the higher result for wt + CpxII- $\Delta N$ . Error bars represent SEM. \* $p < 0.05$ , \*\* $p < 0.01$ , \*\*\* $p < 0.001$ , one way ANOVA test. Figure is taken and modified from Dhara, Yarzagaray et al., 2014.

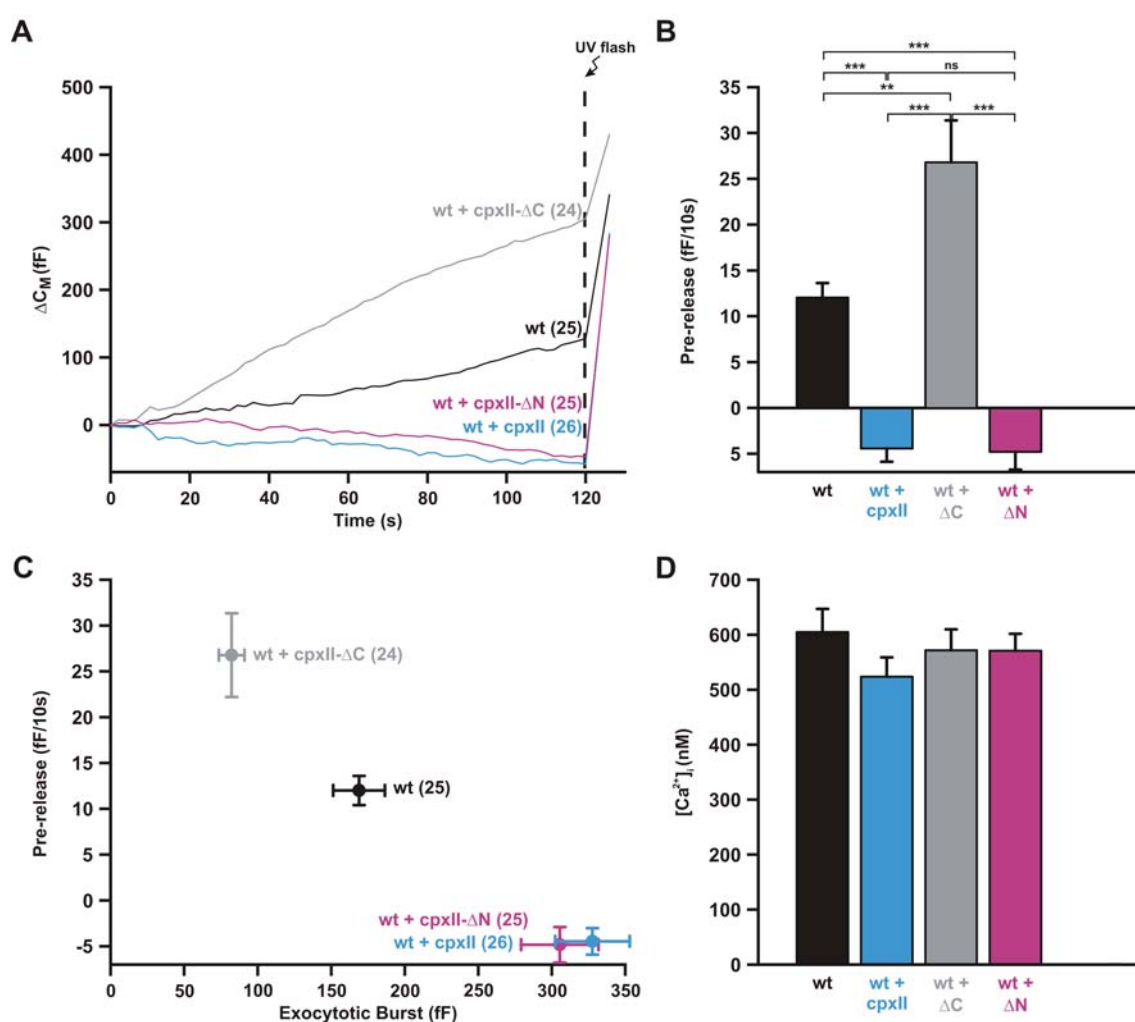


**Fig. 21. The  $\Delta C$ - and  $\Delta N$ -mutant change the tonic secretion beyond levels recorded in wt cells, rising it and lowering it respectively.** (A) Averaged capacitance responses before and after the  $Ca^{2+}$ -triggered stimulus by the UV-flash (dashed line) for the same group of cells as shown in Fig. 9, wt cells (black; n=25), and wt cells expressing either CpxII full-length (blue, wt + CpxII; n=26), or its truncated

mutants (gray, wt + CpxII- $\Delta$ C; n=24; magenta, wt + CpxII- $\Delta$ N; n=25). (B) Quantification of capacitance responses before flash. The truncated mutant  $\Delta$ N is able to clamp the tonic exocytosis and  $\Delta$ C is able to increase it, changing in both cases the wt response. (C) Correlation between the tonic release (y-axis) and the exocytotic burst (x-axis) for the designated groups. The higher the tonic release, the lower the exocytotic burst for wt + CpxII- $\Delta$ C and vice versa for wt + CpxII- $\Delta$ N. (D)  $[Ca^{2+}]_i$  levels before flash are not significant different for the indicated groups. Error bars represent SEM. ns: no significant,  $**p<0.01$ ,  $***p<0.001$ , one way ANOVA test. Figure is taken and modified from Dhara, Yarzagaray et al., 2014.

In the same line, the  $\Delta$ C mutant unclamps tonic secretion at submicromolar  $[Ca^{2+}]_i$  before the UV flash, whereas the  $\Delta$ N mutant hinders premature exocytosis like the wt protein. The direct systematic comparison of tonic secretion and exocytotic burst further corroborates the dependency of the EB size on the extent of preceeding premature exocytosis at submicromolar  $[Ca^{2+}]_i$  (Figure 21). Overall, these results confirm the different phenotypes of the mutant proteins as observed on CpxII null mutant cells.

### 3.1.7 N terminus of CpxII rises the $Ca^{2+}$ affinity of secretion

Timing of fusion events is fundamentally determined by the kinetics of  $Ca^{2+}$  binding to SytI, which functions as the main  $Ca^{2+}$  sensor for exocytosis of chromaffin granules (Voets et al., 2001; Nagy et al., 2006). Accordingly,  $[Ca^{2+}]_i$  changes induced by flash firmly affect the time course of stimulus secretion coupling (Figure 22A). Slower kinetic properties are evidently seen with the truncated  $\Delta$ N mutant expressed on CpxII ko cells compared to control (CpxII protein expressed on CpxII ko cells), when evoked responses are evaluated at different  $[Ca^{2+}]_i$ , especially at low level (Figure 22B and C).

To study this phenomenon in detail, we analyzed secretion over a wide range of  $[Ca^{2+}]_i$  (from  $\sim 5 \mu M$  to  $\sim 70 \mu M$ ) to assess the rates of RRP and SRP, as well as the secretory delay. As shown in Figure 22, a clear difference is observed between  $\Delta$ N mutant and its respective control. The  $\Delta$ N mutant promotes lower rates for RRP and SRP secretion (factor of  $\sim 2$ ). Furthermore, the onset of release is correspondingly longer over the whole range of  $[Ca^{2+}]_i$  (Figure 22D, E and F). Taken together, these results demonstrate that the N terminal domain of CpxII speeds up the RRP and SRP fusion rate and reduces the secretory delay in a  $Ca^{2+}$ -dependent manner. Such alterations of RRP and

SRP fusion rate and delay across a wide range of  $\text{Ca}^{2+}$  concentrations with the  $\Delta\text{N}$  mutant are indicative of a diminished  $\text{Ca}^{2+}$  affinity of synchronous exocytosis.

Evidently, CpxII plays a dual role in fast  $\text{Ca}^{2+}$ -triggered exocytosis in chromaffin cells. CpxII increases the extent of regulated exocytosis by hindering the tonic release pathway (C terminal domain) and independently increases the  $\text{Ca}^{2+}$  affinity of synchronous secretion (N terminal domain).

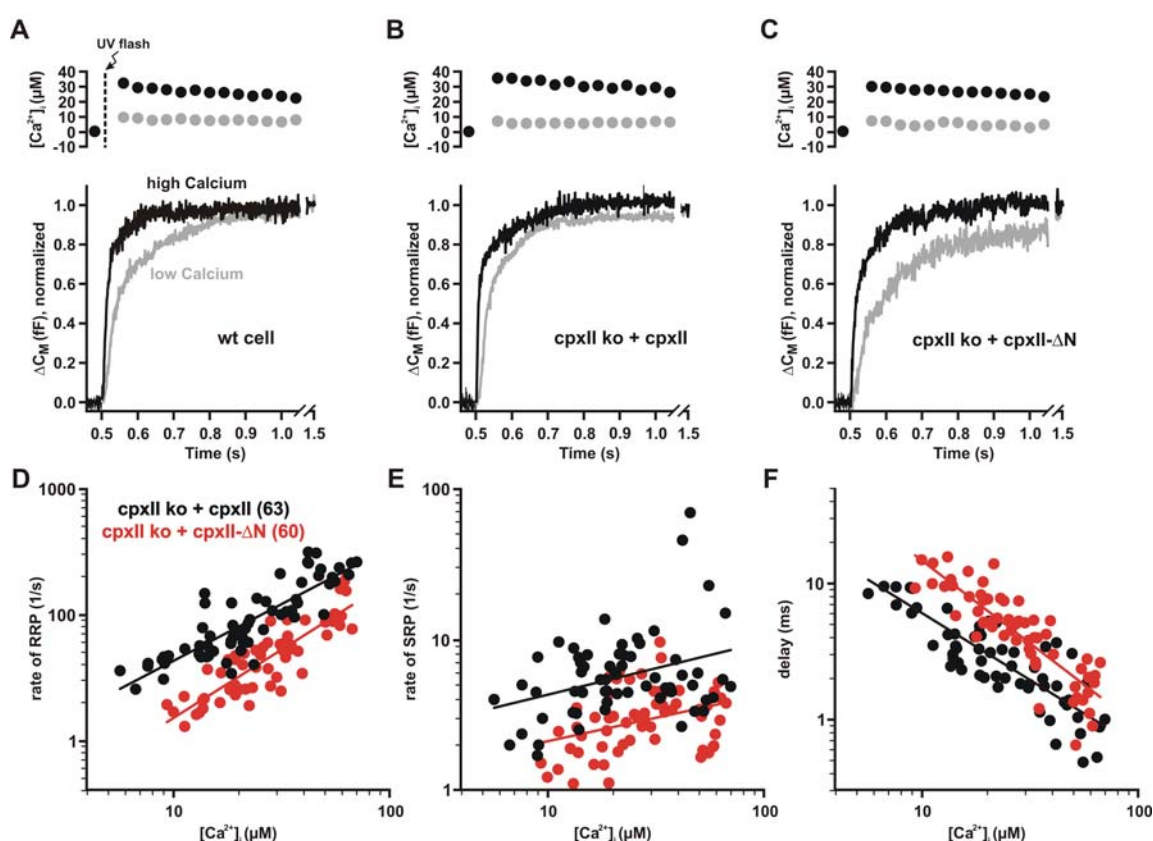


**Fig. 22. N-terminal domain modifies the  $\text{Ca}^{2+}$  affinity of secretion.** (A, B, C) Exemplary recordings of normalized capacitance signals (bottom) in response to low (gray) and high (black)  $[\text{Ca}^{2+}]_i$  levels (top) induced by UV flash (arrow and dashed line). All traces show that high  $\text{Ca}^{2+}$  can speed up the secretion. Note that expression of CpxII full-length protein is able to restore the kinetics properties of the CpxII ko cell to the wt level, and the truncated mutant  $\Delta\text{N}$  exhibits slower response to the comparative  $[\text{Ca}^{2+}]_i$  levels. (D, E, F) RRP fusion rate, SRP fusion rate and the exocytotic delay of CpxII ko cells expressing either CpxII full-length (black, CpxII ko + CpxII; n=63) or N-terminally truncated mutant (red, CpxII ko + CpxII- $\Delta\text{N}$ ; n=60) over the entire range of  $[\text{Ca}^{2+}]_i$  levels (plot using a logarithmic scale for both the x-axis and the y-axis). Continuous lines depict linear regressions. For  $\Delta\text{N}$ -mutant, RRP and SRP rates are slower over the range of taken  $[\text{Ca}^{2+}]_i$  levels and the exocytotic delay is proportionally longer.



### 3.2 Role of the v-SNARE TMD in $\text{Ca}^{2+}$ -triggered exocytosis

For fusion, membranes have to surpass large energy barriers that requires the action of proteins with special properties to lower the energy costs. As experiments made in our laboratory could previously show, v-SNARE proteins drive  $\text{Ca}^{2+}$ -triggered membrane fusion at the millisecond scale (Kesavan et al., 2007). The results have suggested a model in which persistent molecular stress by SNAREs on their transmembrane domain (TMD) leads the vesicle from pre- to postfusional steps during chromaffin granule exocytosis. The interactions of the SNARE motif are well-studied (Sutton et al, 1998; Fasshauer, 1998). In contrast, little is known about the functional relevance of other structures in SNARE proteins, like the TMD. In the second part of this thesis, the function of the lipid-interacting TMD of the vesicular SNARE protein Synaptobrevin II (SybII) in regulated exocytosis was studied (Figure 23). Previous studies have suggested that SNARE TMDs may simply serve as membrane anchor (Zhou et. al., 2013; Pieren et. al., 2015). Structural analyses have shown that SNARE-TMDs are characterized by an overrepresentation of  $\beta$ -sheet promoting  $\beta$ -branched residues (isoleucine, valine; Langosch et al, 2001).  $\beta$ -branched amino acids have the potential to destabilize an  $\alpha$ -helical structure of the TMD due to bulkiness of their side-chain near to the protein backbone. Functional analyses with reconstituted peptides that mimic the TMDs of synaptic or yeast SNAREs have revealed the unusual result that TMDs of v-SNARE proteins without their cytoplasmic domains prompt liposome fusion (Langosch et al., 2001). Clearly, the TMD peptide cannot hold together opposing membranes for fusion. Yet, it is possible that such peptides may provoke local membrane defects and hence cause lipid mixing upon collision between liposomes. Moreover, TMD peptide-driven fusion of liposomes is sequence specific and in contrast to wild type SNARE-TMDs, an oligo-leucine peptide is non-fusogenic indicating that the primary sequence of the TMD, but not overall hydrophobicity, regulates fusogenicity (Langosch et al., 2001). A correlation between the TMD peptide flexibility and its fusogenicity has been proposed (Stelzer et al., 2008). Still, the function of TMD in living cells is unknown and even more unclear is at which step the TMDs may control fast  $\text{Ca}^{2+}$ -triggered exocytosis. Based on the findings with reconstituted fusion models, we set out in the present work to study properties of SNARE-TMDs in fast  $\text{Ca}^{2+}$ -triggered secretion.



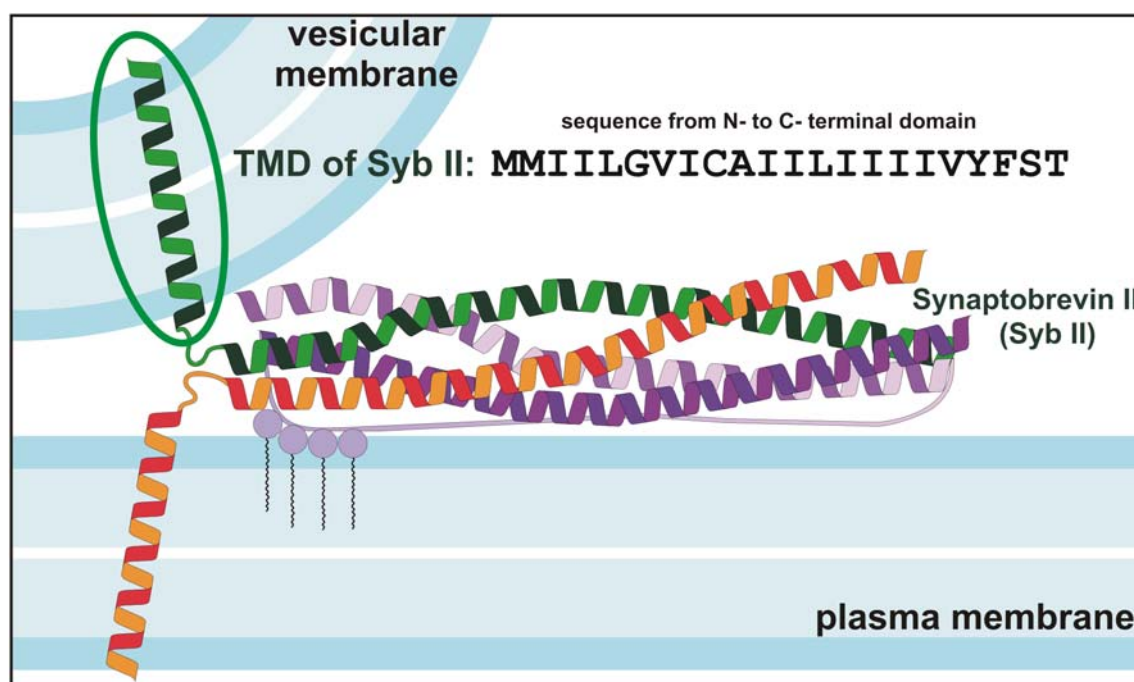


**Fig. 23. The v-SNARE Transmembrane Domain (TMD).** The TMD of SybII (encircled in green) has an overrepresentation of  $\beta$ -branch amino acids as seen in the sequence, since valine (V) residues and isoleucine (I) are highly present.

### 3.2.1 A rigid $\alpha$ -helical structure of the TMD reduces synchronous exocytosis

SybII proteins were expressed carrying mutated TMD in mouse chromaffin cells, which are genetically deficient for SybII and cellubrevin (double knock-out cells, DOKO) and nearly devoid of secretion (Borisovska et al, 2005). In following this strategy,  $\text{Ca}^{2+}$ -dependent exocytosis mediated by the v-SNARE was analyzed in a gain-of-function approach. Like in the Cpx part of this thesis, granule exocytosis in isolated mouse chromaffin cells was synchronized using flash photolysis of caged  $[\text{Ca}^{2+}]_i$  (NP-EGTA), and changes in  $[\text{Ca}^{2+}]_i$  were recorded with a mixture of calcium indicators (Fura-2 and Fura-2/AM) simultaneously with high resolution capacitance measurements in whole-cell patch clamp configuration.

In the first set of experiments, a SybII variant was generated, in which all amino acids within the hydrophobic core of TMD were replaced by leucine (L) residues (Poly-L mutant, Figure 24A). That kind of manipulation should strongly decrease the

---

conformational flexibility of the TMD domain, since L residues commonly favor an  $\alpha$ -helical secondary structure (Krittanaï and Johnson, 2000).

The results reveals that the Poly-L mutant can barely restore the secretory response compared with wt protein (Figure 24B, C and D). Both constituents of the exocytotic burst, the RRP and SRP are equally affected in cells expressing the Poly-L mutant. Moreover, a strong defect in the subsequent, sustained release can be seen, while no changes of the kinetics properties occurred.

In order to rule out the possibility of different expression levels of the protein and proper insertion in the vesicle, confocal imaging and SIM microscopy experiments were respectively performed. Expression of SybII wt protein and its mutant showed no difference in the expression levels (see, Dhara, Yarzagaray et al, 2016). Based on the strong decrease of the exocytotic burst component, we can think of two possible explanations (Figure 24E). On one hand, one might hypothesize that the Poly-L mutation restricts priming of chromaffin granules. Priming of the vesicles could be affected because structural changes in the TMD could interfere with a potential nucleation role of the TMD in controlling the folding of upstream protein regions. However, Poly-L mutation does not disturb the SNARE complex formation (as judged for the binding experiments with the recombinant proteins; see Dhara, Yarzagaray et al, 2016). Thus, the deficiency in the synchronous release in Poly-L expressing cells is not owing to impaired SNARE complex formation (Dhara, Yarzagaray et al, 2016). On the other hand, it is also possible that the conformational flexibility of the TMD is essential for the opening of the initial fusion pore. Indeed, fusion of vesicles could be impaired because of the reduced flexibility of the Poly-L TMD. This mutant may hinder and trap vesicles in a non-fusogenic state. The latter, trapped-state hypothesis, is compatible with the experiments in synthetic liposomes (Langosch et. al., 2001). Furthermore, amperometric experiments performed on chromaffin cells (see, Dhara, Yarzagaray et. al., 2016) could confirm that Poly-L mutant exhibited a clear fusion deficit (as will be discussed below). Such mechanism may lead to a scenario where zipper SNARE complexes are hindered in their ability to surmount the energy barrier of the first intermembrane contact, thereby leaving vesicles in trapped, non-fusogenic state.

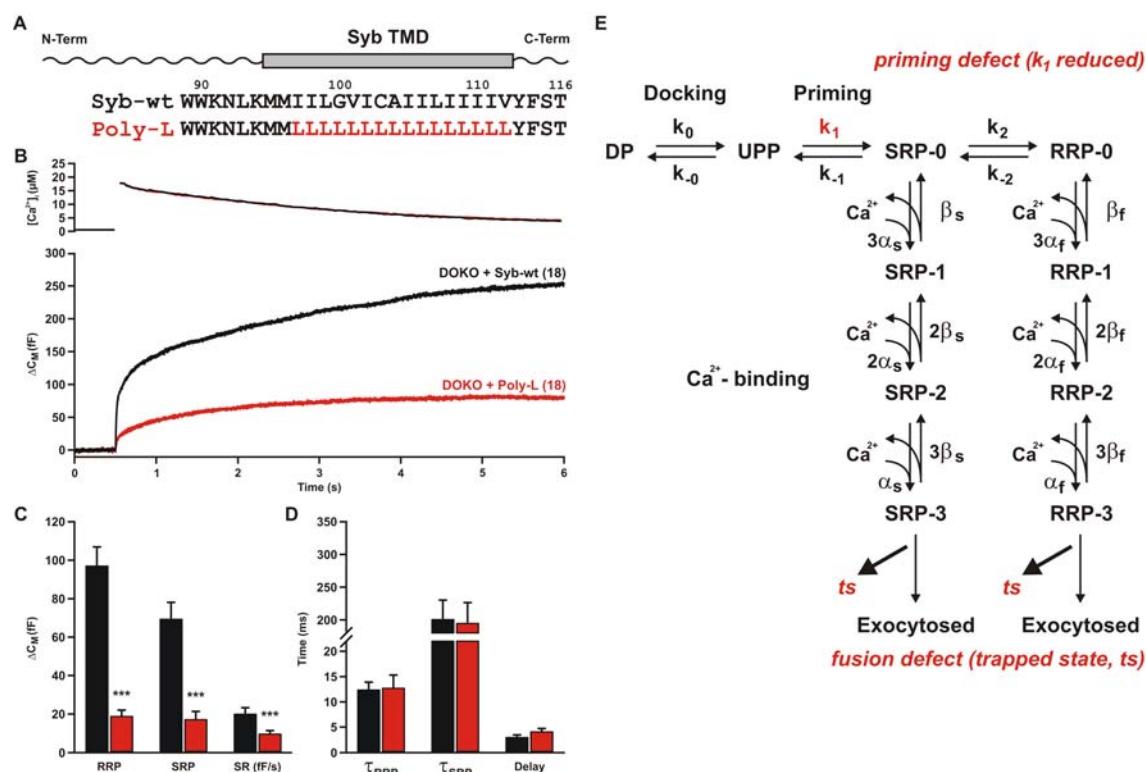


**Fig. 24. A rigid  $\alpha$ -helical structure of v-SNARE TMD reduces synchronous secretion.** (A) Schematic representation of v-SNARE SybII highlighting its TMD (boxed, top), and the amino acid sequences (bottom) for both wild type (syb-wt) and mutant with all amino acids within the TMD substituted for Leucine (poly-L). (B) Averaged flash-induced  $[Ca^{2+}]_i$  levels (top panel) and corresponding capacitance responses (bottom panel) of DOKO cells expressing either SybII (black; n=18) or poly-L (red; n=18). Flash is at t=0.5 s. (C) Analysis of the size of burst phases (RRP and SRP) and sustained rate of secretion (SR, fF/s) by capacitance measurements (bars with same color code as shown in B). RRP, SRP and SR are strongly reduced. (D) Kinetic analysis of the individual traces showed no difference between control and mutant. Error bars represent SEM. \*\*\*p<0.001, Student t-test. (E) Kinetic model of priming and fusion in chromaffin cells highlighting in red the two possible scenarios for the seen effect, the exocytotic response is reduced either by priming defect or fusion defect. Figure is taken and modified from Dhara, Yarzagary et al., 2016.

### 3.2.2 Flexibility of the TMD determines synchronous exocytosis

In following up this hypothesis, amino acids of the lipophilic core of the TMD were substituted by valine (V) residues (Poly-V mutant, Figure 25A) in order to increase conformational flexibility within the TMD.

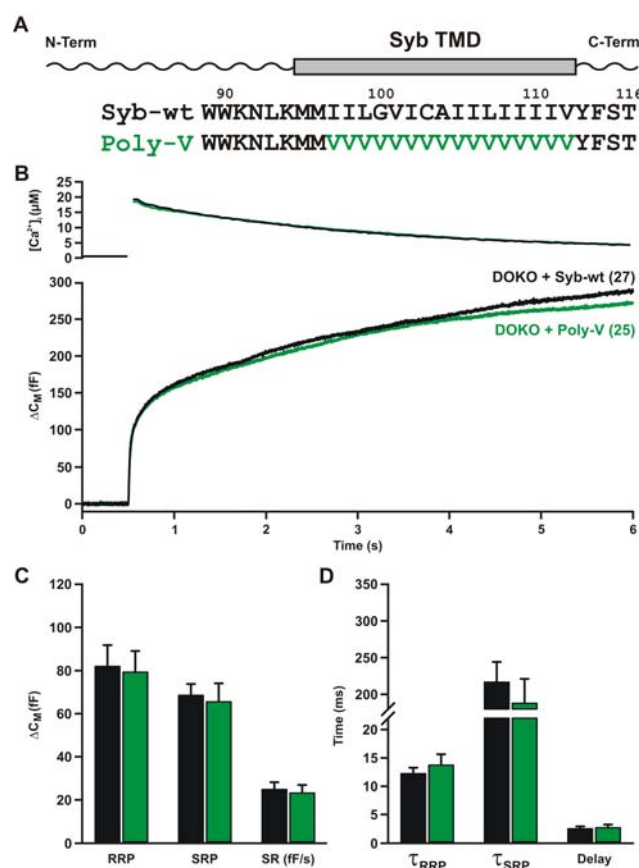


**Fig. 25. Saturation of a  $\beta$ -branch amino acid in v-SNARE TMD is able to restore the exocytotic response.** (A) Illustration of v-SNARE SybII emphasizing its TMD (boxed, top), and the amino acid sequences (bottom) for both wild type (syb-wt) and mutant with all amino acids within the TMD exchanged for Valine (poly-V). (B) Mean flash-induced  $[Ca^{2+}]_i$  levels (upper panel) and corresponding capacitance responses (lower panel) of DOKO expressing either SybII (black;  $n=27$ ) or poly-V (green;  $n=25$ ). Flash is at  $t=0.5$  s. (C) Amplitudes of the two EB components (RRP, SRP) and the sustained rate (SR) for the indicated groups. No difference compared to control. (D) Mean RRP and SRP time constants and the secretory delay are unchanged. Figure is taken and modified from Dhara, Yarzagaray et al., 2016.

The results show that poly-V expressing cells are able to restore the flash-evoked response to the wt level. Neither components of the EB nor the sustained rate of release measured for the Poly-V mutation were different compared to the controls. Similarly, the kinetics properties of the secretion remained unchanged (Figure 25). Thus, Poly-V can functionally substitute the wt protein. Hence, conserved amino acids at defined positions within the SybII TMD are not crucial for vesicle fusion. This finding supports the view that conformational flexibility provided by  $\beta$ -branched residues may facilitate membrane fusion.

### 3.2.3 Single Valine mutations do not affect synchronous secretion

Encouraged by the findings, we extended our structure function analysis to single point mutations. The idea behind the following experiment is to test whether the single V residues present in the original sequence of TMD can be held responsible for the full rescue found with the Poly-V mutant. V residues located in 101 and 112 positions were exchanged to A (V101A mutant, Figure 27A and V112A mutant, Figure 27E). The amino acid A would prefer the  $\alpha$ -helical conformation rather than the  $\beta$ -sheet structure, hence reducing the conformational flexibility of the TMD. Interestingly, those two punctual mutations restore the synchronous secretion with the same efficiency as SybII wt. Neither the extent of the secretory response nor exocytosis timing were altered (Figure 27). Therefore, alterations in the whole structural flexibility of the SybII TMD, rather than a requirement of specific amino acids at key positions, determine the exocytosis of secretory granules.

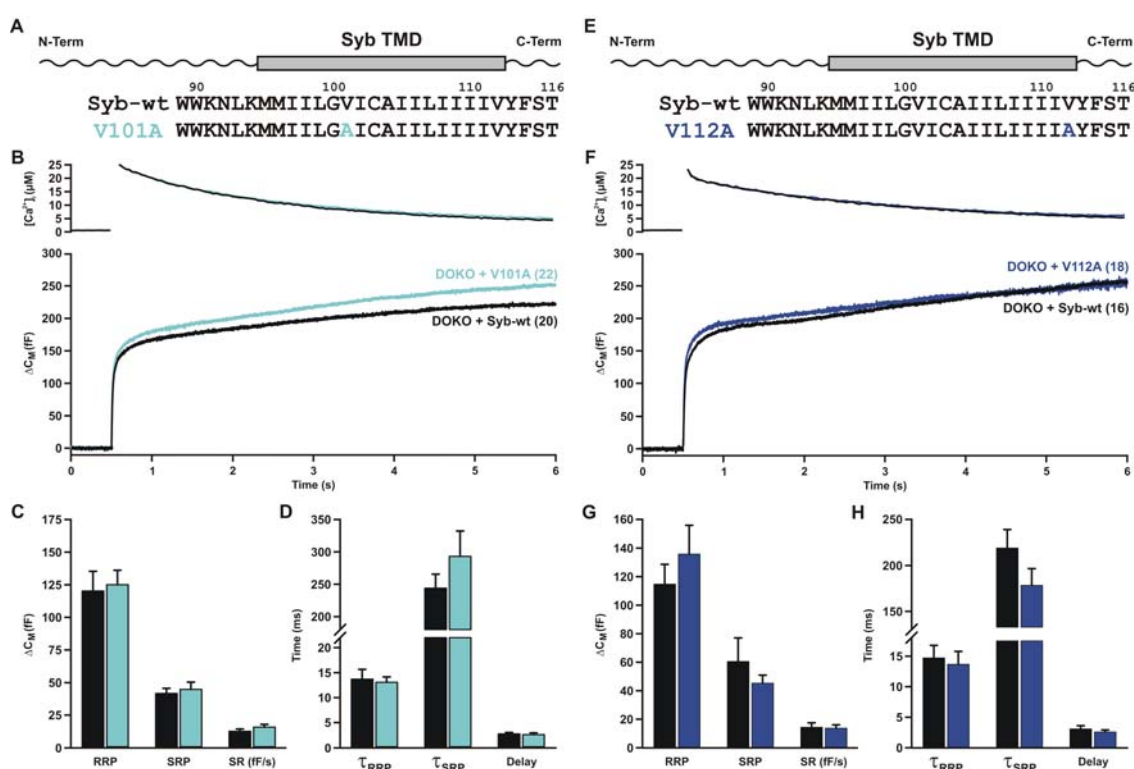


**Fig. 26. Specific mutations on the two Valine residues do not affect the properties of the v-SNARE TMD.** (A, E) Depiction of v-SNARE SybII accentuating its TMD (boxed, top), and the amino acid sequences (bottom) for wild type (syb-wt) and mutants with a specific exchanged of Valine for Alanine (V101A and V112A) within the TMD. (B, F) Averaged flash-induced  $[Ca^{2+}]_i$  levels (top panel) and

corresponding capacitance responses (bottom panel) of DOKO cells expressing either SybII (black; n=20 in B and n=16 in F) or Valine mutation (light blue V101A, n=22 in B and dark blue V112A, n=18 in F). Flash is at  $t=0.5$  s. (C, D, G, F) Amplitudes of the two EB components (RRP, SRP), the rate of sustained release (SR, fF/s), mean RRP and SRP time constants and the secretory delay for the indicated groups (identical color code as shown in B, F). No change was observed in comparison with control. Figure is taken and modified from Dhara, Yarzagaray et al., 2016.

### 3.2.4 Proline mutation probably affects conformational changes in the TMD

In addition to an overrepresentation of  $\beta$ -branched amino acids, the native v-SNARE TMD also has a highly-conserved glycine (G) residue at position 100, which is preserved throughout the animal kingdom, suggesting a possible functional role in membrane fusion. G residues are also well known to disrupt  $\alpha$ -helices, since they cannot support the secondary structure by side-chain-side-chain interactions. Biochemical studies proposed that G destabilizes the  $\alpha$ -helical structure of the TMD and thereby facilitates the fusion of synthetic liposomes (Ollesch et al., 2008). Furthermore, it has been previously reported that the substitution of V101 with a Proline residue (according to Molecular Dynamics simulations, Quint et al., 2010) causes a vastly flexible center in combination with G100. Given these observations, an additional single mutation on the V residue 101 was generated. V was exchanged with Proline (P) residue (V101P mutant, Figure 28A).

Unexpectedly, the exocytotic response of secretory cells was found to be impaired for the V101P. The amplitudes of the two exocytotic burst components, RRP and SRP, were decreased to almost 50% and the sustained phase of secretion (SR) was slightly reduced, while the time constants and the exocytotic delay were unaltered (Figure 28).

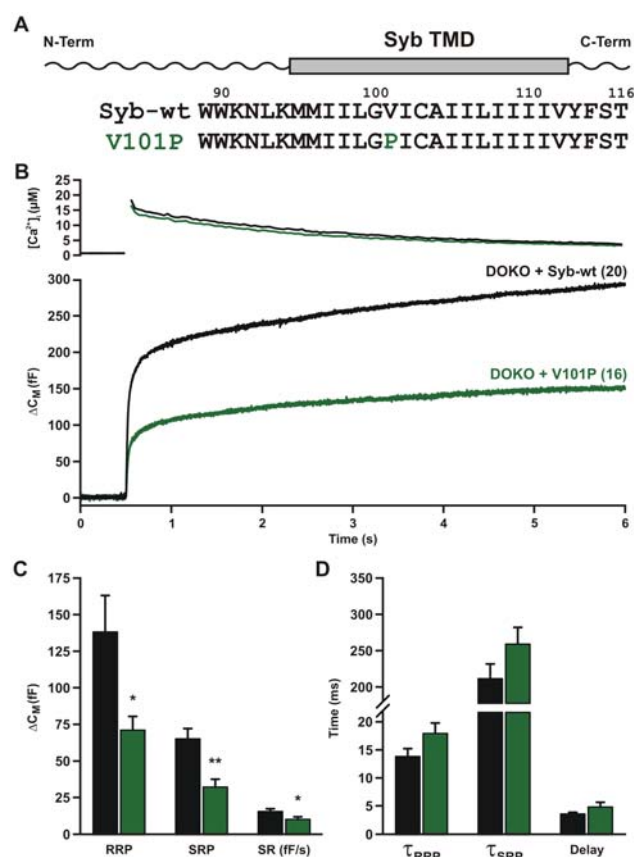


**Fig. 27. Proline mutation in the v-SNARE TMD decreases regulated exocytosis.** (A) Illustration of v-SNARE SybII highlighting its TMD (boxed, top), and the amino acid sequences (bottom) for both wild type (syb-wt) and mutant with amino acid 101 substituted for Proline (V101P). (B) Averaged flash-evoked [Ca<sup>2+</sup>]<sub>i</sub> levels (top panel) and corresponding capacitance responses (bottom panel) of DOKO cells expressing either SybII (black; n=20) or V101P (dark green; n=16). Flash is at t=0.5 s. (C) Analysis of the size of burst phases (RRP and SRP) and sustained rate of secretion (SR, fF/s) by capacitance measurements (bars with same color code as shown in B). RRP, SRP and SR are reduced. (D) Kinetic analysis of the individual traces showed no difference between control and mutant. Error bars represent SEM. \*\*p<0.05, \*\*\*p<0.01, Student t-test.

Evidently, our physiological finding with the V101P mutation appeared to be inconsistent with a simple relationship between TMD flexibility and fusogenicity of the vesicles. Yet, a possible explanation for this apparent divergent result could be that the V101P mutation causes an additional kink in the TMD and changes its overall tilt relative to the membrane. Such a behavior could indeed dominate over an increased flexibility, as judged from MD simulations, and thereby reduce secretion by influencing upstream protein regions.



### 3.2.5 The N-terminal half of the TMD determines fusogenicity

Membranes first meet and merge with their outer leaflets (Figure 29) and transit through a hemifused state before proceeding into complete membrane mixing. To test the significance of TMD-flexibility within different leaflets of the membrane, we generated two mutant proteins, where amino acids within either the N- or the C-terminal half of the TMD are replaced with L residues (Fig. 30A, E).

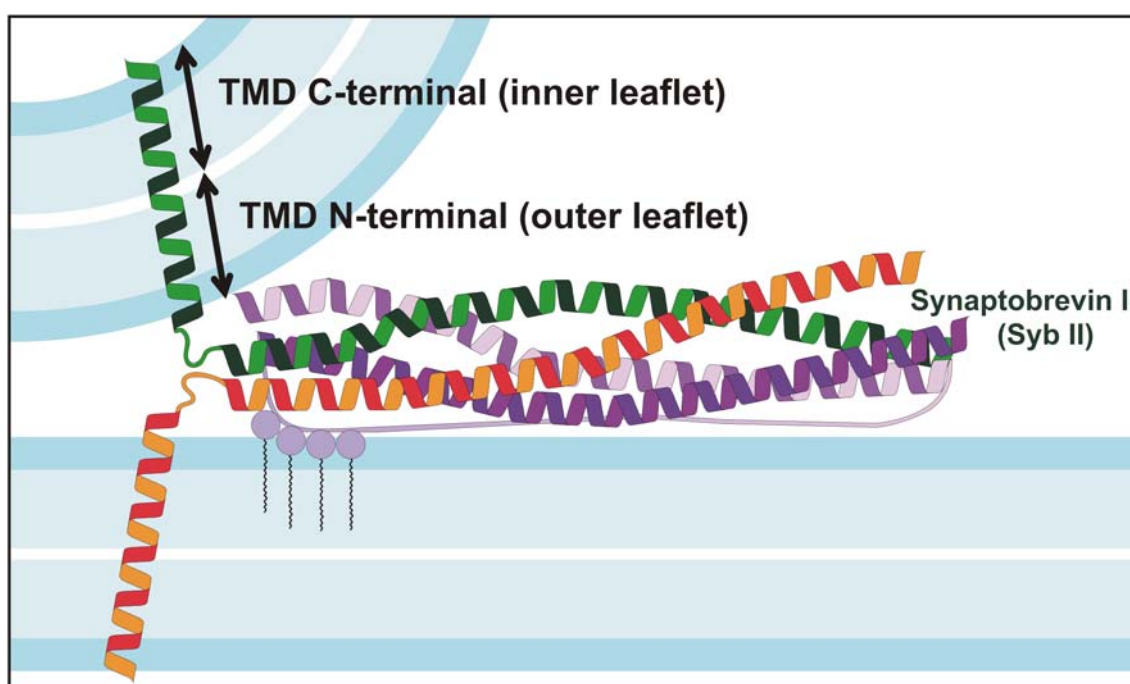


**Fig. 28. The v-SNARE TMD spans both leaflets of the vesicle lipid bilayer.** The TMD of SybII is described in two parts (shown in arrows) in order to distinguish both leaflets (inner and outer) of the vesicle membrane.

Interestingly, L replacement within the N-terminal half of TMD (outer leaflet) failed to restore the exocytotic response (Figure 30F, G and H). In contrast, both magnitude of EB components and kinetic properties were unaffected in Poly-LC mutant (Figure 30B, C and D). These results suggest that SybII TMD has an intrinsic functional polarity, where the N-terminal region is more essential for fusogenicity than the C-terminal region. Given these findings, one might speculate that SybII TMD perturbs lipid packing (enhancing lipid splaying) especially in the cytoplasmic leaflets, thus enabling the first hydrophobic contact for creating a lipid bridge between membranes. Further analysis by my colleague MD (Dhara, Yarzagaray et. al., 2016) extended this view by



showing that TMD backbone, within the outer leaflet, drive fusion pore expansion, most likely by lowering the high membrane curvature of the fusion pore neck.

Overall, the present work provides evidence on how SybII TMD has specific functions that goes beyond passive membrane-anchoring. The interaction between flexible TMDs and the neighboring lipids could induce hydrophobic tail protrusion and consequently membrane fusion.

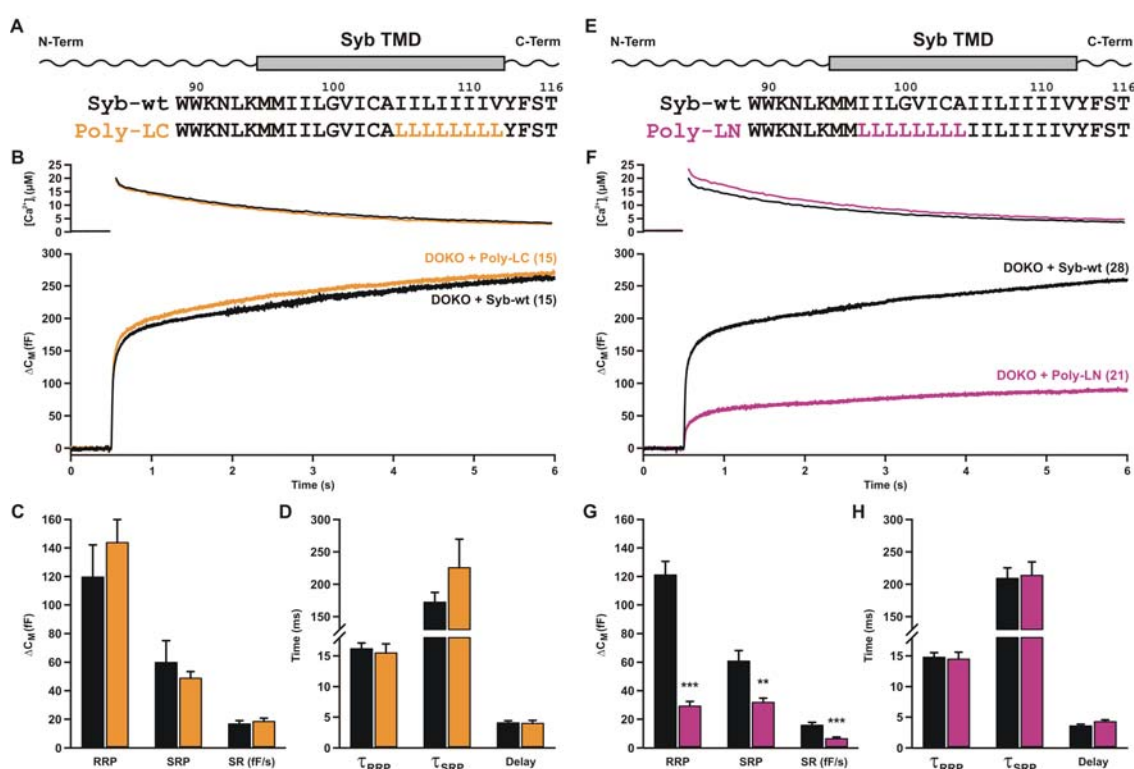


**Fig. 29. The N-terminal half of the v-SNARE TMD provides its flexibility.** (A, E) Schematic representation of v-SNARE SybII emphasizing its TMD (boxed, top), and the amino acid sequences (bottom) for wild type (syb-wt) and mutants with Leucine amino acids within the TMD substituted either very close to the end of C-terminal domain (poly-LC) or close to the N-terminal domain (poly-LN). (B, F) Averaged flash-evoked  $[Ca^{2+}]_i$  increases (top) and parallel capacitance recordings (bottom) of DOKO cells expressing either SybII (black; n=15 in B and n=28 in F) or the indicated mutations (dark yellow poly-LC, n=15 in B and pink poly-LN, n=21 in F). Flash is at t=0.5 s. (C, G) Analysis of the size of burst phases (RRP and SRP) and sustained rate of secretion (SR, fF/s) by capacitance measurements (bars with same color code as shown in B, F). Poly-LN showed a very similar response in comparison with the poly-L (see Fig. 23) suggesting that only this region (half of the TMD) is crucial for the flexibility. (D, H) Kinetic analysis of the individual traces showed no difference between control and mutants. Error bars represent SEM. \*\*\*p<0.01, \*\*\*\*p<0.001, Student t-test. Figure is taken and modified from Dhara, Yarzagary et al., 2016.

### 3.2.6 A TMD with alternating L and V residues support exocytosis like wt protein

We produced a variant where the TMD core was exchanged by an alternating sequence of L and V (termed Poly-LV). In order to match ~50%  $\beta$ -branched residues of the SybII TMD within its N-terminal half (Figure 26A).

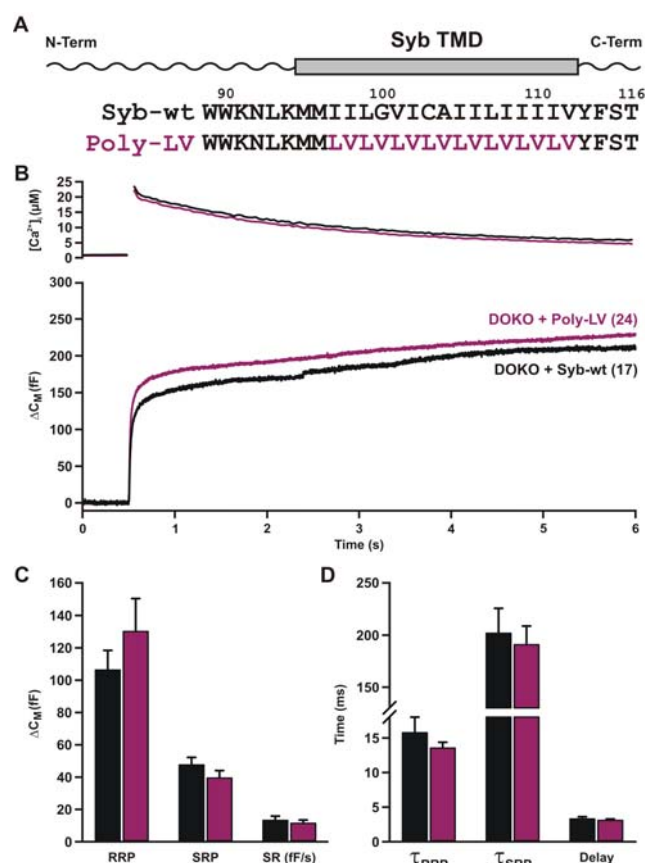


**Fig. 30. Alternating  $\beta$ -branch and non- $\beta$ -branch amino acids in v-SNARE TMD also rebuild synchronous secretion.** (A) Drawing of v-SNARE SybII stressing its TMD (boxed, top), and the amino acid sequences (bottom) for both wild type (syb-wt) and mutant with all amino acids within the TMD replaced for Leucine and Valine interchanging (poly-LV). (B) Averaged flash-evoked  $[Ca^{2+}]_i$  increases (top) and parallel capacitance recordings (bottom) of DOKO cells expressing either SybII (black; n=17) or poly-LV (purple; n=24). Flash is at t=0.5 s. (C, D) Individual capacitance traces were fitted in order to get information on the pool amplitudes (RRP and SRP), sustained rate (SR, fF/s), time constants ( $\tau_{RRP}$  and  $\tau_{SRP}$ ) and exocytotic delay (color code as shown in B). No change observed in comparison with control. Figure is taken and modified from Dhara, Yarzagaray et al., 2016.

---

The amplitude of the EB components and the SR of release, as well as the kinetics in the Poly-LV mutant remained the same in comparison with the control (Figure 26B, C and D). The amino acids L and V are hardly different in their physicochemical properties concerning the hydrophobicity and size. Nevertheless, the different secretory effects emerge from their diverse side-chain mobility, thus affecting side-chain to side-chain interplay and TMD backbone dynamics. Thus, flexibility of the TMD, even if it matches around 50% of the residues, enables membrane fusion.

---

## 4. Discussion

Communication between cells constitutes one of the fundamental processes in all organisms that enable to properly react to diverse stimuli. The basis of intercellular communication comprises the release of neurotransmitters and hormones (signaling molecules), as well as secretion of neuropeptides, small proteins and digestive enzymes. Inside the cell, the signaling molecules are stored in membrane-bound compartments called vesicles, which have to fuse with the plasma membrane in order to release the water-soluble cargo. Intensive research throughout the last 30 years has revealed the central components of the machinery that permits this exocytosis in a regulated manner (see review Rizo and Xu, 2015). The core of the membrane fusion machinery is the soluble NSF attachment protein receptor (SNARE) complex, which is made of a four-helical bundle between the three proteins syntaxin-1, synaptobrevin-II and SNAP-25 (Sutton et al., 1998). These proteins form a stable complex that provides the energy to pull membranes into close proximity rendering them fusion competent (Kesavan et al., 2007). However, SNARE complex formation requires mechanisms that allow synchronization of SNARE action. To accomplish this and to ensure that the membrane fusion is rapid and precise, several proteins serve as regulators, e.g. synaptotagmins and complexins. Additionally, fusion is not exclusively dependent on protein-protein interactions, it is also affected by the surrounding lipids present in either vesicular membrane or plasma membrane (Langosch et al., 2007). *In vitro* studies have shown that the transmembrane regions of the SNARE proteins, spanning the lipid bilayer membranes, are crucial for the fusion reaction (Langosch et al., 2001).

The present work delineates new features of the SNARE regulators, CpxII and SytI, specifically how they regulate synchronized secretion. The experiments elucidate how two different domains of CpxII, the N-terminus (aa 1-29) and the C-terminus (aa 73-134) functionally synergize to enhance synchronous secretion. The first by increasing the  $\text{Ca}^{2+}$  affinity of the release apparatus and the second by blocking premature exocytosis leading to a subsequent boost in flash-evoked response. Moreover, this thesis shows how the lipid-interacting SybII-TMD provides the conformational flexibility that helps membrane fusion, specifically affecting the outer membrane leaflet layer.

#### **4.1 CpxII increases synchronous exocytosis by blocking premature secretion**

Release of neurotransmitters and hormones occurs with exquisite spatial and temporal precision. To accomplish this task, all proteins participating in the fusion machinery have the difficult task of bringing vesicles as near as possible to the plasma membrane (in order to release them as fast as possible when the  $\text{Ca}^{2+}$  signal arrives) and at the very same time preventing their premature exocytosis. This mechanism ensures that enough vesicles are halted in a fusion-competent state, also referred to as primed vesicles, which later are released in a synchronous way in response to a physiological stimulus.

Cpxs are small cytosolic proteins that are well suited to fulfill this task. Previous studies have shown that Cpxs can either facilitate or inhibit SNARE-mediated fusion (see review Brose, 2008). For example, functional analyses have demonstrated that loss of Cpx diminishes evoked release, which would be consistent with its facilitatory role. Yet, different mechanisms have been put forward to explain this phenotype, such as impaired exocytosis activation (Reim et al., 2001; Tang et al., 2006; Xue et al., 2007, 2008, 2009; Strenzke et al., 2009; Cho et al., 2010; Martin et al., 2011; Jorquera et al., 2012; Cao et al., 2013), reduction of vesicle priming (Yang et al., 2010; Kaeser-Woo et al., 2012; Lin et al., 2013), vesicle depletion (Hobson et al., 2011), or alterations in vesicle fusogenicity (Maximov et al., 2009; Xue et al., 2010).

Several studies have also reported elevated asynchronous release due to the loss of Cpx (Yang et al., 2010; Jorquera et al., 2012), a phenotype that rather suggests an inhibitory role of the protein in  $\text{Ca}^{2+}$ -regulated exocytosis. Such opposing views regarding the role of Cpx in membrane fusion might partially be due to the fact that many functional analyses were often hampered by an insufficient control of intracellular  $[\text{Ca}^{2+}]_i$ . Chromaffin cells instead represent a well-suited model system providing both, excellent control of membrane voltage and of intracellular  $\text{Ca}^{2+}$ -signals. Taken advantage of these properties, the present thesis systematically analyzed regulated exocytosis in chromaffin cells in the presence and absence of CpxII, which is the only isoform expressed in these secretory cells (Reim et al., 2001). The results, as outlined in Section 4, permit a quantitative evaluation of tonic and evoked exocytosis measured

from the same group of cells over a wide range of  $[Ca^{2+}]_i$ . The experiments show that loss of CpxII in chromaffin cells increases the tonic release at submicromolar  $[Ca^{2+}]_i$  (~500 nM) with a subsequent reduction of the flash-evoked response. Additionally, CpxII expression increases evoked synchronous release by practically eliminating any tonic secretion at submicromolar  $[Ca^{2+}]_i$  before the triggering flash (Figures 11, 12 and 13). The inverse systematic relationship between both types of secretion (Figure 13C) suggests that CpxII-dependent clamping of tonic exocytosis determines the exocytotic burst size in synchronous exocytosis. As seen in the Fig. 13C, the regression line intercepts the y axis at ~30 fF/10 s (representing ~3 vesicles /s), a value that is similar to the vesicle maximum priming rate at ~500 nM ( $rate_{(500nM)} = 5.35 \times 10^{-3}/s \times 780$  unprimed vesicles = 4 vesicles/s; Sørensen, 2004). Therefore, CpxII is rate limiting in regulating premature secretion that would otherwise outpace synchronous  $Ca^{2+}$ -dependent exocytosis.

#### 4.2 CpxII regulates secretion by influencing SytI in $Ca^{2+}$ -triggered exocytosis

As outline above, the clamping action of CpxII is crucial to determine the magnitude of exocytotic burst. Detailed analysis of the EB components revealed that loss of CpxII also slowed down the stimulus secretion coupling. Thus, CpxII not only affects the magnitude of tonic and synchronous secretion, but also defines kinetic properties of synchronous exocytosis as seen in Figure 11. This effect was surprising, because it is commonly believed that timing of fusion events is mainly determined by the kinetics of  $Ca^{2+}$ -binding to SytI serving as  $Ca^{2+}$ -sensor for exocytosis (Voets et al., 2001; Nagy et al., 2006). Due to the fact that CpxII lacks any  $Ca^{2+}$ -binding sites, the CpxII-mediated acceleration of secretion may be linked to the action of  $Ca^{2+}$  sensors, like Synaptotgamins, in order to control synchronous secretion. Indeed, an attractive explanation could be that CpxII somehow conditions SytI and thereby accelerates the secretion response of chromaffin cells.

Although many studies have suggested a clear interplay between these two SNARE regulators (Giraud et al., 2006; Tang et al., 2006; Chicka and Chapman, 2009; Xu et al., 2010; Krishnakumar et al., 2011; Malsam et al., 2012; Xu et al., 2013), it is still far

---

from clear how Cpx and Syt interact at molecular level and which sequence of molecular steps is important. In the present work, the functions of both CpxII and SytI were studied in isolated mouse chromaffin cells, which were genetically deficient of either CpxII, SytI or both (the novel CpxII/SytI dko). Electrophysiological experiments, where high resolution capacitance recordings were done simultaneously with measurements of a wide range of  $[Ca^{2+}]_i$ , allowing a better understanding of the interplay of these two auxiliary proteins in the context of regulated exocytosis.

In addition to the experiments performed on single ko cells (CpxII ko and SytI ko), the novel CpxII/SytI dko mouse line was also analyzed. Loss of SytI in the absence of CpxII does not further aggravate the CpxII phenotype in chromaffin cells. CpxII ko and CpxII/SytI dko flash-evoked responses are very similar (magnitude of EB components and kinetic properties, Figure 14). As described above, CpxII ko leads to elevated premature exocytosis and thereby reduces both EB components, the ready releasable pool (RRP) and the slow releasable pool (SRP). SytI ko, instead, abolishes selectively the RRP component without affecting premature exocytosis (Figure 15). Thus, both SNARE regulators control the magnitude of synchronous secretion by different molecular mechanisms, but CpxII seems to be the limiting factor and it is likely that its action comes before SytI.

Importantly, the slow kinetics seen with both single ko phenotypes are not additive in the double null mutant, either because a further slowing cannot be measured or both deficiencies affect exocytosis timing by the same molecular mechanism, e.g. loss of CpxII (especially N-terminus) impair the conditioning of SytI and therefore an additional loss of SytI has no effect.

Overall these observations allow several important conclusions. They strongly suggest that both SNARE regulators act in the same molecular pathway for exocytosis, but control the extent of exocytosis by different means. Secondly, they may act interdependently in controlling the kinetics of secretion.

Several studies have established that SytI not only functions as a  $\text{Ca}^{2+}$  sensor for secretion (Voets et al., 2001, Nagy et al., 2006) but also may act as a clamp that hinders SNARE-catalyzed fusion awaiting the arrival of a  $\text{Ca}^{2+}$  signal (Söllner et al., 1993; Littleton et al., 1994; Broadie et al., 1994; Mackler et al., 2002; Pang et al., 2006). These studies have described an increased frequency of spontaneous vesicle fusion events in the absence of SytI (observed in neurons and neuromuscular junctions) as a hint that SytI itself might serve as a clamp. However, the observed increase in spontaneous vesicle fusion in SytI mutants might not be enough to reduce the vesicle pool to the level required to decrease evoked fusion. In stark contrast, findings in the present work are not compatible with the “clamp” action of SytI in chromaffin cells, but are consistent with a significant role of SytI solely in exocytosis timing (Voets et al., 2001; Rettig and Neher, 2002; Nagy et al., 2006). Unlike CpxII, tonic secretion is unchanged in the absence of SytI (Fig. 15), even though the RRP component in the flash-induced release is strongly reduced (Fig. 14). Thus, another mechanism appears to be involved which has consequences in the decrease of RRP component, e.g., loss of SytI may destabilize the equilibrium between the slowly and the readily releasable state of the LDCV fusion machinery (Voets, 2001). Moreover, CpxII expression in SytI ko cells clamps tonic exocytosis with comparable proficiency as seen in wt cells (Fig. 17). The combined set of data shows that clamping of premature secretion is specific for CpxII and not a shared characteristic of SNARE regulators in chromaffin cells. Furthermore, it became clear that clamping is independent of SytI action.

Since tonic secretion is also  $\text{Ca}^{2+}$ -dependent but does not rely on SytI, it remains to be shown which  $\text{Ca}^{2+}$ -sensor is here acting. Indeed, at low  $[\text{Ca}^{2+}]_i$  (~500 nM), additional loss of SytI does not compromise the release of the CpxII ko (Figure 15). An attractive explanation could be that Syt-VII (Schoon et al., 2008) predominantly promotes secretion at low  $[\text{Ca}^{2+}]_i$  whereas both isoforms SytI and Syt-VII may cooperate at high  $[\text{Ca}^{2+}]_i$ . Still it is also possible that SytI is the preferred  $\text{Ca}^{2+}$  sensor for the secretion at different  $[\text{Ca}^{2+}]_i$ , and is only in its absence substituted by Syt-VII.



### 4.3 CpxII has different domains that synergize to elevate synchronous secretion

The crucial role of Cpx in  $\text{Ca}^{2+}$ -evoked neurotransmitter release has been firmly documented (Brose, 2008). To perform its function, its central  $\alpha$ -helix binds to the SNARE complex (Chen et al., 2002). Several studies performed structure function analyses in order to clarify the exact role of Cpx, and astonishingly found that Cpx involves both facilitatory and inhibitory functions. The opposing effects of Cpx suggested facilitatory and inhibitory actions are mediated by distinct molecular mechanisms.

In the present work, simultaneous recordings of capacitance and  $[\text{Ca}^{2+}]_i$  allowed us in the framework of a comprehensive structure-function analysis to assign facilitatory and inhibitory actions of CpxII to distinct regions of protein (Figures 18 to 21). Tonic secretion was blocked by the mutant lacking the N-terminus while synchronous secretion was enhanced, but the kinetics were slowed down as ko cells. Expression on wt cells confirmed the phenotype, showing that the  $\Delta\text{N}$  mutant outcompeted the endogenous protein to slow down secretion. In contrast, tonic secretion was not blocked by the mutant lacking the C-terminus (like ko cells) and therefore the synchronous response was unaltered (again like ko cells). However, the kinetic properties were rescued as CpxII expressing cells. The  $\Delta\text{C}$  mutant outcompeted the endogenous protein in wt cells to increase tonic secretion. These results were unexpected, because the C-terminus has been considered to be functionally inert (Xue et al., 2010). Yet, more recent studies have reported a similar inhibitory effect of this protein domain (Cho et al., 2010; Martin et al., 2011; Kaeser-Woo et al., 2012). Furthermore, it has been shown that the unstructured C-terminus of Cpx binds to lipids (Cho et al., 2010; Kaeser-Woo et al., 2012; Wragg et al., 2013), but the functional importance of this membrane interaction is not understood.

Thus, the N-terminus governs the exocytosis timing, directly or indirectly interacting with SytI (more discussion below). In this context it is important to note that the N-terminus of Cpx, that may bind to the C-terminal SNARE complex or a region of the complex nearby to cause its facilitatory functions (Xue et al., 2007; Xue et al., 2010; Xu

et al., 2013). The C-terminus controls the synchronous secretion by clamping primed vesicles, a mechanism that may also rely binding of this domain to lipids. Another attractive explanation could be that C-terminus of CpxII folds back on the SNARE complex and together with the other potentially inhibitory domain of CpxII, the accessory  $\alpha$ -helix, hinders premature exocytosis (Bowen et al., 2005).

#### **4.4 CpxII N-terminal domain changes the $\text{Ca}^{2+}$ -dependency of primed vesicle fusion**

Loss of CpxII in chromaffin cells is characterized by delayed and slower excitation–secretion coupling, a phenotype that can be separately replicated by expressing the  $\Delta\text{N}$  mutant in CpxII ko (Figure 18) or wt cells (Figure 20). Previous studies on Cpx ko neurons and mutants expressing the protein lacking the first 26 aa (CpxII aa 27–134, similar to the  $\Delta\text{N}$  showed in the present work) exhibited a greater EPSCs (excitatory postsynaptic current) amplitude potentiation upon elevation of external  $\text{Ca}^{2+}$  concentration (12 mM) than wt cells (Xue et al., 2007, 2010). In the present work, analysis of secretion rates versus  $[\text{Ca}^{2+}]_i$  (in the micromolar range) shows that CpxII lacking the N-terminus shifts the  $\text{Ca}^{2+}$  dependency of RRP rate, SRP rate and delay of secretion to higher  $[\text{Ca}^{2+}]_i$  (Figure 22). These results indicate a lower apparent sensitivity to  $\text{Ca}^{2+}$ , which is well explained by a reduced forward rate of  $\text{Ca}^{2+}$  binding. Interestingly, a comparable phenotype is observed with the SytI mutant R233Q, which has a twofold lower affinity for  $\text{Ca}^{2+}$ -dependent lipid binding (Sørensen et al., 2003).

It is important to note that the facilitatory function of CpxII and its N-terminus on evoked secretion in hippocampal neurons and the slower rise time of the evoked endplate response detected at the NMJs of Cpx ko (Jorquera et al., 2012; Lin et al., 2013) is well explained by alterations in the  $\text{Ca}^{2+}$  affinity of secretion observed here in chromaffin cells. Indeed, action potential evoked release in neurons requires fast excitation–secretion coupling due to the short-lasting presynaptic  $\text{Ca}^{2+}$ -rise. Any decrease in  $\text{Ca}^{2+}$ -affinity is expected to go hand in hand with a reduced action potential-evoked response.

Although several studies have highlighted competing functions (facilitatory and inhibitory) for Cpx (e.g., Maximov et al., 2009; Xue et al., 2009), the present work provides a new understanding of CpxII action in  $\text{Ca}^{2+}$ -triggered exocytosis by pointing out two distinct roles and regions of the protein that increase and speed up synchronous secretion.

The precise molecular mechanism, by which speeding of exocytosis is achieved, remains to be clarified. Probably, the N-terminus of CpxII serves as an adaptor for the association of SytI to the partially assembled SNARE complex (see also Neher, 2010). However, a SytI-independent alteration in the  $\text{Ca}^{2+}$  affinity of the release apparatus by CpxII cannot be rigorously excluded.

#### **4.5 v-SNARE TMD provides conformational flexibility that facilitates secretion**

The most probable route of membrane fusion comprises both, protein-protein as well as protein-lipid interactions. Previous work with reconstituted fusion systems suggested that TMDs of the SNARE complex are important in mediating the membrane fusion reaction (Langosch et al., 2001; Hofmann et al., 2006; Ollesch et al., 2008; Poschner et al., 2009). However, little is known about their function in a physiological context. A recent study using cortical neurons testing lipid-anchored variants of Syx and Syb-II suggested that the TMDs are unlikely to be essential for fusion (Zhou et al., 2013). Yet, subsequent work by Jackson and colleagues has clearly shown that the wild-type construct used for restoring the secretion response of SybII-ko neurons was unable to do so because of an added arginine residues at the very end of the TMD hindering full rescue (Chang et al., 2016). This explanation is further verified by previous observations that a similar mutation within the TMD of SybII does not allow to restore exocytosis in chromaffin cells (Ngatchou et al., 2010). Thus, the apparent ability of lipid anchored v-SNARE proteins to restore secretion like the wild-type protein is simply due to inefficient rescue with the wild-type construct used in the study by Zhou et al., 2013.

Furthermore, studies using synthetic liposomes provide a different view where TMDs have crucial properties that facilitates bilayer merger. TMD peptides might induce local

membrane defects and hence producing lipid mixing upon collision with a partner liposome (Langosch et al., 2001; Hofmann et al., 2006; Stelzer et al., 2008; Poschner et al., 2009; Langer et al., 2011). The view of fusogenicity being directly linked to the flexibility of the TMD has also been supported by molecular dynamics simulations (Quint et al., 2010; Risselada et al., 2011).

The results on chromaffin cells in the present work clearly show, within a physiological context (see flash-evoked responses of Poly-L and Poly-V in Figures 24 and 25), that the alterations in the content of  $\beta$ -branched amino acids in the v-SNARE TMD have a strong impact on the secretion response. In particular, lowering the the number of  $\beta$ -branched amino acids strongly diminishes secretion, consistent with a fusion deficit.

Nevertheless, other possibilities that could similarly explain the observed Poly-L phenotype should first be ruled out. For example, expression levels of the tested proteins and their proper sorting to the vesicles. Likewise, an impaired binding of SNARE resulted from the reorganization of the TMD could potentially have severe consequence on a disorientation of the SNARE motif producing priming defects. Experiments by using confocal and structure illumination microscopy have verified that the mutant proteins are expressed as efficient as wt and they are properly sorted to the vesicles (see Dhara, Yarzagaray et al., 2016). The impaired SNARE binding that would cause priming defect seems to be unlikely, because biochemistry experiments with recombinant proteins (see Dhara, Yarzagaray et al., 2016) showed that Poly-L mutant disturbs neither the rate nor the degree of SNARE complex formation. Thus, the release deficiency in Poly-L expressing cells is most likely not due to impaired SNARE complex formation.

An attractive explanation for the observed fusion deficits may indeed be related to alterations in TMD-flexibility. Indeed, MD simulation of the TMDs (embedded in a bilayer with physiological lipid composition, collaboration with Manfred Lindau from the MPI for biophysical Chemistry, Göttingen) have shown that the Poly-Valine mutation increases whereas the Poly-Leucine mutation decrease the conformational flexibility compared with the wild-type TMD (see Dhara, Yarzagary et. al. 2016). These

results together with our physiological observations suggested a clear correlation between content of  $\beta$ -branched amino acids and the fusogenicity of the mutant protein. Whether a direct causality can be deduced from this correlation remains to be shown. Still, it is clearly possible that reduced conformational flexibility of the Poly-L mutant might decrease the probability of lipid splay, hence generating more unsuccessful fusion attempts, leaving vesicles in a “trapped state” (Figure 24E) before membrane fusion. Since fusion mutants are generally expected also to diminish the speed of excitation-secretion coupling (e.g. Kesavan et al., 2007, Weber et al., 2010), the “trapped state” hypothesis would explain why helix-rigidifying mutations do not change the exocytosis timing in  $\text{Ca}^{2+}$ -triggered exocytosis.

Notably, for the Poly-V mutant we observed secretion similar like that of wildtype cells. Evidently, increasing the fraction of  $\beta$ -branched amino acids within the core of SybII TMD domain does not further the EB size. Most likely, docking and priming are rate-limiting reactions (Sorensen, 2009), thus hindering the total exocytotic secretion to rise above wt levels.

#### **4.6 Competing concepts on fusion pores: lipidic vs proteinaceous fusion pores**

In contrast to lipidic fusion intermediates (as discussed above) other concepts have proposed the existence of a proteinaceous fusion pore formed by the TMDs of the SNAREs in the vesicle and plasma membrane (Han et al., 2004; Chang et al., 2015). It has been hypothesized that TMD arranged in barrel like-fashion are aligned in a stacked manner to form a gap-junction like channel through both membranes. Such a putative channel-like organization that may give rise a water-soluble channel and later disassembles by intercalating lipid molecules to allow for fusion pore enlargement.

Clearly, membrane capacitance measurements cannot distinguish between a pure lipidic and a proteinaceous intermediate in membrane fusion. Yet, accompanying amperometric analyses by my colleague MD (Dhara, Yarzagaray et. al., 2016), with the same mutant proteins, have shown with amperometry that TMD variants with hydrophobic, identical residues can rescue or even speed up transmitter release from

single vesicles through the narrow initial fusion pore. Such a result counters the existence of a proteinaceous channel pore, because Poly-L or Poly-V mutants neither exhibit any polarity nor asymmetry with respect to the side chains that could be used to establish an aqueous pathway of a putative channel. Instead, the v-SNARE TMD may provide structural flexibility that could contribute to lipid mixing, thus facilitating a lipidic pore expansion.

#### **4.7 TMD flexibility within the outer vesicular membrane leaflet is crucial for membrane fusion**

To investigate the significance of structural flexibility within subdomains of the TMD, we replaced amino acids either in the N-terminal or in the C-terminal half of the TMD with leucine. Indeed, the Poly-LN mutant (Figure 30, right panel) impairs the synchronous secretion, whereas the Poly-LC mutant (Figure 30, left panel) caused no impairment of exocytosis. These results suggested some functional polarity of the v-SNARE TMD with the N-terminal portion of the TMD being more fusogenic than its C-terminal half. This observation is indeed consistent with the fact that membranes first meet and merge with their cis-oriented leaflets. Given that dehydration of the phospholipid headgroups between the approaching membranes and splaying of lipid acyl chains are very energy demanding steps (Chernomordik et al., 1987), it is possible that structural flexibility of the v-SNARE TMDs delivers some extra energy required to surmount this energy barrier. Indeed, previous coarse-grained models of SNARE mediated membrane fusion suggested not only a similar directionality of v-SNARE TMDs in perturbing lipid packaging, but also showed that lipid splay preferentially occurred in the direct neighborhood of the TMD (Risselada et al., 2011). Splaying of acyl chains likely represents the first hydrophobic encounter to form a lipid bridge between the opposing membranes. The latter hourglass-shaped structure, also referred to as stalk may readily progress to opening of the initial fusion pore that establishes the first aquatic pathway between the vesicle lumen and the extracellular solution.

In conclusion, there is convincing evidence to reach a conclusion that SNARE-complex formation frees energy, which is transmitted to the membranes through the linkers and

TMD as a consistent force to drive exocytosis. This force contributes in strictly arranging the membranes, causing dehydration of the lipid head groups, and the fusion process is controlled by lipid-protein and lipid-lipid interactions. The subsequent events are lipid splaying and stalk formation that initiate a fusion pore and release of the vesicular cargo. The SNAREs remain to drive fusion during the course of these phases.

Overall, SNAREs do not only function as force generators by consistent molecular straining on opposing membranes, but also catalyze membrane fusion via structural flexibility of their TMDs.

#### **4.8 Concluding remarks**

Our results show that the C-terminal domain of CpxII is decisive in clamping SNARE-mediated tonic secretion, consequently resulting in an increased synchronous exocytosis. CpxII N-terminal domain speeds up excitation–secretion coupling and elevates the  $\text{Ca}^{2+}$  affinity of phasic release, possibly by adjusting SytI, the major  $\text{Ca}^{2+}$  sensor. Thus, the present work defines two distinct CpxII actions that synergizes to determine the  $\text{Ca}^{2+}$ -triggered secretion in chromaffin cells. In a separate set of experiments, we could demonstrate that structural flexibility of the SybII-TMD promotes membrane fusion, most likely by perturbing the surrounding lipids on the vesicle membrane. Overall, our data provide evidence for crucial protein-protein as well as protein-lipid interactions that govern vesicle fusion.

---

## 5. Literature

- Archer, D.A.; Graham, M.E. and Burgoyne, R.D. (2002). Complexin regulates the closure of the fusion pore during regulated vesicle exocytosis. *J Biol Chem* 277,18249–18252.
- Ashery, U.; Betz, A.; Xu, T.; Brose, N. and Rettig, J. (1999). An efficient method for infection of adrenal chromaffin cells using the Semiliki Forest virus gene expression system. *Eur. J. Cell Biol.* 78:525-532.
- Ashery, U.; Varoqueaux, F.; Voets, T.; Betz, A.; Thakur, P.; Koch, H.; Neher, E.; Brose, N. and Rettig, J. (2000). Munc13-1 acts as a priming factor for large dense-core vesicles in bovine chromaffin cells. *EMBO J.* 19, 3586–3596.
- Becherer, U. and Rettig, J. (2006). Vesicle pools, docking, priming, and release. *Cell Tissue Res.* 326, 393–407.
- Becherer, U.; Medart, M.R.; Schirra, C.; Krause, E.; Stevens, D.R. and Rettig, J. (2012). Regulated exocytosis in chromaffin cells and cytotoxic T lymphocytes: How similar are they?. *Cell Calcium* 52(3-4), 303-12.
- Blasi, J.; Chapman, E.R.; Link, E.; Binz, T.; Yamasaki, S.; De Camilli, P.; Sudhof, T.C.; Niemann, H. and Jahn, R. (1993). Botulinum neurotoxin A selectively cleaves the synaptic protein SNAP-25. *Nature* 365, 160–163.
- Bollmann, J.H.; Sakmann, B. and Borst, J.G. (2000). Calcium sensitivity of glutamate release in a calyx-type terminal. *Science* 289, 953–957.
- Borisovska, M.; Zhao, Y.; Tsytsyura, Y.; Glyvuk, N.; Takamori, S.; Matti, U.; Rettig, J.; Südhof, T. and Bruns, D. (2005) v-SNAREs control exocytosis of vesicles from priming to fusion. *EMBO J.* 24, 2114 –2126.
- Bracher, A.; Kadlec, J.; Betz, H. and Weissenhorn, W. (2002). X-ray structure of a neuronal complexin-SNARE complex from squid. *J Biol Chem.* 277, 26517-26523.
- Brose, N. (2008). For Better or for Worse: Complexins regulate SNARE function and vesicle fusion. *Traffic* 9(9), 1403-13.
- Brose, N.; Petrenko, A.G.; Südhof, T.C. and Jahn, R. (1992). Synaptotagmin: A Calcium Sensor on the Synaptic Vesicle Surface. *Science* 256, 1021 – 25.
- Bruns, D. (2004). Detection of transmitter release with carbon fiber electrodes. *Methods.* 33:312-321.
- Bruns, D. and Jahn, R. (2002). Molecular determinants of exocytosis. *European Journal of Physiology* 443, 333–338.



- Cai, H.; Reim, K.; Varoqueaux, F.; Tapechum, S.; Hill, K.; Sørensen, J.B.; Brose, N. and Chow, R.H. (2008). Complexin II plays a positive role in  $\text{Ca}^{2+}$ -triggered exocytosis by facilitating vesicle priming. *Proc Natl Acad Sci* 105, 19538 - 19543.
- Carr, C.M. and Munson, M. (2007). Tag team action at the synapse. *EMBO Report* 8(9),34-8.
- Cao, P.; Yang X. and Sudhof, T.C. (2013). Complexin activates exocytosis of distinct secretory vesicles controlled by different synaptotagmins. *J Neurosci.* 33,1714-1727.
- Chapman, E.R. (2008). How does synaptotagmin trigger neurotransmitter release?. *Annual Reviews Biochemistry* 77, 615-41.
- Chang, C.W.; Chiang, C.W.; Gaffaney, J.D.; Chapman, E.R. and Jackson M.B. (2016). Lipid-anchored Synaptobrevin Provides Little or No Support for Exocytosis or Liposome Fusion. *J Biol Chem.* Feb 5;291(6):2848-57.
- Chernomordik, L.V.; Melikyan, G.B. and Chizmadzhev, Y.A. (1987). Biomembrane fusion: a new concept derived from model studies using two interacting planar lipid bilayers. *Biochim Biophys Acta.* Oct 5;906(3):309-52.
- Chicka, M.C. and Chapman, E.R. (2009). Concurrent binding of complexin and synaptotagmin to liposome-embedded SNARE complexes. *Biochemistry.* 48, 657-659.
- Chen, X.; Tomchick, D.R.; Kovrigin, E.; Arac, D.; Machius, M.; Südhof, T.C. and Rizo, J. (2002). Three-dimensional structure of the complexin/SNARE complex. *Neuron* 33: 397-409.
- Cho, R.W.; Song, Y. and Littleton, J.T. (2010). Comparative analysis of *Drosophila* and mammalian complexins as fusion clamps and facilitators of neurotransmitter release. *Mol Cell Neurosci.* 45, 389-397.
- Clary, D.O.; Griff, I.C. and Rothman, J.E. (1990). SNAPs, a family of NSF attachment proteins involved in intracellular membrane fusion in animals and yeast. *Cell.* May 18;61(4):709-21.
- Cole, K.S. (1968). *Membranes, Ions and Impulses.* University of California Press, Berkeley.
- Craxton, M. (2004). Synaptotagmin gene content of the sequenced genomes. *BMC Genomics* Jul 6; 5(1), 43.
- Dhara M, Yarzagaray A, Makke M, Schindeldecker B, Schwarz Y, Shaaban A, Sharma S, Böckmann RA, Lindau M, Mohrmann R, Bruns D. (2016). v-SNARE transmembrane domains function as catalysts for vesicle fusion. *Elife.* 25;5.
- Dhara M, Yarzagaray A, Schwarz Y, Dutta S, Grabner C, Moghadam PK, Bost A, Schirra C, Rettig J, Reim K, Brose N, Mohrmann R, Bruns D. (2014). Complexin

synchronizes primed vesicle exocytosis and regulates fusion pore dynamics. *J Cell Biol.* 204: 1123-40.

DiAntonio, A. and Schwarz T.L. (1994). The Effect on Synaptic Physiology of synaptotagmin Mutations in *Drosophila*. *Neuron* 12, 909–20.

Douglas, W.W. and Rubin R.P. (1963). The mechanism of catecholamine release from the adrenal medulla and the role of calcium in stimulus-secretion coupling. *J Physiol.* Jul; 167(2):288-310.

Ellis-Davies, G.C. and Kaplan, J.H. (1994). Nitrophenyl-EGTA, a photolabile chelator that selectively binds  $\text{Ca}^{2+}$  with high affinity and releases it rapidly upon photolysis. *Proc. Natl. Acad. Sci. U.S.A.* 91, 187-191.

Fasshauer, D.; Sutton, R.B.; Brunger, A.T. and Jahn, R. (1998). Conserved structural features of the synaptic fusion complex: SNARE proteins reclassified as Q- and R-SNAREs. *Proc Natl Acad Sci U S A.* Dec 22;95(26):15781-6.

Felmy, F.; Neher, E. and Schneggenburger, R. (2003). The timing of phasic transmitter release is  $\text{Ca}^{2+}$ -dependent and lacks a direct influence of presynaptic membrane potential. *Proc. Natl. Acad. Sci. U.S.A.* 100, 15200–15205.

Fernandez, I.; Arac, D.; Ubach, J.; Gerber, S.H.; Shin, O.; Gao, Y.; Anderson, R.; Südhof, T.C. and Rizo, J. (2001) Three-dimensional structure of the synaptotagmin 1 C2Bdomain: Synaptotagmin 1 as a phospholipid binding machine. *Neuron* 32, 1057–1069.

Fernandez, J.M.; Neher, E. and Gomperts, B.D. (1984). Capacitance measurements reveal stepwise fusion events in degranulating mast cells. *Nature* 312, 453-455.

Forsythe, I.D. (1994). Direct patch recording from identified presynaptic terminals mediating glutamatergic EPSCs in the rat CNS, in vitro. *J. Physiol.* 479 (Pt 3), 381–387.

Geppert, M.; Goda, Y.; Hammer, R.E.; Li, C.; Rosahl, T.W.; Stevens, C.F. and Südhof, T.C. (1994). Synaptotagmin I: A major  $\text{Ca}^{2+}$  sensor for transmitter release at a central synapse. *Cell* 79, 717–727.

Gillis, K.D. (1995). Techniques for membrane capacitance measurements. *Single-Channel Recording*, 2<sup>nd</sup> edition. 155-198.

Gillis, K.D. (2000). Admittance-based measurement of membrane capacitance using the EPC-9 patch-clamp amplifier. *Pflugers Arch* 439, 655-664.

Giraud, C.G.; Eng, W.S.; Melia, T.J. and Rothman, J.E. (2006). A clamping mechanism involved in SNARE-dependent exocytosis. *Science*. Aug 4;313(5787):676-80. Epub 2006 Jun 22.

- Giraudo, C.G.; Garcia-Diaz, A.; Eng, W.S.; Chen, Y.; Hendrickson, W.A.; Melia, T.J. and Rothman, J.E. (2009). Alternative zippering as an on-off switch for SNARE-mediated fusion. *Science*. 323, 512-516.
- Gustavsson, N.; Lao, Y.; Maximov, A.; Chuang, J.C.; Kostromina, E.; Repa, J.J.; Li, C.; Radda, G.K.; Südhof, T.C. and Han, W. (2008). Impaired insulin secretion and glucose intolerance in synaptotagmin-7 null mutant mice. *Proc Natl Acad Sci* 105, 3992 - 3997.
- Gustavsson, N.; Wei, S.H.; Hoang, D.N.; Lao, Y.; Zhang, Q.; Radda, G.K.; Rorsman, P.; Südhof, T.C. and Han, W. (2009). Synaptotagmin-7 is a principal  $\text{Ca}^{2+}$  sensor for  $\text{Ca}^{2+}$ -induced glucagons exocytosis in pancreas. *J Physiol* 587, 1169 - 1178.
- Grynkiewicz, G.; Poenie, M. and Tsien, R.Y. (1985). A new generation of  $\text{Ca}^{2+}$  indicators with greatly improved fluorescence properties. *J Biol Chem* 260, 3440-3450.
- Hamill, O.P.; Marty, A.; Neher, E.; Sakmann, B. and Sigworth, F.J. (1981). Improved patch-clamp techniques for high-resolution current recording from cells and cell-free membrane patches. *Pflugers Arch* 391, 85-100.
- Han, X.; Wang, C.T.; Bai, J.; Chapman, E.R. and Jackson, M.B. (2004). Transmembrane Segments of Syntaxin Line the Fusion Pore of  $\text{Ca}^{2+}$ -Triggered Exocytosis. *Science*. Apr 9;304(5668):289-92.
- Hanson, P.I.; Roth, R.; Morisaki, H.; Jahn, R. and Heuser, J.E. (1997). Structure and conformational changes in NSF and its membrane receptor complexes visualized by quick-freeze/deep-etch electron microscopy. *Cell*. Aug 8;90(3):523-35.
- Heidelberger, R.; Heinemann, C.; Neher, E. and Matthews, G. (1994). Calcium dependence of the rate of exocytosis in a synaptic terminal. *Nature* 371, 513–515.
- Heinemann, C.; Chow, R.H.; Neher, E. and Zucker, R.S. (1994). Kinetics of the secretory response in bovine chromaffin cells following flash photolysis of caged  $\text{Ca}^{2+}$ . *Biophysical Journal* 67, 2546–2557.
- Hobson, R.J.; Liu, Q.; Watanabe, S. and Jorgensen, E.M. (2011). Complexin maintains vesicles in the primed state in *C. elegans*. *Curr Biol*. 21, 106-113.
- Hofmann, M.W.; Peplowska, K.; Rohde, J.; Poschner, B.C.; Ungermann, C. and Langosch, D. (2006). Self-interaction of a SNARE transmembrane a domain promotes the hemifusion-to-fusion transition. *J Mol Biol*. Dec 15;364(5):1048-60.
- Huntwork, S. and Littleton, J.T. (2007). A complexin fusion clamp regulates spontaneous neurotransmitter release and synaptic growth. *Nat Neurosci*. 10, 1235-1237.
- Jahn, R. (2004). Principles of exocytosis and membrane fusion. *Ann N Y Acad Sci*. Apr;1014:170-8.

- Jahn, R. and Fasshauer, D. (2012). Molecular machines governing exocytosis of synaptic vesicles. *Nature* 490, 201–7.
- Jahn, R. and Scheller, R.H. (2006) SNAREs - engines for membrane fusion. *Nature Reviews Molecular Cell Biology* 7, 631– 643.
- Jorquera, R.A.; Huntwork-Rodriguez, S.; Akbergenova, Y.; Cho, R.W. and Littleton, J.T. (2012). Complexin controls spontaneous and evoked neurotransmitter release by regulating the timing and properties of synaptotagmin activity. *J Neurosci.* 32,18234-18245.
- Kaesler-Woo, Y.J.; Yang, X. and Sudhof, T.C. (2012). C-terminal complexin sequence is selectively required for clamping and priming but not for  $\text{Ca}^{2+}$  triggering of synaptic exocytosis. *J Neurosci.* 32, 2877-2885.
- Kasson, P.M.; Lindahl, E. and Pande, V.S. (2010). Atomic-resolution simulations predict a transition state for vesicle fusion defined by contact of a few lipid tails. *PLoS Comput Biol.* 2010 Jun 24;6(6):e1000829.
- Kesavan, J.; Borisovska, M. and Bruns, D. (2007). v-SNARE actions during  $\text{Ca}^{2+}$ -triggered exocytosis. *Cell* 131(2), 351-63.
- Klingauf, J. and Neher, E. (1997). Modeling buffered  $\text{Ca}^{2+}$  diffusion near the membrane: implications for secretion in neuroendocrine cells. *Biophys J* 72, 674-690.
- Konishi, M.; Hollingworth, S.; Harkins, A.B. and Baylor, S.M. (1991). Myoplasmic calcium transients in intact frog skeletal muscle fibers monitored with the fluorescent indicator fura-2. *J Gen Physiol* 97, 271-301.
- Krishnakumar, S.S.; Radoff, D.T.; Kummel, D.; Giraudo, C.G.; Li, F.; Khandan, L.; Baguley S.W., Coleman, J.; Reinisch, K.M.; Pincet, F. and Rothman, J.E. (2011). A conformational switch in complexin is required for synaptotagmin to trigger synaptic fusion. *Nat Struct Mol Biol.* 18, 934-940.
- Krittana, C. and Johnson, W.C. Jr. (2000). The relative order of helical propensity of amino acids changes with solvent environment. *Proteins.* May 1;39(2):132-41.
- Kummel, D.; Krishnakumar, S.S.; Radoff, D.T.; Li, F.; Giraudo, C.G.; Pincet, F.; Rothman, J.E. and Reinisch, K.M. (2011). Complexin cross-links prefusion SNAREs into a zigzag array. *Nat Struct Mol Biol.* 18, 927-933.
- Langer, M. and Langosch, D. (2011). Is lipid flippase activity of SNARE transmembrane domains required for membrane fusion?. *FEBS Lett.* Apr 6;585(7):1021-4.
- Langosch, D.; Crane, J.M.; Brosig, B.; Hellwig, A.; Tamm, L.K. and Reed, J. (2001). Peptide mimics of SNARE transmembrane segments drive membrane fusion depending on their conformational plasticity. *J Mol Biol.* Aug 24;311(4):709-21.

- Langosch, D.; Hofmann, M. and Ungermann, C. (2007). The role of transmembrane domains in membrane fusion. *Cell Mol Life Sci.* 2007 Apr;64(7-8):850-64.
- Lin, M.Y.; Rohan, J.G.; Cai, H.; Reim, K.; Ko, C.P. and Chow, R.H. (2013). Complexin facilitates exocytosis and synchronizes vesicle release in two secretory model systems. *J Physiol.* 591, 2463-2473.
- Lin, R.C. and Scheller, R.H. (1997). Structural organization of the synaptic exocytosis core complex. *Neuron.* 1997 Nov;19(5):1087-94.
- Lindau, M. and Neher, E. (1988). Patch-clamp techniques for time-resolved capacitance measurements in single cells. *Pflugers Arch* 411, 137-146.
- Littleton, J.T.; Stern, M.; Perin, M. and Bellen, H.J. (1994). Calcium dependence of neurotransmitter release and rate of spontaneous vesicle fusions are altered in *Drosophila* synaptotagmin mutants. *Proc Natl Acad Sci* 91, 10888–10892.
- Liu, J.; Wei, Y.; Guo, T.; Xie, X.; Jiang, J. and Sui, S.F. (2007). The positively charged residues in the fragment 71–77 of complexin is required for its binding to SNARE complex. *IUBMB Life* 59, 84–89.
- Mackler, J.M.; Drummond, J.A.; Loewen, C.A.; Robinson, I.M. and Reist, N.E. (2002). The C2B Ca<sup>2+</sup>-binding motif of synaptotagmin is required for synaptic transmission *in vivo*. *Nature* 418, 340 - 44.
- Malsam, J.; Seiler, F.; Schollmeier, Y.; Rusu, P.; Krause, J.M. and Sollner, T.H. (2009). The carboxy-terminal domain of complexin I stimulates liposome fusion. *Proc Natl Acad Sci U S A.* 106, 2001-2006.
- Martens, S. and McMahon, H.T. (2008). Mechanisms of membrane fusion: disparate players and common principles. *Nature Review Molecular Cell Biology* 9(7), 543-56.
- Martin, J.A.; Hu, Z.; Fenz, K.M.; Fernandez, J. and Dittman, J.S. (2011). Complexin has opposite effects on two modes of synaptic vesicle fusion. *Curr Biol.* 21, 97-105.
- Marz, K.E. and Hanson, P.I. (2002). Sealed with a twist: complexin and the synaptic SNARE complex. *Trends Neuroscience* 25, 381–383.
- Markvoort, A.J. and Marrink, S.J. (2011). Lipid acrobatics in the membrane fusion arena. *Curr Top Membr.* 68:259-94.
- Mayer, A.; Wickner, W. and Haas, A. (1996). Sec18p (NSF)-driven release of Sec17p (alpha-SNAP) can precede docking and fusion of yeast vacuoles. *Cell.* Apr 5;85(1):83-94.
- Maximov, A.; Shin, O.H.; Liu, X. and Südhof, T.C. (2006). Synaptotagmin-12, a synaptic vesicle phosphoprotein that modulates spontaneous neurotransmitter release. *J. Cell Biology* 176, 113–124.

- Maximov, A.; Tang, J.; Yang, X.; Pang, Z.P. and Sudhof, T.C. (2009). Complexin controls the force transfer from SNARE complexes to membranes in fusion. *Science* 323, 516 - 521.
- Melicoff, E.; Sansores-Garcia, L.; Gomez, A.; Moreira, D.C.; Datta, P.; Thakur, P.; Petrova, Y.; Siddiqi, T.; Murthy, J.N.; Dickey, B.F.; Heidelberger, R. and Adachi, R. (2009). Synaptotagmin-2 controls regulated exocytosis but not other secretory responses of mast cells. *J Biol Chem* 284, 19445 - 19451.
- McMahon, H.T.; Missler, M.; Li, C. and Sudhof, T.C. (1995). Complexins: cytosolic proteins that regulate SNAP receptor function. *Cell* 83, 111–119.
- Moser, T. and Neher, E. (1997). Estimation of mean exocytic vesicle capacitance in mouse adrenal chromaffin cells. *Proc. Natl. Acad. Sci. U.S.A.* 94, 6735–6740.
- Nagy, G.; Kim, J.H.; Pang, Z.P.; Matti, U.; Rettig, J. and Südhof, T.C. (2006). Different effects on fast exocytosis induced by synaptotagmin 1 and 2 isoforms and abundance but not by phosphorylation. *J Neurosci* 26, 632–643.
- Neher, E. (1998). Vesicle pools and  $\text{Ca}^{2+}$  microdomains: new tools for understanding their roles in neurotransmitter release. *Neuron* 20(3), 389-99.
- Neher, E. and Marty, A. (1982). Discrete changes of cell membrane capacitance observed under conditions of enhanced secretion in bovine adrenal chromaffin cells. *Proc Natl Acad Sci USA* 79, 6712-6716.
- Neher, E. and Sakmann, B. (1976). Noise analysis of drug induced voltage clamp currents in denervated frog muscles fibres. *J Physiol* 258, 705-729.
- Ngatchou, A.N.; Kisler, K.; Fang, Q.; Walter, A.M.; Zhao, Y.; Bruns, D.; Sørensen, J.B. and Lindau, M. (2010). Role of the synaptobrevin C terminus in fusion pore formation. *PNAS* 107:18463–18468.
- Novick, P.; Field, C. and Schekman, R. (1980). Identification of 23 complementation groups required for post-translational events in the yeast secretory pathway. *Cell* Aug;21(1):205-15.
- Ollesch, J.; Poschner, B.C.; Nikolaus, J.; Hofmann, M.W.; Herrmann, A.; Gerwert, K. and Langosch, D. (2008). Secondary structure and distribution of fusogenic LV-peptides in lipid membranes. *Eur Biophys J.* Apr;37(4):435-45.
- Ono, S.; Baux, G.; Sekiguchi, M.; Fossier, P.; Morel, N.F.; Nihonmatsu, I.; Hirata, K.; Awaji, T.; Takahashi, S. and Takahashi, M. (1998). Regulatory roles of complexins in neurotransmitter release from mature presynaptic nerve terminals. *Eur J Neurosci* 10: 2143–2152.

- Pabst, S.; Hazzard, J.W.; Antonin, W.; Südhof, T.C.; Jahn, R.; Rizo, J. and Fasshauer D. (2000). Selective interaction of complexin with the neuronal SNARE complex. Determination of the binding regions. *J Biol Chem.* Jun 30;275(26):19808-18.
- Pang, Z.P.; Sun, J.; Rizo, J.; Maximov, A. and Sudhof, T.C. 2006. Genetic analysis of synaptotagmin 2 in spontaneous and  $\text{Ca}^{2+}$ -triggered neurotransmitter release. *EMBO Journal* 25, 2039 – 50.
- Pieren, M.; Desfougères, Y.; Michailat, L.; Schmidt, A. and Mayer A. (2015). Vacuolar SNARE Protein Transmembrane Domains Serve as Nonspecific Membrane Anchors with Unequal Roles in Lipid Mixing. *J Biol Chem.* May 15;290(20):12821-32.
- Popov, S.V. and Poo, M.M. (1993). Synaptotagmin: A Calcium-Sensitive Inhibitor of Exocytosis?. *Cell* 73, 1247 - 49.
- Poschner, B.C.; Quint, S.; Hofmann, M.W. and Langosch, D. (2009). Sequence-Specific Conformational Dynamics of Model Transmembrane Domains Determines Their Membrane Fusogenic Function. *J Mol Biol.* Feb 27;386(3):733-41.
- Quint, S.; Widmaier, S.; Minde, D.; Hornburg, D.; Langosch, D. and Scharnagl, C. (2010). Residue-specific side-chain packing determines the backbone dynamics of transmembrane model helices. *Biophys J.* Oct 20;99(8):2541-9.
- Rabl, K.; Cadetti, L. and Thoreson, W.B. (2005). Kinetics of exocytosis is faster in cones than in rods. *J Neurosci* 25, 4633-4640.
- Reim, K.; Mansour, M.; Varoqueaux, F.; McMahon, H.T.; Sudhof, T.C.; Brose, N. and Rosenmund, C. (2001). Complexins regulate a late step in  $\text{Ca}^{2+}$ -dependent neurotransmitter release. *Cell.* 104, 71-81.
- Reim, K.; Wegmeyer, H.; Brandstätter, J.H.; Xue, M.; Rosenmund, C.; Dresbach, T.; Hofmann, K. and Brose, N. (2005). Structurally and functionally unique complexins at retinal ribbon synapses. *J Cell Biol* 169, 669–680.
- Rettig, J. and Neher, E. (2002). Emerging roles of presynaptic proteins in  $\text{Ca}^{2+}$ -triggered exocytosis. *Science* 298, 781-785.
- Risselada, H.J.; Kutzner, C. and Grubmüller, H. (2011). Caught in the act: visualization of SNARE-mediated fusion events in molecular detail. *Chembiochem.* May 2;12(7):1049-55.
- Rizo, J. and Rosenmund, C. (2008). Synaptic vesicle fusion. *Nature Structural Molecular Biology* 15(7), 665-74.
- Rizo, J. and Xu, J. (2015). The Synaptic Vesicle Release Machinery. *Annu Rev Biophys.* 2015;44:339-67.

- Sakmann, B. and Neher, E. (1995). *Single Channel Recording*, 2<sup>nd</sup> ed., Plenum, New York, pp. 700.
- Shao, X.; Davletov, B.A.; Sutton, R.B.; Südhof, T.C. and Rizo, J. (1996). Bipartite  $\text{Ca}^{2+}$ -binding motif in C2 domains of synaptotagmin and protein kinase C. *Science* 273, 248–251.
- Schaub, J.R.; Lu, X.; Doneske, B.; Shin, Y.K. and McNew, J.A. (2006). Hemifusion arrest by complexin is relieved by  $\text{Ca}^{2+}$ -synaptotagmin I. *Nat Struct Mol Biol.* 13, 748–750.
- Schneggenburger, R. and Neher, E. (2000). Intracellular calcium dependence of transmitter release rates at a fast central synapse. *Nature* 406, 889–893.
- Schoch, S.; Deak, F.; Königstorfer, A.; Mozhayeva, M.; Sara, Y.; Südhof, T.C. and Kavalali, E.T. (2001). SNARE function analyzed in synaptobrevin/VAMP knockout mice. *Science* 294, 117–1122.
- Schonn, J.S.; Maximov, A.; Lao, Y.; Südhof, T.C. and Sørensen J.B. (2008). Synaptotagmin-1 and -7 are functionally overlapping  $\text{Ca}^{2+}$  sensors for exocytosis in adrenal chromaffin cells. *Proc. Natl. Acad. Sci. USA.* 105(10), 3998–4003.
- Seiler, F.; Malsam, J.; Krause, J.M. and Sollner, T.H. (2009). A role of complexin-lipid interactions in membrane fusion. *FEBS Lett.* 583, 2343–2348.
- Simon, S.M. and Llinas, R.R. (1985). Compartmentalization of the submembrane calcium activity during calcium influx and its significance in transmitter release. *Biophysical Journal* 48, 485–498.
- Söllner, T.; Bennett, M.K.; Whiteheart, S.W.; Scheller, R.H. and Rothman J.E. (1993). A Protein Assembly-Disassembly Pathway In Vitro That May Correspond to Sequential Steps of Synaptic Vesicle Docking, Activation, and Fusion. *Cell* 75, 409–18.
- Söllner, T.; Whiteheart, S.W.; Brunner, M.; Erdjument-Bromage, H.; Geromanos, S.; Tempst, P. and Rothman J.E. (1993). SNAP receptors implicated in vesicle targeting and fusion. *Nature*. 1993 Mar 25;362(6418):318–24.
- Sørensen, J.B.; Nagy, G.; Varoqueaux, F.; Nehring, R.B.; Brose, N.; Wilson, M.C. and Neher, E. (2003). Differential control of the releasable vesicle pools by SNAP-25 splice variants and SNAP-23. *Cell* 114, 75–86.
- Sørensen, J.B. (2004). Formation, stabilisation and fusion of the readily releasable pool of secretory vesicles. *Eur. J. Physiol.* 448, 347–362.
- Sørensen J.B.; Matti, U.; Wei, S.H.; Nehring, R.B.; Voets, T.; Ashery, U.; Binz, T.; Neher, E. and Rettig, J. (2002). The SNARE protein SNAP-25 is linked to fast calcium triggering of exocytosis. *Proc. Natl. Acad. Sci. USA* 99, 1627–1632.



- Stelzer, W.; Poschner, B.C.; Stalz, H.; Heck, A.J. and Langosch, D. (2008). Sequence-specific conformational flexibility of SNARE transmembrane helices probed by hydrogen/deuterium exchange. *Biophys J.* Aug;95(3):1326-35.
- Stevens, D.R.; Schirra, C.; Becherer, U. and Rettig, J. (2011). Vesicle pools: lessons from adrenal chromaffin cells. *Frontiers Synaptic Neuroscience* 3(2), 1 - 9.
- Strenzke, N.; Chanda, S.; Kopp-Scheinflug, C.; Khimich, D.; Reim, K.; Bulankina, A.V.; Neef, A.; Wolf, F.; Brose, N.; Xu-Friedman, M.A. and Moser, T. (2009). Complexin-I is required for high-fidelity transmission at the endbulb of Held auditory synapse. *J Neurosci.* 29, 7991-8004.
- Südhof, T.C. and Rizo, J. (1996). Synaptotagmins: C2-Domain Proteins That Regulate Membrane Traffic. *Neuron* 17, 379–388.
- Sutton, R. B.; Fasshauer, D.; Jahn, R. and Brunger, A. T. (1998). Crystal structure of a SNARE complex involved in synaptic exocytosis at 2.4 Å resolution. *Nature* 395, 347–353.
- Tang, J.; Maximov, A.; Shin, O.H.; Dai, H.; Rizo, J. and Südhof, T.C. (2006). A complexin/synaptotagmin 1 switch controls fast synaptic vesicle exocytosis. *Cell.* 126, 1175-1187.
- Tokumaru, H.; Umayahara, K.; Pellegrini, L.L.; Ishizuka, T.; Saisu, H.; Betz, H.; Augustine, G.J. and Abe, T. (2001). SNARE complex oligomerization by synaphin/complexin is essential for synaptic vesicle exocytosis. *Cell* 104: 421–432.
- Tokumaru, H.; Shimizu-Okabe, C. and Abe, T. (2008). Direct interaction of SNARE complex binding protein synaphin/complexin with calcium sensor synaptotagmin 1. *Brain Cell Biol.* 36, 173-189.
- Ubach, J.; Zhang, X.; Shao, X.; Südhof, T.C. and Rizo, J. (1998). Ca<sup>2+</sup> binding to synaptotagmin: How many Ca<sup>2+</sup> ions bind to the tip of a C2-domain?. *EMBO Journal* 17, 3921–3930.
- Voets, T. (2000). Dissection of three Ca<sup>2+</sup>-dependent steps leading to secretion in chromaffin cells from mouse adrenal slices. *Neuron* 28, 537–545.
- Voets, T.; Moser, T.; Lund, P.E.; Chow, R.H.; Geppert, M.; Südhof, T.C. and Neher, E. (2001). Intracellular calcium dependence of large dense-core vesicle exocytosis in the absence of synaptotagmin I. *Proc. Natl. Acad. Sci. U. S. A.* 98, 11680–11685.
- Voets, T.; Neher, E. and Moser, T. (1999). Mechanisms underlying phasic and sustained secretion in chromaffin cells from mouse adrenal slices. *Neuron* 23, 607–615.
- Weber, T.; Zemelman, B.V.; McNew, J.A.; Westermann, B.; Gmachl, M.; Parlati, F.; Söllner, T.H. and Rothman, J.E. SNAREpins: minimal machinery for membrane fusion. *Cell.* 1998 Mar 20;92(6):759-72.

- Wilson, D.W.; Wilcox, C.A.; Flynn, G.C.; Chen, E.; Kuang, W.J.; Henzel, W.J.; Block, M.R.; Ullrich, A. and Rothman J.E. (1989). A fusion protein required for vesicle-mediated transport in both mammalian cells and yeast. *Nature*. Jun 1;339(6223):355-9.
- Wojcik, S.M. and Brose, N. (2007). Regulation of membrane fusion in synaptic excitation-secretion coupling: speed and accuracy matter. *Neuron*. 55:11–24.
- Wragg, R.T.; Snead, D.; Dong, Y.; Ramlall, T.F.; Menon, I.; Bai, J.; Eliezer, D. and Dittman, J.S. (2013). Synaptic vesicles position complexin to block spontaneous fusion. *Neuron*. 77, 323-334.
- Xu, J.; Mashimo, T. and Südhof, T.C. (2007). Synaptotagmin-1, -2, and -9:  $\text{Ca}^{2+}$ -sensors for fast release that specify distinct presynaptic properties in subsets of neurons. *Neuron* 54, 567–581.
- Xue, M.; Craig, T.K.; Xu, J.; Chao, H.T.; Rizo, J. and Rosenmund, C. (2010). Binding of the complexin N terminus to the SNARE complex potentiates synaptic-vesicle fusogenicity. *Nature Structural Molecular Biology* 17, 568–575.
- Xue, M.; Lin, Y.Q.; Pan, H.; Reim, K.; Deng, H.; Bellen, H.J. and Rosenmund, C. (2009). Tilting the balance between facilitatory and inhibitory functions of mammalian *Drosophila* Complexins orchestrates synaptic vesicle exocytosis. *Neuron* 64, 367-380.
- Xue, M.; Reim, K.; Chen, X.; Chao, H.T.; Deng, H.; Rizo, J.; Brose, N. and Rosenmund, C. (2007). Distinct domains of complexin I differentially regulate neurotransmitter release. *Nature Structural Molecular Biology* 14, 949–958.
- Xue, M.; Stradomska, A.; Chen, H.; Brose, N.; Zhang, W.; Rosenmund, C. and Reim, K. (2008). Complexins facilitate neurotransmitter release at excitatory and inhibitory synapses in mammalian central nervous system. *PNAS USA*. 105, 7875-7880.
- Yang, X.; Kaeser-Woo, Y.J.; Pang, Z.P.; Xu, W. and Südhof, T.C. (2010). Complexin clamps asynchronous release by blocking a secondary  $\text{Ca}^{2+}$  sensor via its accessory alpha helix. *Neuron*. 68, 907-920.
- Yamashita, T.; Hige, T. and Takahashi, T. (2005). Vesicle endocytosis requires dynamin-dependent GTP hydrolysis at a fast CNS synapse. *Science* 307, 124-127.
- Yoon, T.Y.; Lu, X.; Diao, J.; Lee, S.M.; Ha, T. and Shin, Y.K. (2008). Complexin and  $\text{Ca}^{2+}$  stimulate SNARE-mediated membrane fusion. *Nat Struct Mol Biol*. 15, 707-713.
- Yoshihara, M. and Littleton, J.T. (2002). Synaptotagmin I Functions as a Calcium Sensor to Synchronize Neurotransmitter Release. *Neuron* 36, 897–908.

## 6. Publications

Dhara M\*, Yarzagaray A\*, Makke M, Schindeldecker B, Schwarz Y, Shaaban A, Sharma S, Böckmann RA, Lindau M, Mohrmann R, Bruns D. (2016). v-SNARE transmembrane domains function as catalysts for vesicle fusion. *Elife*. 25;5.

Dhara M\*, Yarzagaray A\*, Schwarz Y, Dutta S, Grabner C, Moghadam PK, Bost A, Schirra C, Rettig J, Reim K, Brose N, Mohrmann R, Bruns D. (2014). Complexin synchronizes primed vesicle exocytosis and regulates fusion pore dynamics. *J Cell Biol*. 204: 1123-40.

Borisovska M, Schwarz YN, Dhara M, Yarzagaray A, Hugo S, Narzi D, Siu SW, Kesavan J, Mohrmann R, Böckmann RA, Bruns D (2012). Membrane-proximal tryptophans of synaptobrevin II stabilize priming of secretory vesicles. *J Neurosci*. 32:15983-97.

**\* Joint first authorship**